JOINT CONFERENCES ON ADVANCED MATERIALS

The 10th Conference
on Functional and Nanostructured Materials

FNMA'13

The 12th Conference
on Intermolecular and Magnetic Interactions in Matter

IMIM'13

8–12 September 2013
Poros Island, Greece

ABSTRACT BOOK

TITLE

Joint Conferences on Advanced Materials:

The 10^{th} Conference on Functional and Nanostructured Materials – FNMA'13

The 12^{th} Conference on Intermolecular and Magnetic Interactions in Matter – IMIM'13

8–12 September 2013, Poros, Greece – Abstract Book

EDITORS

Jarosław Rybicki and Krzysztof W. Wojciechowski

TYPESETTING USING TEX

BOP, www.bop.com.pl

TASK PUBLISHING 2013
GDAŃSK

ISBN 978-83-930549-9-2

FNMA'13 IMIM'13
Joint Conferences on Advanced Materials

Organizers

Department of Solid State Physics, Faculty of Physics,
University of Athens, Greece
Department of Solid State Physics, Gdansk University of Technology, Poland
Institute of Physics, Faculty of Mechanical Engineering and Mechatronic,
West Pomeranian University of Technology, Szczecin, Poland
Lublin University of Technology, Poland
University of Zielona Gora, Poland
Institute of Molecular Physics, Polish Academy of Sciences, Poznan, Poland
PWSZ im. Prezydenta St. Wojciechowskiego, Kalisz, Poland

In cooperation with:
TASK – Academic Computer Centre in Gdansk, Poland
Poznan Supercomputing and Networking Center, Poland
Intel Corporation Polish Physical Society

Honorary Chairman

G. J. Papadopoulos (Athens, Greece)

Scientific Committee

A. Alderson (Bristol, UK) • F. J. Baltá-Calleja (Madrid, Spain) • J. Barnaś (Poznan, Poland) • J. Bernholc (Raleigh, USA) • X. M. Duan (Beijing, China) • J. Felba (Wroclaw, Poland) • J. Grima (Msida, Malta) • B. Grzybowski (Evanston, USA) • W. G. Hoover (Ruby Valley, USA) • A. B. Kolomeisky (Houston, USA) • A. A. Kornyshev (London, UK) C. A. Londos (Athens, Greece) • H. Mizuta (Southampton, UK) • A. Morawski (Szczecin, Poland) • B. Padlyak (Lviv, Ukraine) • G. Papavasiliou (Athens, Greece) V. Radmilovic (Berkeley, USA) • P. Siskos (Athens, Greece) • W. Sadowski (Gdansk, Poland) – Co-Chairman • F. Scarpa (Bristol, UK) • K. Schulte (Hamburg, Germany) T. Tsuboi (Kyoto, Japan) • P. Varotzos (Athens, Greece) • K. W. Wojciechowski (Poznan, Poland) – Co-Chairman • N. I. Zheludev (Southampton, UK)

Programme Committee

M. Dudek (Zielona Gora, Poland) • N. Gouskos (Athens, Greece) • R. Gunnella (Camerino, Italy) • W. Kempinski (Poznan, Poland) • S. Kruchinin (Kiev, Ukraine) • J. Olchowik (Lublin, Poland) • U. Narkiewicz (Szczecin, Poland) D. Petridis (Athens, Greece) – Co-Chairman • J. Rybicki (Gdansk, Poland) – Co-Chairman • Ch. Trapalis (Athens, Greece) • J. Typek (Szczecin, Poland)

Organizing Committee

N. Gouskos (Athens, Greece) – Chairman • C. Aidinis (Athens, Greece) A. Guskos (Szczecin, Poland) • M. Nakonieczny (Gdansk, Poland) • A. Rybicka (Gdansk, Poland) • J. Rybicki (Gdansk, Poland) • Sz. Winczewski (Gdansk, Poland) – Secretary • B. Zapotoczny (Zielona Gora, Poland) • G. Zolnierkiewicz (Szczecin, Poland)

CONTENTS

On the 80^{th} birthday of Professor George J. Papadopoulos

In the evening preceding the canonical date (7^{th} July 2013) the blissful eightieth Birthday of Professor Emeritus of the University of Athens George J. Papadopoulos was celebrated in a coherently vibrant festive Assembly of Relatives, Colleagues and Friends, enjoying the stream of a broad variety of ambrosia and the catalysis of hilarious wines and contributing lovingly to the authentic and mystifying enthusiasm permeating the local atmosphere.

His Daughters, Helen and Emma, scintillating with affection for and righteously taking pride in their Father, and his kind Spouse, Helen, ever paying devoted attention to co-operating with him for the proper flow of the celebration, kept being witnesses as the graceful paragons of honouring the importance of the ceremony. The Colleagues and Friends-and-Followers (and among them the composer of this Brief Report, having been blessed both to have experienced the Professor's inspiring Tuition, apocalyptic of the celestial Beauty and fantastic Charm of Physics, as a 1979–1982 Student and to have been belonging to his regular Team of Office Visitors since around 1990) were exchanging memories of old and recent manifestations of the Professor's multi-facetted charismatic personality:

Not only has he been functioning beneficially and fruitfully within the international Academic Community (in the U.K., Belgium, Greece, his heroic Homeland Cyprus, and elsewhere) for already almost half a century both as a magnetising Professor and an unparalleled autonomous original Researcher, but he has also been communicating with his Colleagues and Followers as a surprisingly profound Physical and (socially) Empirical Philosopher, always eagerly and efficiently offering invaluable scientific enlightenment and friendly support. This Reporter is one of those who perceive and admit Prof. Papadopoulos as their adored Mentor and (academic and life-affairs) Advisor.

Furthermore, his vigorous, just, and uninterrupted Leadership quality has been evidenced and praised during, in particular, both his Direction of the Solid State

Physics Section of the Department of Physics at the University of Athens (for consecutive Terms before and after 1990) and his Presidency of the Hellenic Physical Society (for three Terms in series, covering the 2002–2008 period): By virtue of his talent for inspiring and convincing he has in either case equally succeeded in taming inter-Colleague misunderstandings and, having identified the genuine dexterity of each Group Member, in earnestly encouraging everyone to be systematically applying the personal advantage for serving the collective need and advancement.

We are, therefore, straightforwardly declaring our gratitude and expressing our best heartfelt Birthday Wishes to our beloved and, in accordance with our Conscience, unique Mentor, Philosopher, and Archon of our Spiritual and Friendly eternal Symposium, Professor George J. Papadopoulos!

E. A. Anagnostakis

Simulating the thermal expansion properties of triangular lattices

K. Aquilina[1], R. Gatt[2], J. N. Grima[1,2]

[1] *Department of Chemistry, Faculty of Science, University of Malta Msida MSD 2080, Malta*

[2] *Metamaterials Unit, Faculty of Science, University of Malta Msida MSD 2080, Malta*

Materials having a negative coefficient of thermal expansion exhibit the counterintuitive property of undergoing a decrease in dimensions on heating and an increase in dimensions on cooling. This atypical behaviour renders such a material very appealing to various fields of engineering and science. One of the primary causes giving rise to such a property may be comprehended in the terms of the structural geometry of the material, presenting a relatively simplistic case which could be described through analytical and computational models.

A novel method which aims to computationally describe this mechanistic cause of negative thermal expansion for a theoretical triangular framework is proposed and implemented. This is employed through Empirical Modelling Using Dummy Atoms (EMUDA) and Molecular Dynamics. The theoretical framework, composed of equilateral corner-shared triangles, is based on naturally occurring high temperature polymorphs of silica. It was determined that the thermal expansion behaviour is highly dependent on the equilibrium angles between the triangles constituting the framework, presenting a simplistic method of controlling the thermal expansion behaviour. Furthermore, the basic assumptions which need to be assumed in order to describe such a geometry analytically were also formulated. This was further developed by calculating a set of statistical values and distributions which may be directly followed by to the derivation of such an analytical model.

Acknowledgements
The support of the University of Malta is gratefully acknowledged.

Studies of nitriding and reduction processes in system nanocrystalline iron-ammonia-hydrogen at 350°C

W. Arabczyk, R. Pełka, B. Wilk, K. Kiełbasa, R. Wróbel

Institute of Chemical and Environment Engineering
West Pomeranian University of Technology
Pulaskiego 10, 70-322 Szczecin, Poland

Studies of a nanocrystalline iron nitriding process and reduction of the obtained nanocrystalline iron nitrides were performed. Ammonia-hydrogen mixtures of different composition ($p_{NH_3}/p_{H_2} = \text{var}$) were applied as a reacting agent. The fused ammonia iron catalyst promoted with oxides of aluminum, calcium and potassium was used for testing. The composition of the catalyst, as determined by ICP-AES, expressed in the weight percent was: Al_2O_3 – 3.3%, CaO – 2.8% K_2O – 0.65%, oxygen in the form of iron oxides – 6.5%. The average size of iron nanocrystallites was 20 nm (as determined by XRD). The thermogravimetric measurements were performed in a tubular differential reactor equipped with a system that also allowed the gas phase composition analysis.

The nitriding process and reduction of the obtained iron nitrides were performed isothermally at a temperature of 350°C and at atmospheric pressure. Stationary states, in which an equilibrium between the gas phase and solid holds, occurred for certain nitriding potentials (defined as $P = p_{NH_3}/p_{H_2}^{3/2}$).

The average crystallite sizes of iron and iron nitride γ'-Fe_4N were measured by the Scherrer method and the phase composition was determined by the Rietveld method for the obtained samples corresponding to the particular stationary states. It was found that the average size of nanocrystallites of both iron and iron nitrides decreased along with an increase in the nitriding potential.

The obtained results were compared with the data for the temperature of 475°C [1]. At the temperature of 475°C an increase in the nitriding degree of nanocrystalline iron was observed only to a level corresponding to nitride Fe_4N – no further increase in the nitriding degree occured. Higher nitriding degrees were observed at the temperature of 350°C, and the resulting material was characterized by nitriding degrees close to those corresponding to the Fe_2N phase. The hysteresis phenomenon in the system nitriding degree – the nitriding potential was observed during the nitriding and reduction of iron nitrides.

Acknowledgements
Scientific work of one of the authors (R. Pełka) supported from the budget of the Iuventus Plus program for science in 2012–2013, IP No. 2011040771.

References
[1] K. Kiełbasa, PhD Thesis, West Pomeranian University of Technology, Szczecin, 2013

On the mechanical properties of C_6H_6: an organic molecule having delocalised electrons

K. M. Azzopardi[1], D. Attard[1], R. Gatt[1], J. N. Grima[1,2]

[1] *Metamaterials Unit, Faculty of Science, University of Malta Msida MSD 2080, Malta*

[2] *Department of Chemistry, Faculty of Science, University of Malta Msida MSD 2080, Malta*

Auxetic materials exhibit the counterintuitive property of expanding laterally when uniaxially stretched. The extent of this property is quantitatively measured by the Poisson's ratio which assumes negative values for such materials. This property has been reported in a number of systems ranging from macro-structures to micro-structured materials and molecular systems. In this study, DFT methods were used to analyse the mechanical properties, particularly the Poisson's ratio, of solid benzene in its various phases (I, I', II, III, III', IV, V) in view of the reports made relating to its potential to exhibit auxetic behaviour in one of its phases. The results obtained through these simulations suggest that out of the seven phases, Benzene I, I', II and III can exhibit auxetic behaviour. The systems are highly anisotropic and when auxeticity is present it is predicted to be present off-axis and in a limited range except for Benzene I' in the XY plane, which shows auxeticity for all off-axis angles, with the lowest Poisson's ratio being ~ -0.4 at around $\sim 60^\circ$ with respect to Z.

Phase	Plane	Auxeticity Range ($\sim^\circ$)		Maximum Auxeticity ($^\circ$)	Maximum Auxeticity (ν)
Benzene I	XZ	35	55	45	-0.3
Benzene I'	XY	0	360	59	-0.4
	XZ	43	49	45	-0.04
Benzene II	XY	30	65	45	-0.11
Benzene III	XY	30	65	45	-0.11
Benzene III'	N/A	N/A	N/A	N/A	N/A
Benzene IV	N/A	N/A	N/A	N/A	N/A
Benzene V	N/A	N/A	N/A	N/A	N/A

Table 1: Summary of the auxeticity present in the phases of solid state benzene

Acknowledgements
This research is funded by a grant awarded to Keith M. Azzopardi through the Strategic Educational Pathways Scholarship (Malta). These scholarships are part-financed by the European Union – European Social Fund (ESF) under Operational Programme II – Cohesion Policy 2007–2013, "Empowering People for More Jobs and a Better Quality of Life" and a grant from Malta Council for Science & Technology.

Negative thermal expansion from partially closed rotating rigid units

M. Bajada[1], D. Attard[1], S. Scerri[1], J. N. Grima[1,2]

[1] *Department of Chemistry, Faculty of Science, University of Malta Msida MSD 2080, Malta*

[2] *Metamaterials Unit, Faculty of Science, University of Malta Msida MSD 2080, Malta*

Negative thermal expansion (NTE), or *thermal contraction*, is the phenomenon by which a structure or material exhibits a shrinkage when subjected to an increase in temperature. Due to their intriguing, counterintuitive properties and attractive features for use in numerous applications, popularity in the field has grown tremendously in the past decades.

This work is concerned with an extended preliminary investigation of the fundamental models initially developed by Dove, Heine and others, within the domain of the 'rigid unit mode' (RUM) approach. In essence, their work was based on modelling the NTE capabilities of *fully open, two dimensional* framework structures, composed of rigid units, under the thermal excitation of low frequency phonon modes (or RUMs), which leads to a "rocking-type motion" of the units and results in a subsequent shrinkage in the unit cell. Although such models offered a deep insight to the relation between phonon modes, NTE and geometrical constraints, there appeared to be little or no mention of how the systems would behave, were they to be found in various *non-fully open* conformations. Thus, the need was felt to develop a generic model that could account for this relatively unknown factor in such 2D structures, whilst keeping in line with certain concepts and assumptions, both used and derived in previous works by Dove et al., with particular focus on the RUM formalism. This model was instigated by mapping the potential expression for the rotational motion of the rigid units in an arbitrary framework structure, to a probability distribution function, that was to represent a weighting factor for the unit cell area at different rotational angles. By calculating this overall weighted area at various temperatures, and integrating by means of an iterative process, the thermal expansion properties of the structure could be studied in terms of the changes in its unit cell area. Through this method, it has been shown that a number of 2D framework structures composed of various geometrical shapes, not only exhibited NTE in their fully open conformations, but also in a number of non-fully open forms. Particularly, quadrilateral based systems showed signs of NTE throughout the range of the initial angles specified, whereas the equilateral triangular based array displayed NTE effects and positive thermal expansion, within separate ranges of such initial angles. The difference in thermal properties observed in these two categories is purely a result of geometrical effects, since the same model (based on the same assumptions), was applied for all the cases studied.

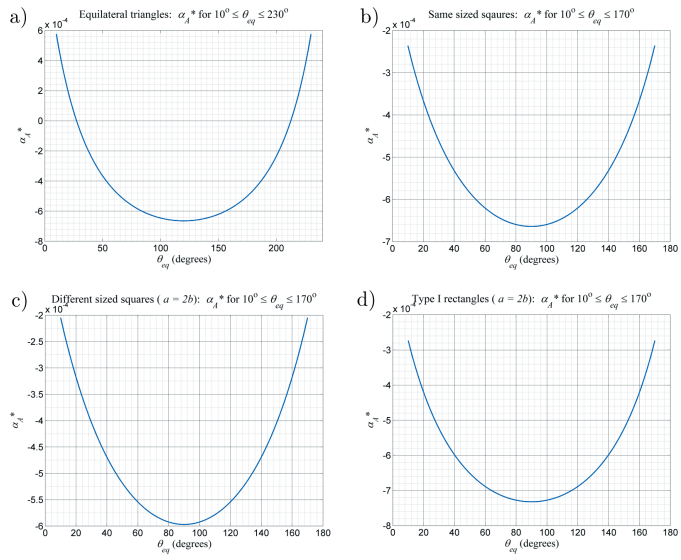

Figure 1: 2D plots of the *effective area coefficient of thermal expansion*, α_A*, for varying equilibrium angles, Θ_{eq}

Acknowledgements
The support of the University of Malta, is gratefully acknowledged.

Compensation of Eu^{3+} ions in Ca^{2+} sites in β-Ca_2SiO_4 doped with europium

A. Baran, J. Barzowska, M. Grinberg, K. Szczodrowski

Institute of Experimental Physics, University of Gdansk
Wita Stwosza 57, 80-952 Gdansk, Poland

Silicate materials have good thermal and chemical stability, therefore doped Eu^{3+}/ Eu^{2+} are perspective phosphors for white LEDs. In β-Ca_2SiO_4, the Eu ion replaces the Ca^{2+} ion and occupies two different sites which are characterized by 7 and 8 fold coordination of O^{2-}. Synthesis in an air atmosphere provides β-Ca_2SiO_4:Eu^{3+}. The Eu^{2+} ion can be obtained by synthesis in a reducing atmosphere (H_2, N_2) or by performing a reduction after synthesis as the second step of the process. The reduction process is reversible and the ratio of Eu^{2+} to Eu^{3+} can be controlled. The excitation spectrum of Eu^{3+} contains a broad band peaked at about 5 eV that can be attributed to the charge transfer (CT) transition and allows the position of the Eu^{2+} ground state to be fixed with respect to the valence band of β-Ca_2SiO_4 for the case when the Eu^{3+} f-f emission is observed. The emission of Eu^{2+} is dominated by $4f^65d \rightarrow 4f^7$ transitions with bands peaked at 2.5 eV and 2 eV.The excitation spectrum of Eu^{2+} consists of several bands related to transitions to the split levels of the $4f^65d$ electronic configuration, peaked at 3.5 eV. Since no emission quenching and no anomalous luminescence in the case of Eu^{2+} ions in β-Ca_2SiO_4 are observed the ground state energy of Eu^{2+} should be placed more than 3.5 eV below the conduction band edge. The band gap obtained using synchrotron radiation was 6.8 eV. These data and the excitation spectra of the Ca_2SiO_4:Eu^{2+} and Ca_2SiO_4:Eu^{3+} allow estimating the lattice relaxation energy related to an increase in the number of electrons from 6 to 7 when $Eu^{3+} \rightarrow Eu^{2+}$ occurs as greater than 0.75 eV. The processes that control the amount of Eu^{2+} and the Eu^{3+} emission are discussed by means of the Fermi level energy and by consideration of the influence of the potentials of Ca vacancies or/and other defects that appear as charge compensation for Eu^{3+} in the Ca^{2+} site. The obtained spectroscopic results for samples containing different amounts of Eu^{3+} and Eu^{2+} lead to the conclusion that compensation defects control the Fermi energy and cause the band bending due to the fact that they appear at a short distance from Eu^{3+}. The quantitative relation that determines the existence of Eu^{2+} and/or Eu^{3+} is discussed considering the defect formation energy and the difference between energies of Eu^{2+} and Eu^{3+} in the band gap.

Acoustic variant of parameters for anisotropic Poisson's ratios in cubic crystals

V. Belomestnykh, E. Soboleva

Yurga Institute of Technology of National Research Tomsk Polytechnic University
Leningradskaya 26, 652050, Yurga, Kemerovo Region, Russia

The work suggests new calculation correlations for four Poisson's ratios ($\sigma_{\langle 100,001\rangle}$, $\sigma_{\langle 110,001\rangle}$, $\sigma_{\langle 110,1\bar{1}0\rangle}$, $\sigma_{\langle 111,111\rangle}$) in cubic crystals where a combination of two acoustic parameters was used based on the data of the propagation velocity of longitudinal elastic waves in crystallographic direction $\langle 100\rangle$ and two transverse elastic waves in directions $\langle 100\rangle$ and $\langle 110\rangle$.

The calculation capability of the suggested correlations was tested on 30 substances with the basic types of chemical bonds in solids (metal, covalent, ion, molecular) with intentionally various values of elastic anisotropy and centricity of interatomic forces. Some of the received $\sigma_{\langle hk\ell\rangle}$ values are of special interest as they fall into the primary category and the mechanisms of abnormal Poisson's ratios with different signs (positive and negative) are being intensively studied now [1,2]. The traditional parameters for receiving anisotropic Poisson's ratios are tensor components of compliance s_{ij} and rigidity c_{ij} constants. These are correspondingly s_{11}, s_{12}, s_{44} or c_{11}, c_{12}, c_{44} for the cubic crystals. The calculation formulas are given in the top part of Table 1.

Parameters	$\sigma_{\langle 100\rangle}$	$\sigma_{\langle 110,001\rangle}$	$\sigma_{\langle 110,1\bar{1}0\rangle}$	$\sigma_{\langle 111\rangle}$
c_{ij}	$\dfrac{c_{12}}{c_{11}+c_{12}}$	$\dfrac{2c_{12}c_{44}}{3Bc_s+c_{11}c_{44}}$	$\dfrac{3Bc_s-c_{11}c_{44}}{3Bc_s+c_{11}c_{44}}$	$\dfrac{3B-2c_{44}}{6B+2c_{44}}$
a^2, A	$\dfrac{(a^2-2)}{2(a^2-1)}$	$\dfrac{2A(a^2-2)}{(3+A)a^2-4}$	$\dfrac{(3-A)a^2-4}{(3+A)a^2-4}$	$\dfrac{1.5a^2-A-2}{3a^2+A-4}$

Note: $B=\frac{1}{3}(c_{11}+2c_{12})$, $c_s=\frac{1}{2}(c_{11}-c_{12})$.

Table 1: Calculated correlations for anisotropic Poisson's ratios in cubic crystals

The suggested parameter, A, actually is a factor of the elastic anisotropy of cubic crystals $\left(A=\frac{c_{44}}{c_s}=\frac{2c_{44}}{c_{11}-c_{12}}\right)$. The other parameter, a^2, as far as we know, is not named in the elasticity theory and expressed through c_{ij}, equals the following relation $a^2=\frac{c_{11}}{c_s}=\frac{2c_{11}}{c_{11}-c_{12}}$.

We suggest to present new parameters for calculating anisotropic Poisson's ratios in cubic crystals as squared ratios of sound velocities $a^2=\left(\frac{\upsilon_L}{\upsilon_t}\right)^2_{\langle 100\rangle}$ and $A=\left(\frac{\upsilon_{L\langle 100\rangle}}{\upsilon_{t_2\langle 110\rangle}}\right)^2$, where υ_L – the velocity of a purely transversal wave in an unbounded medium, υ_t and υ_{t_2} – the velocities of purely longitudinal waves in $\langle 100\rangle$ and $\langle 110\rangle$ crystallographic

No.	Substance	a^2	A	B [GPa]	$\sigma_{\langle 100,001\rangle}$	$\sigma_{\langle 110,001\rangle}$	$\sigma_{\langle 110,1\bar{1}0\rangle}$	$\sigma_{\langle 111,111\rangle}$	σ	Reference c_{ij}
1	Ag	8.111	3.014	103.63	0.430	0.823	−0.092	0.306	0.369	[3]
2	W	3.342	0.995	308.07	0.286	0.286	0.289	0.287	0.287	[3]
3	Re	3.021	1.016	342.2	0.253	0.255	0.245	0.249	0.251	[3]
4	Na	12.23	6.975	6.593	0.455	1.210	−0.446	0.236	0.362	[3]
5	C (diamond)	2.263	1.211	442.0	0.104	0.115	0.009	0.046	0.070	[3]
6	Ge	3.200	1.663	75.417	0.273	0.365	0.025	0.156	0.207	[3]
7	PbSe	2.155	0.262	40.80	0.067	0.027	0.627	0.356	0.267	[3]
8	CuI	6.295	2.540	35.547	0.406	0.707	−0.036	0.281	0.342	[4]
9	LiF	3.169	1.880	61.843	0.269	0.383	−0.039	0.118	0.186	[3]
10	NaCl	2.734	0.722	24.77	0.212	0.172	0.361	0.280	0.255	[3]
11	NaCN	4.650	0.061	18.07	0.363	0.031	0.945	0.491	0.468	[5]
12	$AgPO_3$	4.639	1.004	29.50	0.363	0.364	0.361	0.362	0.362	[6]
13	Tl_3TaS_4	2.598	0.169	23.90	0.187	0.048	0.792	0.436	0.370	[7]
14	Ar (4.2 K)	2.685	0.807	2.66	0.203	0.178	0.303	0.251	0.233	[8]
15	Ne (24.3 K)	5.318	2.727	0.88	0.384	0.684	−0.096	0.221	0.303	[3]
16	$In_{0.73}Tl_{0.27}$ (125 K)	8110	1904	40.54	0.500	1.996	−0.997	0.406	0.475	[9]
17	USb	1.866	0.170	55.67	−0.077	−0.024	0.668	0.356	0.227	[10]
18	USe (0 K)	1.726	0.095	57.33	−0.189	−0.039	0.757	0.389	0.229	[10]
19	UTe	1.777	0.127	39.67	−0.144	−0.037	0.710	0.369	0.222	[11]
20	PuTe	1.805	0.987	94.0	−0.122	−0.121	−0.115	−0.117	−0.119	[12]
21	$Tm_{0.99}Se$ (4.2 K)	1.529	0.220	25.0	−0.444	−0.224	0.273	0.092	−0.114	[13]
22	SmB_6	1.719	0.322	93.33	−0.195	−0.106	0.352	0.173	0.041	[14]
23	$Sm_{0.75}Y_{0.25}S$	1.427	0.360	8.33	−0.671	−0.519	−0.292	−0.342	−0.500	[15]
24	$Sm_{0.75}La_{0.25}S$	1.556	0.479	13.0	−0.400	−0.302	−0.055	−0.127	−0.240	[16]
25	$Sm_{0.75}Tm_{0.25}S$	1.521	0.612	11.33	−0.460	−0.393	−0.247	−0.282	−0.365	[17]
26	FeS_2	2.309	0.650	154.67	0.118	0.091	0.322	0.227	0.188	[18]
		1.768	0.516	90.47	−0.151	−0.108	0.176	0.074	−0.010	[19]
27	$NaClO_3$	2.819	0.671	26.027	0.225	0.173	0.404	0.304	0.275	[20]
		1.495	0.288	6.83	−0.511	−0.318	0.059	−0.059	−0.242	[21]
28	$CeRu_2$ (2 K)	23.18	3.360	151.83	0.477	0.992	−0.086	0.427	0.454	[22]
		51.36	6.545	157.82	0.490	1.329	−0.383	0.437	0.469	
29	V_3Si (4.2 K)	3.441	0.971	17.58	0.295	0.290	0.309	0.300	0.298	[23]
		119.7	50.73	17.75	0.496	1.858	−0.890	0.312	0.440	
30	Nb_3Sn (4.2 K)	3.603	0.600	15.43	0.308	0.214	0.518	0.379	0.354	[23]
		2.780	0.205	16.13	0.219	0.065	0.768	0.433	0.375	

Table 2: Parameters A^2, A, bulk modulus (B) and Poisson's ratios in cubic crystals

directions accordingly (the wave is polarized in $\langle 1\bar{1}0\rangle$ direction). New calculation formulas for $\sigma_{\langle hk\ell\rangle}$ are shown in the bottom part of Table 1.

Table 2 makes evident that modulus B is maximal for the diamond (442 GPa) and minimal for neon (0.88 GPa). Low modulus values are also observed for solid samarium monosulfide-based solutions when 25% of samarium ions are replaced by ions of yttrium, lanthanum and thulium. This condition leads to unusual mechanical properties of the given crystals – single sign longitudinal and transverse deformations (the crystals extend/contract in the orthogonal direction under longitudinal tension/compression).

Thus, the following facts should be noted:

1. Compounds of uranium, plutonium, thulium and samarium are axial auxetics. Pyrite and Sodium chlorate may also be included into this group (further study is required).

2. 9 of 30 crystals are non-axial auxetics (negative Posson's ratios in $\langle 110\rangle$ direction).

3. Four objects demonstrate all four anisotropic and isotropic negative Poisson's ratios – plutonium telluride and mixed samarium sulphide-based systems.

4. Seven substances, if FeS_2 and $NaClO_3$ included, are real auxetics in the full sense of this word.

5. Solid solution of $Sm_{0.75}Y_{0.25}S$ has the maximal negative isotropic Poisson's ratio (-0.500) and In-Tl alloy has the maximal positive $\sigma = 0.475$. One of anisotropic Poisson's ratios in this alloy (in $\langle 110.001\rangle$ direction) is the largest ($\approx +2$), and another (in $\langle 110, 1\bar{1}0\rangle$ direction) is the smallest (almost -1).

6. In tungsten, rhenium and silver phosphate all Poisson's ratios in the basic directions in monocrystals and medium in the polycrystals equal each other (as a result of elastic isotropy).

7. Calculations of anisotropic Poisson's ratios in cubic crystals with the application of the new suggested parameters A and a^2 allow receiving the same values as those received by traditional calculations $\sigma_{\langle hk\ell\rangle} = f(c_{ij})$ (Table 1).

Acknowledgements
This work was supported by RFBR grant No 13-08-98014 r_sibir_a to conduct fundamental research.

References

[1] Konyok D A, Wojciechowski K V, Pleskachevsky Yu M, Shilko S V 2004 *Mechanics of composite materials and constructions* **10** 35
[2] Tokmakova S P 2005 *Phys. Stat. Sol. (b)* **242** 721
[3] Franzevich I N et al. 1982 *Elastic constants and modules of elasticity of metals and non-metals*, Kiev, Naukova dumka
[4] Hanson R C et al. 1972 *Appl. Phys. Lett.* **21** 490
[5] Haussühl S et al. 1977 *Acta Cryst.* **A33** 847
[6] Saunders G A et al. 1996 *Phys. Rev. B* **53** 5287

[7] Blistanov A A et al. 1982 Acoustic crystals. Reference book. Edited by M P Shaskolskaya M: Nauka
[8] Simmons G, Wang H 1971 *Single crystal elastic constants and calculated aggregate properties: A handbook. Sec. edition*, Cambridge, Massachusetts and London
[9] Gunton D J, Saunders G A 1975 *Proc. R. Soc. Lond.* **343** 63
[10] Neuenschwander J et al. 1986 *Physica. B* **144** 66
[11] Mendik M, Wachter P 1993 *Physica. B* **190** 72
[12] Mendik M et al. 1993 *Physica B* **186–188** 678
[13] Boppart H et al. 1980 *Solid State Communic.* **35** 483
[14] Tamaki A et al. 1985 *J. Magn. Magnetic Mater.* **47–48** 469
[15] Hailing Tu et al. 1984 *J. Phys. C: Solid State Phys.* **17** 4559
[16] Shärer U, Wachter P 1995 *Solid State Communic.* **96** 497
[17] Shärer U et al. 1998 *Physica B* **244** 148
[18] Benbattouche N et al. 1989 *J. Phys. D.: Appl. Phys.* **22** 670
[19] Voigt W 1888 *J. Annalen der Physic und Chemie* **35** 642
[20] Belomestnykh V N, Soboleva E G 2009 *Acoustic, elastic and inelastic properties of sodium halogenate crystals*, Tomsk
[21] Voigt W, 1893 *Aus. den Gött. Nackrichten* **6** 719
[22] Suzuki T et al. 1996 *J. Phys. Soc. Japan.* **65** 2753
[23] Testardi L et al. 1977 *Superconducting compositions with β-tungsten structure.*

Anisothropy of dynamic elastic modules and interatomic oscillations anharmonicity in Cu_3Au alloy at low temperatures

V. Belomestnykh, E. Tesleva

Yurga Institute of Technology of National Research Tomsk Polytechnic University
Leningradskaya 26, 652050, Yurga, Kemerovo Region, Russia

The elastic properties of crystals are the most needed (important) properties of all solids developing as a result of strain due to external influence. The elastic properties of crystals are characterized by different modules and elastic constants adequately revealing the nature of interatomic force bonds which is one of the main problems (tasks) of the solid state physics. The elastic properties anisotropy shows interatomic bond strength in different crystal planes [1].

It is very important for the condensed state physics to know about the non-linear properties of substances. The anharmonic properties of solids are related to the deviation of medium behavior from the Hooke's law. It means that the correlation between stress and strain becomes non-linear. The Grüneisen parameter serves as an anharmonicity measure of interatomic (intermolecular) vibrations and non-linear interatomic force interaction.

Formerly, we studied the elastic properties and anharmonic effects in metallic, ion, covalent, ion-covalent and molecular cubic monocrystals with lattices of various types. For example, work [1] studied orientational order-disorder of alkaline metals cyanides. The investigation showed that the Grüneisen parameter reached its maximum value of 4.5 in the field (area) of structural change at disorder. It is of interest to study the elastic properties anisotropy and interatomic interaction anharmonicity in double alloys with the positional order-disorder. From the great number of alloys studied we shall consider the A_3B type of alloy, Cu_3Au, with a simple stehiometry and formula. In the low temperatures area the given alloy has a cubic face-centered lattice with a $Pm\bar{3}m$ space group where face centers are occupied by copper atoms and cube corners by aurum atoms. Work [2] studied the rigidity constants of order and disorder Cu_3Au forms in the temperature area of 4.2–300 K.

According to the data on c_{ij} of a Cu_3Au crystal we calculated purely longitudinal and purely transverse waves velocities in three crystallographic directions, elastic anisotropy factor (A), Cauchy correlation (Δ) and temperature dependence of the elastic modules (Young's modulus E, shear modulus G and adiabatic modulus B) for the order as well as for the disorder forms [1,3,4].

The temperature changes of Cu_3Au properties under consideration (Figs. 1–4) are linear between the temperatures of 4.2–300 K, while the sound velocities and elastic modules are slowly decreasing with the temperature rise and Poisson's ratios and the Grüneisen parameters show a tendency of growth (in all Figures the results for the

order phase are shown by darker symbols, while those for the disorder phase – by lighter ones).

Table 1 compares the results of calculations of purely longitudinal and purely transverse waves velocities in three crystallographic directions, the elastic anisotropy factor and the Cauchy correlation. The given results show that:

– all acoustic modes demonstrate normal regularity with the rise of temperature (the transmission velocities of order and disorder Cu_3Au decrease),

T, K	[100]		[110]		[111]		A	Δ
	υ_L	υ_t	υ_L	υ_{t2}	υ_L	υ_t		
0	3912	2442	4352	1526	4489	1882	2,559	1,786
	3891	2453	4352	1489	4495	1867	2,715	1,778
20	3913	2443	4353	1527	4490	1883	2,559	1,784
	3891	2454	4353	1490	4496	1867	2,715	1,777
40	3912	2442	4352	1525	4489	1881	2,564	1,785
	3890	2454	4352	1487	4495	1866	2,722	1,778
60	3911	2438	4350	1523	4487	1878	2,563	1,793
	3887	2453	4350	1485	4494	1865	2,728	1,778
80	3908	2433	4346	1518	4482	1873	2,567	1,802
	3884	2449	4346	1483	4489	1862	2,727	1,782
100	3905	2427	4341	1514	4477	1868	2,571	1,811
	3880	2445	4341	1478	4485	1857	2,736	1,787
120	3903	2419	4337	1509	4473	1862	2,571	1,825
	3879	2436	4337	1473	4480	1851	2,734	1,804
140	3899	2412	4331	1504	4465	1857	2,572	1,835
	3875	2429	4331	1468	4472	1845	2,736	1,814
160	3894	2406	4325	1499	4459	1852	2,576	1,842
	3872	2420	4325	1463	4466	1838	2,734	1,829
180	3888	2400	4318	1494	4452	1846	2,580	1,849
	3866	2412	4318	1456	4459	1831	2,746	1,840
200	3886	2393	4313	1489	4447	1841	2,581	1,862
	3862	2406	4313	1451	4454	1826	2,752	1,849
220	3884	2385	4309	1485	4442	1835	2,581	1,877
	3861	2399	4309	1446	4449	1820	2,754	1,864
240	3880	2379	4305	1480	4437	1829	2,586	1,886
	3858	2391	4305	1441	4443	1814	2,756	1,877
260	3878	2372	4300	1475	4431	1824	2,586	1,900
	3857	2384	4300	1438	4438	1809	2,747	1,889
280	3876	2364	4296	1470	4427	1818	2,587	1,915
	3855	2376	4296	1433	4433	1803	2,749	1,904
300	3872	2360	4292	1465	4423	1813	2,595	1,922
	3852	2370	4292	1428	4429	1798	2,755	1,915

Note: 1. $\upsilon_{t1[110]} = \upsilon_{t[100]}$
2. upper value – ordered form, lower value – disordered form

Table 1: Longitudinal waves velocities (υ, m/s), elastic anisotropy factor and Cauchy correlation of Cu_3Au alloy

– the elastic anisotropy factor values in both phases and their increase (growth) with the rise of temperature point at the high-degree elastic anisotropy in the alloy;

– the Cauchy correlation between 0–300 K grows by 8% which means great deviations from the central forces model;

– the acoustic parameters of order and disorder alloys are changed simultaneously (synchronously) in the whole temperature range.

Figure 1 shows diagrams $E = f(T)$, $G = f(T)$, $B = f(T)$. The elastic modules of anisotropic Cu_3Au decrease with the temperature growth, Young's modulus having the maximum change, shear modulus – the minimum.

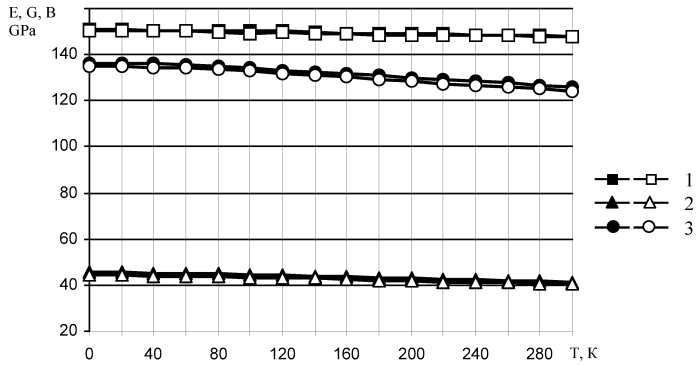

Figure 1: Temperature dependence of elastic modules of Cu_3Au alloy: 1 – Young's modulus, 2 – shear modulus, 3 – adiabatic modulus

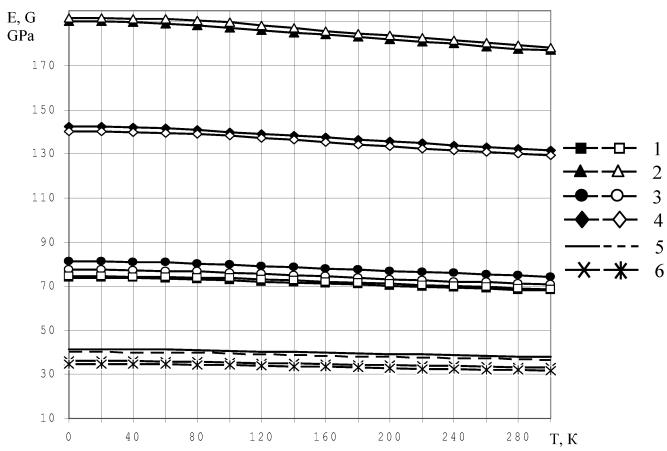

Figure 2: Temperature dependence of Cu_3Au elastic modules in various crystallographic directions: 1 – $G_{\langle 100\rangle}$, 2 – $E_{\langle 111\rangle}$, 3 – $E_{\langle 100\rangle}$, 4 – $E_{\langle 110\rangle}$, 5 – $G_{\langle 110\rangle}$, 6 – $G_{\langle 111\rangle}$

The elastic properties anisotropy influences the Young's modulus and shear modulus correlation in various crystallographic directions (Figure 2). The elastic modules

correlations of Cu_3Au alloy are similar to those of lithium halogenides at $A > 1$: $E_{langle111\rangle} > E_{\langle110\rangle} > E_{\langle100\rangle}$ and $G_{\langle100\rangle} > G_{\langle110\rangle} > G_{\langle111\rangle}$.

The temperature changes of the Poisson's ratio in the Cu_3Au alloy along various crystallographic directions are shown in Figure 3. The correlation $\sigma_{\langle110,001\rangle} > \sigma_{\langle100\rangle} > \sigma_{\langle111\rangle} > \sigma_{\langle110,1\bar{1}0\rangle}$ is true within the temperature range of 4.2–300 K. Negative values of Poisson's ratio in $\langle110, 1\bar{1}0\rangle$ direction are possible if the material is extending in the given direction. These abnormal strain properties are characteristic of a new class of materials – "aucsetics", being very perspective for practical application [5].

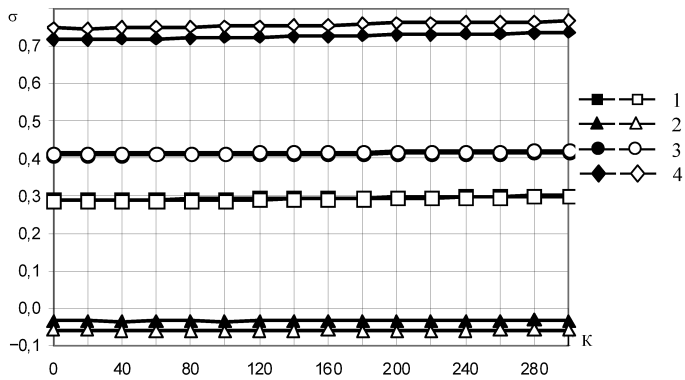

Figure 3: Poisson's ratios temperature dependence in Cu_3Au alloy in various crystallographic directions: 1 – $\langle111\rangle$, 2 – $\langle110, 1\bar{1}0\rangle$, 3 – $\langle100\rangle$, 4 – $\langle110, 001\rangle$

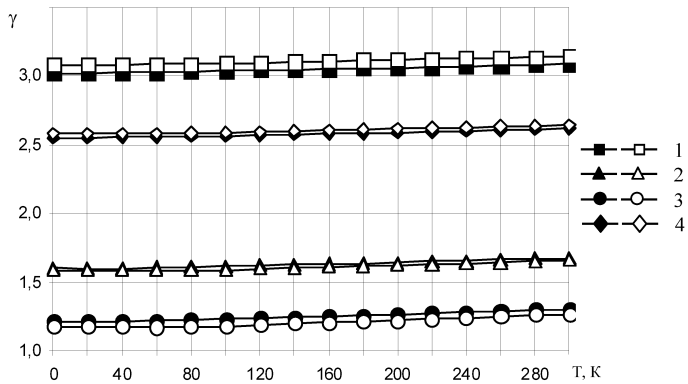

Figure 4: Grüneisen parameter anisotropy of Cu_3Au alloy: 1 – $\gamma_{2[110]}$, 2 – $\gamma_{1[110]}$, 3 – $\gamma_{[100]}$, 4 – $\gamma_{[111]}$

Acknowledgements
This work was supported by RFBR grant No 13-08-98014 r_sibir_a to conduct fundamental research.

References

[1] Belomestnykh V N, Tesleva E P 2009 *Anharmonic effects in solid bodies (acoustic aspects)* Tomsk (in Russian)
[2] Flinn P A, McManus G M, Rayne J A 1960 *J. Phys. Chem. Solids.* **15** 189
[3] Leibfried G, Ludvig V 1963 *Theory of anharmonic effects in crystals* Foreign literature, Moscow
[4] Belomestnykh V N 2004 *Technical Physics Letters* **30** (3) 14 (in Russian)
[5] Konek D A, Voitsekhovsky K B, Pleskachevsky Y M, Shilko S V 2004 *Mechanics of composite materials and constructions* **10** (1) 35 (in Russian)
[6] Belomestnykh V N, Tesleva E P 2009 *Works of VI International scientific conference-school "Fundamental and applied science of materials"* (in Russian)

Nanomechanical properties of metallic *fcc* nanorods from molecular simulations with the Sutton-Chen force field

M. Białoskórski[1,2], J. Rybicki[1,2,3]

[1] *Department of Solid State Physics, Faculty of Applied Physics and Mathematics*
Gdansk University of Technology
G. Narutowicza 11/12, 80-233 Gdansk, Poland

[2] *TASK Computer Centre, Gdansk University of Technology*
G. Narutowicza 11/12, 80-233 Gdansk, Poland

[3] *Institute of Mechatronics, Nanotechnology and Vacuum Techniques*
Koszalin University of Technology
Sniadeckich 2, 75-453 Koszalin, Poland

Basic elastic constants (Young's modulus, Poisson's ratio, shear modulus) were determined for several monocrystalline, metallic (Ni, Cu, Pt, Au) nanorods using molecular dynamics with the Sutton-Chen force field. Stress-strain curves were also calculated and discussed.

Acknowledgements
This work was supported by grants N519 024 32/3053 and N519 577 838 of the Polish Ministry of Science and Education. The calculations were performed at the TASK Computer Centre (Gdansk, Poland).

Triple-bonds functionalizing CVD-produced parylene layers

M. Bobrowski[1,2]

[1] *Department of Solid State Physics, Gdansk University of Technology*
G. Narutowicza 11/12, 80-233 Gdansk, Poland
[2] *TASK Computer Center, Gdansk University of Technology*
G. Narutowicza 11/12, 80-233 Gdansk, Poland

Chemical vapor deposition (CVD) of [2,2]paracyclophanes leading to parylene polymers requires neither catalysts nor solvents to result in inherently clean products. The obtained polymer layers are extremely adjusted, tailored and tight and possess desirable mechanical and optical characteristics which make them promising in electronics, medicine and optics. Parylene CVD can be used with liquid substrates which significantly extends the area of possible applications (especially due to the stability of the final product).

Recently it has been demonstrated that the CVD of parylene C (poly[2-chloroxylylene]) over a series of unsaturated fluorenes as well as over acrylates evokes chemical binding between the polymer and fluorenes and between the parylene and the acrylates, respectively, as is explicitly proven by the FT-IR and FT-Raman spectra. In both cases the substrates were liquids containing reactants while the parylene was deposited over the liquids. These observations were followed by theoretical studies revealing that the reactions likely involved double CC bonds (in fluorenes and acrylates) and parylene radical chains, and possible mechanisms were proposed. An important conclusion was formulated on the basis of those experimental and theoretical considerations performed over a relatively short time period; namely, it became apparent that various novel functional parylene thin layers might be easily produced and applied (e.g., to sophisticated materials in many types of devices) using practically the same or slightly modified facile technological process.

In the present work we discuss triple-bond molecules based parylenes functionalization. The simplest model - acetylene - as well as other reactants were picked up for quantum chemical as well as kinetic studies. We applied standard methods based on the statistical Markov laws analysis to achieve information on sequence distributions in the terminal model. The results revealed high reactivity of triple bonds, in comparison to vinyl moieties. The first-order structure of the resulting copolymers was achieved and analyzed.

Acknowledgements
The investigations were supported by Grant No. 6416/B/T02/2011/40 funded by the National Science Center in Poland. Calculations were carried out on the supercomputers of the Computer Center of the Metropolitan Academic Network (CC MAN) at the Gdansk University of Technology in Poland.

Cement mortars modified with magnetite before and after magnetization

J. Borucka-Lipska[1], N. Guskos[2,3], G. Zolnierkiewicz[3], J. Typek[3], A. Guskos[3], W. Kiernożycki[1]

[1] *Department of Concrete Constructions and Technology of Concrete Civil Engineering and Architecture Faculty, West Pomeranian University of Technology Al. Piastow 50, 70-311 Szczecin, Poland*

[2] *Department of Solid State Physics, Faculty of Physics, University of Athens Panepistimiopolis, 15 784 Zografou, Athens, Greece*

[3] *Institute of Physics, West Pomeranian University of Technology Al. Piastow 48, 70-311 Szczecin, Poland*

The research program included the design of cement mortars modified with magnetite. The number of basic components was based on the normalized ratio of cement mortar, where the ratio of individual components, such as cement, aggregates, water was 1:3:0.5. The ZP I mortar was modified by adding magnetite in an amount of 20% of cement by weight, and the ZP II mortar was modified by replacing 20% of cement by magnetite. Both the mortars were made of Portland cement-based CEM I 42.5 R and natural aggregate, fraction 0–2 mm. The detailed composition of mortars is shown in Table 1.

The compressive strength test was performed on the bar dimensions of $40 \times 40 \times 160$ mm. The samples were disbanded after 24 hours and stored at 20°C and at the humidity of 98%. After 28 days of ripening, half-made mortar samples ZP I and ZP II were magnetized, then all the samples were tested in a destructive testing machine. The applied external magnetic field was used up to 1 T. The results obtained are shown in Table 2.

The obtained results showed a decrease in the compressive strength of mortar ZP II of about 12.12 MPa with the increasing concentration of magnetite. An increase in the compressive strength was observed in mortars subjected to magnetization: in ZP I and ZP II by 8.14% and 8.52%, respectively (Table 2). Magnetite in cement mortar does not participate in the binding process, while the magnetization of mortars modified with an addition has an effect on the increase in the compressive strength.

Figure 1 presents the FMR spectra of sample ZP II before magnetization at room temperature (RT). Similar spectra were recorded for sample ZP I. The FMR spectra could be well fitted by two Lorentzian lines with the following parameters: $H_r(1) = 1480(50)$ G, $\Delta H_{pp}(1) = 1410(50)$ G, $A_{pp}(1) = 21600(200)$; $H_r(2) = 3093(4)$ G, $\Delta H_{pp}(2) = 780(7)$ G, $A_{pp}(2) = 65800(500)$ for sample ZP I and $H_r(1) = 1560(50)$ G, $\Delta H_{pp}(1) = 1360(50)$ G, $A_{pp}(1) = 22600(300)$; $H_r(2) = 3076(4)$ G, $\Delta H_{pp}(2) = 731(7)$ G, $A_{pp}(2) = 66500(500)$ for sample ZP II. The FMR parameters show small differences between samples ZP I and ZP II. These have some essential influence on the mechanical properties of sample ZP I and ZP II before magnetization but the increase

Composition of ZP I						
	Units	Sand	Cement	Water	Magnetite	W/C
m	g	1350.00	450	225	90	0.5
ρ	g/cm^3	2.65	3.10	1.00	4.21	
V	cm^3	509.43	145.16	225	21.38	
Composition of ZP II						
	Units	Sand	Cement	Water	Magnetite	W/C
m	g	1350.00	360	225	90	0.63
ρ	g/cm^3	2.65	3.10	1.00	4.21	
V	cm^3	509.43	116.13	225	21.38	

Table 1: Composition of mortars modified with magnetite

Composition	Value of destructive force F_c [kN]	Compressive strength f_c [MPa]	Average compressive strength f_{cm} [MPa]
ZP I Untreated	86	53.75	49.90
	87	54.38	
	82	51.25	
	78	48.75	
	71	44.38	
	75	46.88	
ZP I After magnetization	89	55.63	53.96
	84	52.50	
	85	53.13	
	87	54.38	
	84	52.50	
	89	55.63	
ZP II Untreated	61.78	38.61	37.78
	61.19	38.24	
	59.18	36.99	
	54.64	34.15	
	62.77	39.23	
	63.09	39.43	
ZP II After magnetization	64.82	40.51	41.00
	62.42	39.01	
	68.88	43.05	
	66.09	41.31	
	65.65	41.03	
	65.71	41.07	

Table 2: Results of compressive strength

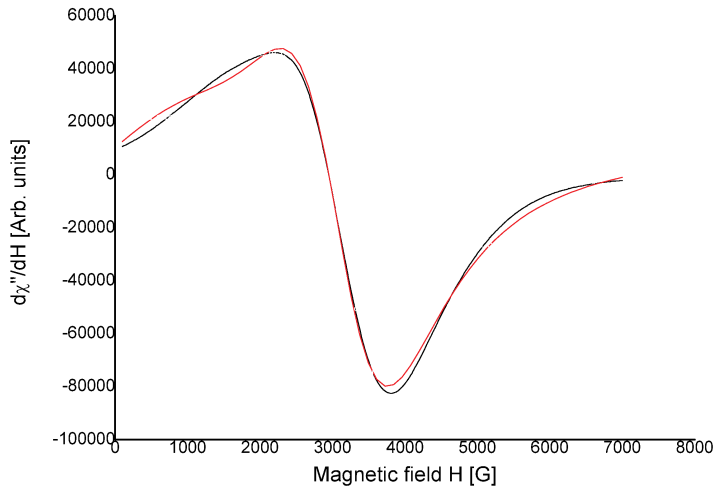

Figure 1: Experimental (black) and fitted (red) FMR spectra of sample ZP II before magnetization at RT

in compressive strength due to magnetization is almost the same in both cases. After magnetization only slight differences in the above magnetic parameters were observed.

Magnetic properties of few-layer graphene

P. Bougiatioti[1], S. Glenis[1], V. Likodimos[1,2], N. Guskos[1,3]

[1] *Department of Solid State Physics, University of Athens Panepistimiopolis, 15 784 Zografou, Athens, Greece*

[2] *Institute of Advanced Materials, Physicochemical Processes, Nanotechnology and Microsystems, NCSR "Demokritos" Aghia Paraskevi Attikis, 15 341 Athens, Greece*

[3] *Institute of Physics, West Pomeranian University of Technology Al. Piastow 17, 70-310 Szczecin, Poland*

Graphene is the basic two-dimensional structural unit of graphite. Due to its unique electrical, thermal, optical and mechanical properties graphene attracts particular interest from both the fundamental and applied research perspective. The aim of this work is to study the structural and magnetic properties of few-layer graphene. Raman spectroscopy was applied on different graphene specimens to identify the number of layers and the defect density. Static magnetic measurements were subsequently employed in order to investigate the diamagnetic character and the paramagnetic contributions in the magnetization of few-layer graphene powder specimens (4–5 layers). According to our results, neither ferromagnetism nor strong paramagnetism could be resolved at any temperature. Rather, the few-layer graphene is found to be strongly diamagnetic, similar to 3D-graphite, exhibiting a weak paramagnetic contribution below 60 K. The underlying paramagnetism is attributed to the presence of localized moments at defects of graphene layers.

Solvent effects on the Young's moduli and other properties of polyurehtane foam

J.-P. Brincat[1], A. Buttigieg[1], R. Gatt[1], J. N. Grima[1,2]

[1] *Metamaterials Unit, Faculty of Science, University of Malta Msida MSD 2080, Malta*

[2] *Department of Chemistry, Faculty of Science, University of Malta Msida MSD 2080, Malta*

Auxetics are counterintuitive materials which become fatter rather than thinner when uniaxially stretched. Polyurethane foams can be made to exhibit such a property via two different processes, based on a thermo-mechanical or a chemo-mechanical method. This study attempts to investigate the chemo-mechanical effects of solvents on conventional polyurethane foam. It will be shown that different solvent will effect the Young's moduli of the foam to different degrees, giving an indication of the solvents which may be best suited for the conversion of conventional foams to auxetic foams.

Acknowledgements
This research work is partly funded by the University of Malta, and the Malta Council for Science and Technology. The authors would also like to thank Methode Electronics Malta Ltd.

Synthesis and characterization of poly(butylene terephthalate) nanocomposites reinforced with oxidized carbon nanofibers

W. Brostow[1], G. Broza[1], E. Piesowicz[2], M. Nachman[2], S. Paszkiewicz[2], Z. Rosłaniec[2]

[1] *Department of Material Science and Engineering, University of North Texas Denton, USA*

[2] *Institute of Materials Science and Engineering, Westpomeranian University of Technology Al. Piastow 19, 70-310 Szczecin, Poland*

Carbon nanofibers (CNFs) with a diameter between 200 and 350 nm, used as filler in thermoplastic composites, have the potential to both reinforce the polymer and reduce the electrical resistivity. We obtained poly(butylene terephthalate) (PBT) as matrix + CNFs nanocomposites by introducing CNFs into a 1,4-butanodiol during the synthesis of PBT. The polymers with carbon nanofibers and plasma oxidized CNFs were synthesized using an in situ polycondensation reaction process. After polycondensation the nanocomposites were extruded and then injection molded. The addition of only a small amount of CNFs to the matrix is sufficient to improve the dynamical mechanical (DMA) properties [1–3].

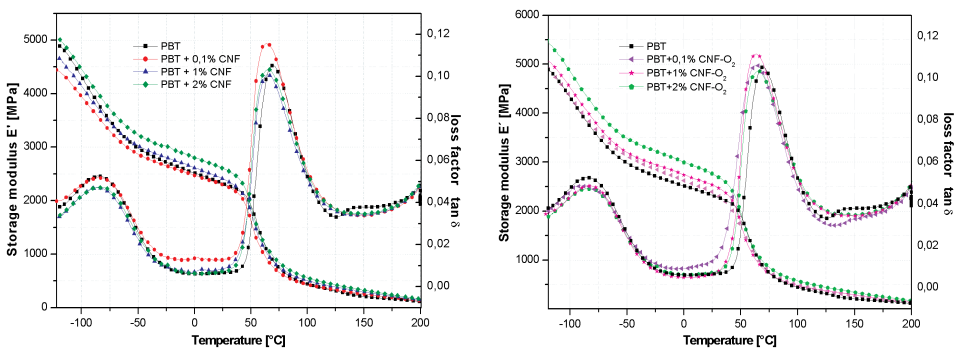

Figure 1: Storage modulus E', loss modulus E'' and $\tan\delta$ as a function of temperature for PBT nanocomposites

An increase in the crystallization temperature was observed. It can be explained by induced nucleation by the CNFs. The degree of crystallinity X_c for all composites is higher in comparison to the pure PBT. Table 1 shows the differences in the melting and in crystallization temperatures.

Sample	T_{m1} [°C]	T_c [°C]	T_{m2} [°C]	D_{Hm} (mJ/mg)	X_c (%)
PBT	226.8	186.8	226.1	49.42	35.3
PBT + 0.1% CNF	223.0	195.0	221.9	58.01	41.4
PBT + 1.0% CNF	109.9	24.4	222.2	53.12	37.9
PBT + 2% CNF	223.6	198.6	222.5	53.04	37.9
PBT + 0.1% oxid. CNF	224.0	195.7	222.5	52.42	37.4
PBT + 1% oxid. CNF	224.1	195.3	222.6	47.27	33.8
PBT + 2% oxid. CNF	224.4	198.1	222.7	52.02	37.2

Table 1: Thermal properties of the prepared PBT nanocomposites

References

[1] Z. Rosłaniec 2005 *Handbook of Condensation Elastomers*, Wiley-VCH Weinheim, Chapter 3, 77–116

[2] R. K. Adams, G. K. Hoeschele, W. K. Witsiepe 2004 *Thermoplastic Elastomers* (Ed. G. Holden, H. R. Kricheldorf, R. P. Quirk), 3rd Edition, Hanser, Chapter 8, 183–216

[3] N. Guskos, M. Maryniak, J. Typek, P. Podsiadły, U. Narkiewicz, E. Senderek, Z. Rosłaniec 2009 *Journal of Non-Crystalline Solids* **355**

An investigation on stent geometries

A. Casha[1,2], R. Gatt[1], K. Dudek[1], W. Wolak[1], L. Mizzi[1], D. Attard[1], H. Vella[3], K. Busuttil[4], J. N. Grima[1,5]

[1] *Metamaterials Unit, Faculty of Science, University of Malta*
Msida MSD 2080, Malta

[2] *Faculty of Medicine and Surgery, University of Malta*
Msida MSD 2080, Malta

[3] *Halmann Vella Limited, The Factory*
Mosta Road, Lija, LJA 9016 Malta

[4] *Tek Mould Precision Engineering Limited*
B12A, Qasam Industriali, Bulebel, Zejtun, ZTN 3000

[5] *Department of Chemistry, Faculty of Science, University of Malta*
Msida MSD 2080, Malta

It is now known that auxetic and related systems may have an important role in the biomedical industry, such as in the production of stents with superior qualities. This paper looks at some modelling work we performed on biomedical devices based on auxetic and related systems. In particular the use of auxetic and related systems in the design of stents is discussed.

Acknowledgements
The support of the University of Malta, the Malta Council for Science and Technology and the Commerce Division (Malta) is gratefully acknowledged.

On the negative properties of the AlPOs APC and APD: a molecular modelling study

R. Cauchi[1], M. Zammit[1], D. Attard[1], R. Gatt[1], J. Rybicki[3,4], Sz. Winczewski[3,4], J. N. Grima[1,2]

[1] *Department of Chemistry, Faculty of Science, University of Malta Msida MSD 2080, Malta*

[2] *Metamaterials Unit, Faculty of Science, University of Malta Msida MSD 2080, Malta*

[3] *TASK Computer Centre G. Narutowicza 11/12, 80-233 Gdansk, Poland*

[4] *Department of Solid State Physics Faculty of Technical Physics and Applied Mathematics, Gdansk University of Technology G. Narutowicza 11/12, 80-233 Gdansk, Poland*

The Poisson's ratios, isothermal compressibilities and thermal expansion coefficients of common materials normally have positive values but, in some unusual cases, they may also have negative values. A number of studies performed on zeolite systems have shown that these frameworks have the potential to exhibit such anomalous thermo-mechanical properties. This work shall present an investigation on the potential that particular aluminophosphates (AlPOs) may have in exhibiting such counterintuitive properties through the study of the related APC and APD frameworks. In particular it will be shown that these frameworks have the potential to exhibit negative thermo-mechanical properties, and that topotactical transformation of the frameworks have an effect on the properties such systems exhibit. Moreover it will be shown that a system may indeed exhibit a combination of more than one negative thermo-mechanical property as shall be exemplified via the molecular dynamics simulations work on the APC framework.

Acknowledgements
This research is funded by a grant awarded to Reuben Cauchi through the Strategic Educational Pathways Scholarship (Malta). These scholarships are part-financed by the European Union – European Social Fund (ESF) under Operational Programme II – Cohesion Policy 2007–2013, "Empowering People for More Jobs and a Better Quality of Life" and a grant from Malta Council for Science & Technology.
Parts of the calculations were performed at the TASK Academic Computer Centre in Gdansk, Poland. While some of the research has been carried out using computational facilities procured through the European Regional Development Fund, Project ERDF-080 'A Supercomputing Laboratory for the University of Malta' (http://www.um.edu.mt/research/scienceeng/erdf_080).

Defect engineering strategies in Si, $Si_{1-x}Ge_x$ and Ge

A. Chroneos[1,2], C. A. Londos[3], E. N. Sgourou[3]

[1] *Materials Engineering, The Open University Milton Keynes MK7 6AA, United Kingdom*

[2] *Department of Materials, Imperial College London SW7 2AZ, United Kingdom*

[3] *University of Athens, Solid State Physics Section Panepistimiopolis, 15 784 Zografou, Athens, Greece*

Semiconductor materials such as silicon (Si), silicon germanium ($Si_{1-x}Ge_x$) alloys and germanium (Ge) are very important for nanoelectronics and/or photovoltaic applications. This is driven by their advantageous materials properties, however, their defect processes (e.g. diffusion) need to be controlled to optimize their application in devices. In the present contribution developments in the study of impurities including dopant-defect interactions, diffusion and point defect engineering are discussed. In particular we investigate the association of lattice vacancies and oxygen interstitials (known as A-centers) in both Si and $Si_{1-x}Ge_x$ alloys, and vacancies with donor (E-centers) atoms in Ge. Both A- and E-centers can become populous and have to be controlled especially under irradiation conditions. The results are discussed in view of recent theoretical and experimental studies aiming to constrain A- and E-centers through the use of defect engineering strategies such as isovalent doping.

Nanomaterials in environment

M. Cieszyńska[1], K. Sosnowiec[1], G. Gałęzowska[1], L. Wolska[1,2]

[1] *Department of Environmental Toxicology, Faculty of Health Sciences with Subfaculty of Nursing and Institute of Maritime and Tropical Medicine Medical University of Gdansk Powstania Styczniowego 9b, 81-519 Gdynia, Poland*

[2] *Faculty of Chemistry, Gdansk University of Technology G. Narutowicza 11/12, 80-233 Gdansk, Poland*

In recent years, growing application and production of materials containing nanoparticles have been observed in various areas of life, particularly in many industry sectors. In consequence, increasingly frequent, uncontrolled emission of nanoparticles to various elements of the environment: surface water, soil, bottom deposits and sludge sediments should be considered. Nanomaterials belonging to the so called newly emerging compounds comprise a variety of particles the impact of which on aquatic and terrestrial organisms has not been fully identified, hence, they may pose a potential threat to living organisms from different trophic levels and inhabiting different ecosystems. Nowadays, the toxicity of nanomaterials is still a problem in the common use of many technologies and applications of nanoproducts. This in particular concerns the bioavailability of nanoparticles and the mechanisms of their transmission in the trophic chain.

The results of studies of toxicity of nanoparticles, particularly those containing titanium, zinc, silver, cerium and fullerenes (C_{60}) will be discussed in the presentation.

Use of different materials and magnetron sputtering process in sample preparation for scanning electron microscopy

S. Czernik[1], D. Plewik[1], J. M. Olchowik[2]

[1] *Centre for Research on Innovation*
Pope John Paul II State School of Higher Education in Biala Podlaska
Sidorska 105, 21-500 Biala Podlaska, Poland

[2] *Institute of Renewable Energy Engineering, Lublin University of Technology*
Nadbystrzycka 40B, 20-618 Lublin, Poland

Scanning electron microscopy requires that the sample should conduct electricity or be covered with a conductive layer. The most common metal used for covering samples is gold, due to its good conductive and chemical properties. Although gold is normally used for covering samples, it is also very expensive, therefore, we began to try other metals. We used a magnetron sputtering process to cover our samples in the LINE 440 sputtering machine (Alliance Concept) and Hitachi TM3000 Table top SEM. The samples were covered with copper, copper-gallium alloy, tin and tin oxide. The resulting image quality was comparable with samples covered with gold found in the literature.

Magnetic properties of double-wall carbon nanotubes

A. Diamantopoulou[1], S. Glenis[1], V. Likodimos[1,2], N. Guskos[1,3]

[1] *Department of Solid State Physics, University of Athens Panepistimiopolis, 15 784 Zografou, Athens, Greece*

[2] *Institute of Advanced Materials, Physicochemical Processes Nanotechnology and Microsystems, NCSR "Demokritos" Aghia Paraskevi Attikis, 15 341 Athens, Greece*

[3] *Institute of Physics, West Pomeranian University of Technology Al. Piastow 17, 70-310 Szczecin, Poland*

Electron spin resonance (ESR) spectroscopy was applied to probe the magnetic properties of double-wall carbon nanotubes (DWNTs). ESR measurements revealed a narrow resonance line of low intensity in the $g = 2.0$ region for DWNTs, superimposed on the broad ferromagnetic resonance signal of the catalyst particles. This ESR line was analyzed by the superimposition of a narrow and broad resonance signal attributed to defect spins located on the inner and outer shells of the DWNTs. The corresponding spin susceptibility (χ_s) increased rapidly for temperatures up to 10 K for both the inner and outer tube ESR lines, revealing the presence of ferromagnetic behavior at low temperatures. The Curie-Weiss temperatures determined from the temperature dependence of the inverse spin susceptibility (χ_s) were ca. 8 and 12 K for the inner and outer DWNT shells, respectively. However, a distribution of transitions temperatures was evidenced at lower temperatures with a lower bound of 3.0 K for both DWNT shells. The observed behavior was related to the weakly varying ferromagnetic interactions between defect spins on the inner and outer DWNT shells and possibly their exchange interactions with conduction electrons.

Hybrid quantum-classical approach for dynamical simulations of metallic systems

J. Dziedzic[1,2,3], J. Rybicki[1,2]

[1] *Faculty of Technical Physics and Applied Mathematics*
Gdansk University of Technology
G. Narutowicza 11/12, 80-233 Gdansk, Poland

[2] *TASK Computer Centre, Gdansk University of Technology*
G. Narutowicza 11/12, 80-233 Gdansk, Poland

[3] *[also at] School of Chemistry, University of Southampton*
Highfield, SO17 1BJ, United Kingdom

The increasing technological significance of nanoscale systems is the driving force for their study. High costs and difficulties of experimental analysis lead to the use of computer simulation at the atomistic level for the investigation of the properties and behaviour of such systems. Simulations of this kind traditionally fall into one of two categories – classical (e.g. molecular dynamics, MD) or quantum-mechanical (QM, *ab initio*). The conceptual simplicity of the MD approach allows treating larger systems, but simple empirical interatomic potentials usually cannot capture all the relevant effects. *Ab initio* methods are of use only in the smallest systems, up to a thousand of atoms, because of their high computational effort. Multiscale approaches, which combine the two methodologies are a new addition to the toolbox of the computational material scientist [1].

We present a multiscale method targeted at atomistic simulations (including non-equilibrium) of metals in which selected regions are modelled using a quantum-mechanical approach (tight-binding, TB [2,3] or density functional theory, DFT), while the rest of the system is treated with molecular-dynamics employing (in this case) the Sutton-Chen [4] many-body interaction potential. The parameters of the underlying MD potential are re-parametrized locally on-the-fly by the employment of an extension to the Learn-on-the-Fly [5] technique, in order to reproduce the forces obtained by local QM calculations. The technique is parallel-ready, with both the quantum-based calculation and the force-fitting procedure scalable to several tens of processors [6].

Apart from the presentation of the method and implementation in computer code, the results of a series of validation and productions simulations will be presented, demonstrating the accuracy and practicality of the approach.

References

[1] Bernstein N, Kermode J R and Csànyi G 2009 *Rep. Prog. Phys.* **72** 026501
[2] Cohen R, Mehl M and Papaconstantopoulos D 1994 *Phys. Rev.* **B 50** 14694

[3] Mehl M, Papaconstantopoulos D, Kioussis N and Herbranson M 2000 *Phys. Rev.* **B 61** 4894
[4] Sutton A P and Chen J 1990 *Phil. Mag. Lett* **61** 139
[5] Csànyi G, Albaret T, Payne M C and De Vita A 2004 *Phys. Rev. Lett* **93** 175503
[6] Dziedzic J, Bobrowski M, Rybicki J 2011 *Phys. Rev. B* **83**

Hartree-Fock exchange with linear-scaling cost

J. Dziedzic[1,2], C.-K. Skylaris[1]

[1] *School of Chemistry, University of Southampton Highfield, SO17 1BJ, United Kingdom*

[2] *[also at] Faculty of Applied Physics and Mathematics, Gdansk University of Technology G. Narutowicza 11/12, 80-233 Gdansk, Poland*

In density functional theory (DFT), local and semilocal exchange functionals have long been known to incorrectly describe the energetics of small molecules [1], among other deficiencies. So-called hybrid functionals include a fraction of Hartree-Fock exchange (HFx) in the exchange-correlation functional, providing a more accurate description of geometries and of several properties, such as bond energies and band gaps, particularly for metal oxides [2]. Because of the non-locality, the computational effort of a straightforward implementation of HFx scales with the fourth power of the system size. A wide variety of techniques have been proposed that aim to either reduce the prefactor, or to offer better ('reduced') scaling.

We present a resolution-of-identity-based approach [3] for calculating Hartree-Fock exchange energy and hybrid exchange-correlation functionals with a computational cost that scales linearly with the number of atoms. We describe how the necessary approximations are well-controlled, and discuss the conditions that need to be satisfied for the proposed technique to be numerically stable and accurate. We briefly describe the implementation of this approach in the linear-scaling DFT code ONETEP [4], which can perform DFT calculations with near-complete basis set accuracy.

We validate the proposed approach against energies, forces and equilibrium bond-lengths [2,5], computed with conventional, cubic-scaling DFT codes, demonstrating excellent agreement, even with approaches using an all-electron description and Gaussian basis sets. We show qualitative agreement between B3LYP calculations performed with our technique and the predictions [6] of DFT+U for the binding of O_2 and CO to a simplified model of myoglobin. We also present benchmarks for larger systems, demonstrating that the computational effort of the proposed approach indeed scales linearly with size of the system.

References

[1] M. Marsman, J. Paier, A. Stroppa and G. Kresse, *J. Phys. Cond. Matt.* **20**, 064201 (2008)
[2] V. N. Staroverov, G. E. Scuseria, J. Tao and J. P. Perdew, *J. Chem. Phys.* **23**, 12129 (2003)
[3] J. Dziedzic, Q. Hill and C-K. Skylairs, *J. Chem. Phys* (submitted)
[4] C.-K. Skylaris, P. D. Haynes, A. A. Mostofi and M. C. Payne, *J. Chem. Phys.* **122**, 084119 (2005)
[5] N. D. M. Hine, M. Robinson, P. D. Haynes, C.-K. Skylaris, M. C. Payne and A. A. Mostofi, *Phys. Rev. B* **83**, 195102 (2011)
[6] D. J. Cole, D. D. O'Regan and M. C. Payne, *J. Phys. Chem. Lett.* **3**, 1448 (2012)

An investigation of hierarchical structures composed of rotating rigid units

R. Gatt[1], J. Azzopardi[2], K. M. Azzopardi[1], L. Mizzi[1], J. N. Grima[1,2]

[1] *Metamaterials Unit, Faculty of Science, University of Malta Msida MSD 2080, Malta*

[2] *Department of Chemistry, Faculty of Science, University of Malta Msida MSD 2080, Malta*

Over the past years, several geometry / deformation mechanism based models have been proposed to generate and/or explain auxetic behaviour. These include the re-entrant mechanism, rotating rigid units and chiral systems. This paper presents some of the recent developments made by the University of Malta group which discusses how multi-level auxetic systems may be constructed where more-than one geometry / deformation mechanisms are introduced at different levels of the structure. For example, as illustarted in Figure 1 below, one may construct a multi-level auxetic systems based on the rotating squares mechanism where the rigid square in the regular rotating squares model is replaced by a sub-set of rotating polygons, (or other units such as chiral units) which also have auxetic potential. We show how the overall properties of such systems will be dependent on how and when the different mechanisms at the different levels operate relative to each other, where different deformation mechanisms, and hence different properties, come into play at different strains.

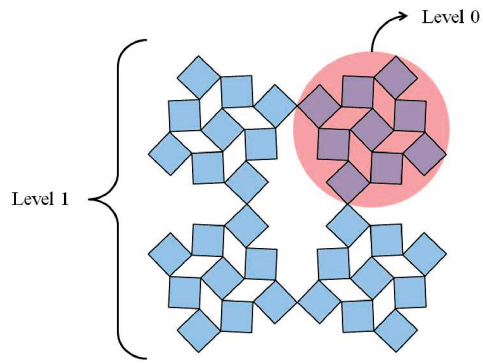

Figure 1: Multi-level auxetic system

Acknowledgements
This research work is partly funded by the University of Malta, and the Malta Council for Science and Technology.

Negative properties in ordered β-cristobalite

R. Gatt[1], D. Bugeja[2], K. M. Azzopardi[1], L. Mizzi[1], D. Gambin[1], J. N. Grima[1,2]

[1] *Metamaterials Unit, Faculty of Science, University of Malta Msida MSD 2080, Malta*

[2] *Department of Chemistry, Faculty of Science, University of Malta Msida MSD 2080, Malta*

Materials exhibiting negative properties, such as negative Poisson's ratio, that is the ability to get fatter rather than thinner when uniaxially stretched (auxetic) and negative thermal expansion, i.e. the ability to shrink when heated, have attracted a lot of interest in view of their many potential applications.

In this study, the negative Poisson's ratio and negative thermal expansion in orthorhombic β-cristobalite were investigated and it was shown that this material can exhibit both negative effects. In particular, the negative Poisson's ratio was predicted by both force-field based simulations using the CVFF force-field and the more fundamental DFT calculations, which methods were also used to confirm that this effect is manifested as a result of relative rotation of semi-rigid units which project as connected squares in the (001) plane where negative Poisson's ratio's was found. It was concluded that while the DFT shows greater on-axis auxeticity, overall the two methods produce highly comparable results and thus the CVFF force-field is appropriate for simulating the properties of this phase of cristobalite. The CVFF force-field was also used to simulate the effect of temperature on orthorhombic β-cristobalite using NPT molecular dynamics simulations where the structure was simulated over a temperature range of 530–620 K with negative thermal expansion being predicted along the [001] direction.

Auxeticity in ceramic type frameworks

R. Gatt[1], D. Gambin[1], J. N. Grima[1,2]

[1] *Metamaterials Unit, Faculty of Science, University of Malta Msida MSD 2080, Malta*

[2] *Department of Chemistry, Faculty of Science, University of Malta Msida MSD 2080, Malta*

Auxetic materials are materials which exhibit the anomalous behaviour of getting fatter rather than thinner when stretched i.e. they exhibit a negative Poisson's ratio. Several material classes have been studied for their potential to exhibit auxetic behaviour, particularly ceramic materials such as $\alpha-$cristobalite, $\beta-$cristobalite, NAT, THO and EDI.

The Poisson's ratio of six SiO_2 equivalents of the frameworks of the previously unstudied ceramics AEN, BOF, cordierite, danburite, caesium aluminium titanate and gallium phosphate will be investigated through force-field based simulations. Energy expressions for these systems were constructed using COMPASS, CVFF, BKS and Burchart force-fields. Of the six ceramic frameworks studied, three where shown to have the potential of exhibiting a negative Poisson's ratio, namely danburite, BOF and gallium phosphate. In particular it was shown that the SiO_2 equivalent framework of danburite exhibits auxetic behaviour in all the three major planes with maximum auxeticity being exhibited for loading at 45° off-axis. In the case of the SiO_2 equivalent framework of BOF maximum auxetic behaviour was exhibited in the (001) plane for loading on-axis, whilst in the case of the SiO_2 equivalent of the $GaPO_4$ framework, auxetic behaviour was exhibited in the (010) and (100) planes with its maximum value exhibited for loading at 45° off-axis. Furthermore, a study on the deformation mechanism of the SiO_2 equivalent of the $GaPO_4$ framework has shown that the auxetic behaviour can be explained via a combined tetrahedral model where rotation and deformation of the tetrahedra occur concurrently. This is very significant as it further confirms that relative rotation of semi-rigid units, in this case semi-rigid tetrahedra, is an important mechanism for the generation of auxetic behaviour.

Acknowledgements
The support of the University of Malta, is gratefully acknowledged.

Advanced functional ceramics

M. Gazda

Faculty of Applied Physics and Mathematics, Gdansk University of Technology
G. Narutowicza 11/12, 80-233 Gdansk, Poland

Ceramic materials are one of the most important materials in contemporary technology. They are used both as structural and functional materials. In the lecture functional ceramics will be briefly described. The following topics will be covered:

- Introduction: definitions of relevant terms; examples of fields in which advanced functional materials are relevant (smart structures and materials; microelectronics, electrical insulation, electromagnetic shielding, communication, stealth technology, optics, lighting, lasers, light detectors, batteries, energy harvesting, energy conversion, heating, ...).
- General description of ceramics: chemical bonds, structures and phase transitions, examples of various properties of ceramic materials.
- Methods of synthesis and shaping of ceramic materials: solid state synthesis, hydrothermal synthesis, Pechini method, etc.
- Examples of functional ceramics and nanoceramics:
  - Titanium oxide – a simple oxide with many interesting functions;
  - Perovskites – a family of complex oxides in which examples of almost all possible properties may be found (insulators, conductors and superconductors, piezo-and ferroelectrics, catalysts, ionic conductors, magnetic materials, etc.);
  - Other ceramics, e.g. spinels, fluorites etc.
- Ceramic composites and nanocomposites.
- Summary.

References

[1] M. A. Pena and J. L. G. Fierro, *Chem. Rev.* 2001, **101**, 1981–2017
[2] A. Manan, Y. Iqbal, M. ur Rahman, M. Khan *J. Pak. Mater. Soc.* 2008, **2**, 1
[3] J. Nowotny, T. Bak, M. K. Nowotny, L. R. Sheppard, *International Journal of Hydrogen Energy* 2007, **32**, 2609

Non-debye dipolar relaxation of ethylene glycol embedded in ZSM-5 zeolite host matrix – computer simulation study

K. Górny, Z. Dendzik, M. Pabiszczak, Z. Gburski

Institute of Physics, University of Silesia
Uniwersytecka 4, 40-007 Katowice, Poland

We performed fully atomistic molecular dynamics simulations of ethylene glycol confined inside a ZSM-5 zeolite in order to study the effect of the spatial confinement and interaction between the embedded molecules and internal surface of the host channels on the dynamics of the system. We found a change in the thermal activation characteristic as well as a considerable deviation of the dynamics in this system from the almost purely exponential relaxation observed in bulk ethylene glycol liquid.

Structural and dynamical properties of n-CB liquid crystal layer on graphene surface – computer simulation study

K. Górny, Z. Dendzik, B. Sawicki, Z. Gburski

Institute of Physics, University of Silesia
Uniwersytecka 4, 40-007 Katowice, Poland

An ultrathin film of mesogenic molecules 5CB and 6CB located on a graphene surface was investigated by means of the molecular dynamics (MD) technique. Graphene is only one atom thick, optically transparent, chemically inert and an excellent conductor. These properties seem to make this material an excellent candidate for applications in various photonic devices including the new generation of liquid crystal displays. We wanted to check if, and how, the peculiarities of the dynamics of molecules near graphene sheet influence the liquid crystalline properties (spatial ordering, reorientational dynamics, dipolar/dielectric relaxation) of the thin layer of mesogene molecules. The dynamical and structural observables were calculated for several temperatures: the mean square displacement, the translational and angular velocity autocorrelation function, the second-rank order parameter and total dipole moment autocorrelation function.

Negative properties from magnetic mechanical metamaterials

J. N. Grima[1,2], R. Caruana-Gauci[1], K. W. Wojciechowski[3], M. R. Dudek[4]

[1] *Metamaterials Unit, Faculty of Science, University of Malta Msida MSD 2080, Malta*

[2] *Department of Chemistry, Faculty of Science, University of Malta Msida MSD 2080, Malta*

[3] *Institute of Molecular Physics, Polish Academy of Sciences M. Smoluchowskiego 17, 60-179 Poznan, Poland*

[4] *Institute of Physics, Zielona Gora University 65-069 Zielona Gora, Poland*

During the past months, advances in the understanding of auxetic systems having magnetic insertions have been made. It was shown that these novel magnetic mechanical metamaterials exhibit highly interesting properties which may depend on the externally applied magnetic fields, such as tunable Poisson's ratios, bi-stability or multi-stability, and other electromagnetic-mechanical effects. The properties exhibited by these systems are affected by several variables such as the relative position and orientation of the magnetic insertion/s within the structure, the geometry of the system and the magnetic strength of the magnetic components, including that of the external magnetic field.

A case study of a system having one magnetic insertion in a rotating rigid unit auxetic system will be considered so as to fully comprehend the versatility of such magneto-auxetic systems. Such a system, by a careful choice of the characteristics pertaining to the system, can be fine-tuned and tailor-made for particular practical applications. Such applications vary from smart filters, to strain dependent sensors, to systems which require an instantaneous change in their macroscopic properties.

Acknowledgements
The support of the University of Malta is gratefully acknowledged.

Auxetic behaviour in graphene having random vacancy defects: a preliminary study

J. N. Grima[1,2], M. C. Grech[1], R. Cauchi[2], R. Gatt[1], D. Attard[1]

[1] *Metamaterials Unit, Faculty of Science, University of Malta Msida MSD 2080, Malta*

[2] *Department of Chemistry, Faculty of Science, University of Malta Msida MSD 2080, Malta*

In view of its many unusual and superior properties, graphene is widely considered to be one of the wonder materials of the twenty-first century. In this work, force-field based simulations were used to simulate the structural and mechanical properties of defective graphene sheets in an attempt to introduce auxeticity into these materials. The systems studied had a varying amount of randomly distributed and oriented single and double vacancies which were simulated using the COMPASS, pcff, Dreiding, cvff and Universal force-fields. These force-fields were chosen since their parameters adequately model pristine graphene and its defective equivalent ones and a validation study performed on pristine graphene suggested that all of these force-fields yield results that are in good agreement with published results obtained both via computational and experimental studies.

It was shown that the cvff, Dreiding and Universal force-fields are likely to be able to model defective graphene adequately since the simulated mechanical properties obtained using these force-fields compared extremely well with those obtained by Dettori et al. who studied defective graphene with low concentrations of defects using tight binding atomistic simulations. It was also shown that these force-fields consistently suggest that defective graphenes adopt a highly wrinkled 3-dimensional conformation and also exhibit lower Poisson's ratio than their pristine counterparts. In particular, it was shown that a high level of defects, some of the samples studied deformed in an auxetic manner when strained under tension in their zigzag direction. All this is very significant, not only since the systems studied here are the thinnest real auxetic systems discovered so far, but also since graphene is also known to exhibit some other extremely useful and superior properties, some of which may be enhanced through the auxetic effect.

Acknowledgements
This research is partially funded by a grant awarded to Reuben Cauchi through the Strategic Educational Pathways Scholarship (Malta). These scholarships are part-financed by the European Union – European Social Fund (ESF) under Operational Programme II – Cohesion Policy 2007–2013, "Empowering People for More Jobs and a Better Quality of Life". The research has been carried out using computational facilities procured through the European Regional Development Fund, Project ERDF-080 'A Supercomputing Laboratory for the University of Malta' (http://www.um.edu.mt/research/scienceeng/erdf 080).

Studying the negative thermal expansion in framework structures through a geometrical approach

J. N. Grima[1,2], S. Scerri[1], M. Bajada[1], D. Attard[2]

[1] *Department of Chemistry, Faculty of Science, University of Malta Msida MSD 2080, Malta*

[2] *Metamaterials Unit, Faculty of Science, University of Malta Msida MSD 2080, Malta*

The manner with which materials change shape and size when they are subjected to changes in temperature is described and quantified through their thermal expansion coefficients (CTEs). Although most materials expand when heated (positive CTEs), materials which shrink on heating (negative CTEs or negative thermal expansion, NTE) are not unheard of. A number of mechanisms which may lead to such behaviour have been studied, with one of the most important being that based on rigid unit modes (RUMs) where the NTE is achieved from the relative rotation of rigid units.

The work presented here is aimed at extending current models, based on 2D systems made from connected squares, to more general systems made from connected parallelograms, rectangles, rhombi and different-sized rectangles. Analytical models for the area CTEs for each of these networks were derived using an approach based on that developed by Welche, Heine and Dove (Phys. Chem. Minerals (1998), 26(1), p. 63–77), in an attempt to determine the optimal structure for maximal NTE from among those considered. These models suggest that, all the structures considered have the potential to exhibit NTE, with some of the structures exhibiting far superior NTE properties than the well-known network of squares. Furthermore, it was found that in most cases, the extent of NTE is primarily determined from the way that the

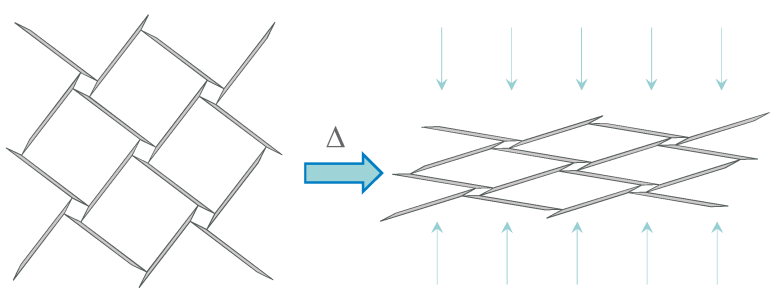

Figure 1: An example model of a NTE material

units are connected to each other and from the shape of the rigid units (side lengths ratio and/or internal angle). However, in general it was found that networks which are characterised by large pores have a better potential to exhibit large NTE. It was found that using rigid units which are more 'pencil-like', i.e. flatter and elongated, help to attain a larger pore size and thus a more negative CTE.

Acknowledgements
The support of the University of Malta is gratefully acknowledged.

Investigating the effect of extra framework species on the mechanical properties of zeolites

J. N. Grima[1,2], M. V. Wood[1]

[1] *Metamaterials Unit, Faculty of Science, University of Malta Msida MSD 2080, Malta*

[2] *Department of Chemistry, Faculty of Science, University of Malta Msida MSD 2080, Malta*

Materials with a negative Poisson's ratio, i.e. auxetic materials, exhibit the unexpected property of becoming wider when stretched and thinner when compressed [1]. This rare property, which is very much dependent on the geometry of the material, results in the enhancement of various macroscopic properties of the material and makes auxetics superior to their conventional counterparts in many practical applications [2].

It is known that some zeolite frameworks may exhibit this unusual property [3], through the rotating squares mechanism and the rotating triangles mechanism, where the corners of the squares or triangles are oxygen atoms [4].

This paper discusses a methodology for simulating zeolites with cations and water molecules is described. This methodology was applied on a number of zeolites with the scope of assessing the contribution of cations and water molecules on the mechanical properties and on the way the system responds to applied loads (i.e. the deformation mechanism). Two zeolites were studied, NAT and EDI which were found to exhibit auxetic behaviour through a rotating squares mechanism (Figure 1).

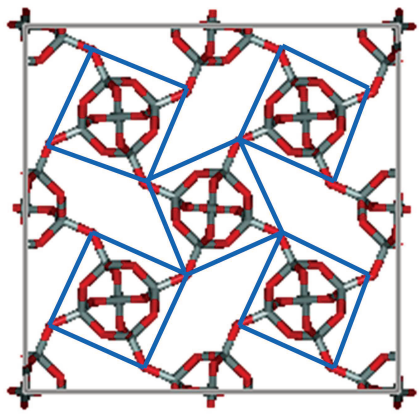

Figure 1: The rotating squares mechanism observed in the zeolite: NAT

It was also found that cations and water molecules do play an important role on the Poisson's ratios although in most cases, the auxetic behaviour is retained. While cations reduced the auxeticity of the structure by a small degree, the addition of water molecules had a greater effect rendering the structures less auxetic. This observation was explained by the fact that the structures were also observed to be stiffer with the inclusion of water and cations. Essentially the water and cations seemed to be 'in the way', preventing the 'hinging oxygen atoms' from deforming as much as was possible in response to loading.

Acknowledgements
The support of the University of Malta is gratefully acknowledged.

References

[1] K. E. Evans, M. A. Nkansah, I. J. Hutchinson and S. C. Rogers, *Nature*, **353** (1991) 124
[2] J. N. Grima, *University of Malta Annual Report* (2002)
[3] J. N. Grima, R. Jackson, A. Alderson and K. E. Evans *Adv. Mater.* **12** (2000) 1912
[4] J. N. Grima and K. E. Evans, *J.Mat.Sci.Lett.*, **19** (2000) 1563
[5] Molecular Simulations Inc. (MSI), San Diego, California, currently incorporated within Accelrys (http://www.accelrys.com)
[6] A. Alderson, J. Rasburn, K. E. Evans and J. N. Grima, *Membrane Technology*, **137** (2001) 6

Opto-electrical properties of SnO_2 layers obtained in various process conditions by Line 440 magnetron sputtering

T. Grudniewski[1], J. M. Olchowik[2]

[1] *Centre for Research on Innovation*
Pope John Paul II State School of Higher Education in Biala Podlaska
Sidorska 105, 21-500 Biala Podlaska, Poland

[2] *Institute of Renewable Energy Engineering, Lublin University of Technology*
Nadbystrzycka 40B, 20-618 Lublin, Poland

Magnetron sputtering systems are one of the most promising methods of preparation of chip layers for different applications [1,2]. While testing a line 440 alliance concept machine the authors decided to perform several tests (which led to the obtained SnO_2) with different process parameters. SnO_2 is still the most irreplaceable material (due to its transparency)for electrodes. The authors changed the gas composition, pressure, temperature and glass substrate to obtain as much information as possible about the created layers. Then, the resistance, transparence, absorbance and other measurable parameters were tested. The results of the experiments allow performing various processes according to the application requirements. Moreover, the authors prepared tests with two different layer combinations and characterized them.

References

[1] S. Takeda, S. Suzuki, H. Odaka, H. Hosono, *Thin Solid Films*, **392**, 2001
[2] K. Mech, R. Kowalik, P. Żabiński, *Archives of Metallurgy and materials*, **56**, 2011
[3] A. Chowdhuri, D. Haridas, K. Sreenivas, V. Gupta, *International Journal of Smart Sensing and Intelligent Systems*, **2**, 2009

Computer implementation of moving boundary problem in Matlab environment for modeling epitaxial growth process

S. Gulkowski, J. M. Olchowik

Faculty of Environmental Engineering, Lublin University of Technology
Nadbystrzycka 38, 20-618 Lublin, Poland

This paper presents computational implementation of the moving interface problem for the epitaxial lateral overgrowth application. Due to the possibility of producing high quality and low cost silicon substrates the ELO technology may find application in the photovoltaic industry. As the lateral growth process depends on many technological parameters such as the system temperature , cooling rate, solvent and geometry of the mask, it is difficult to find optimized settings of these factors in experimental research. Numerical analysis of the growth process leads to better understanding of the influence of the parameters on the final shape of the layer. For this reason, a computational model was proposed. The approach presented in the model is based on the assumption that growth is only diffusion controlled and the most important process which determines the velocity of the interface is the mass transport into the grown surface. Therefore, it is very important to determine the concentration gradients in the vicinity of the interface very precisely. The adaptive mesh method was used to achieve high precision of calculations. The problem under study requires also calculations of the interface position which changes in time. It means that the simulation domain changes in time, too. A special script was implemented in the Matlab environment in order to solve this problem numerically and the results were shown.

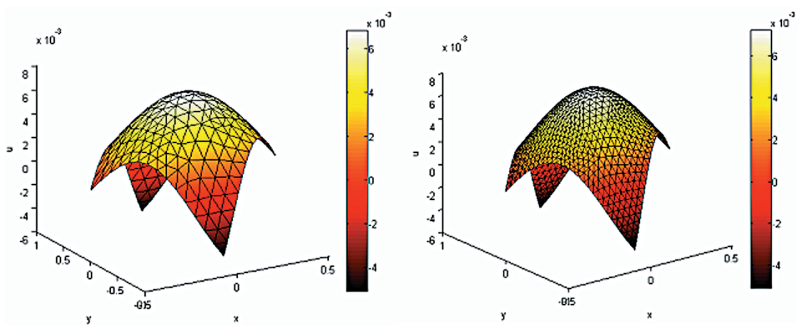

Figure 1: Comparison of calculation results for two different triangle mesh sizes

FMR and photocatalytic investigations of nNi-TiO_2 ($n = 1\%$, 5% and 10%) compounds

N. Guskos[1,2], A. Guskos[2], S. Glenis[1], G. Zolnierkiewicz[2], J. Typek[2], P. Berczynski[2], D. Dolat[3], B. Grzmil[3], B. Ohtani[4], A. W. Morawski[3]

[1] *Department of Solid State, Faculty of Physics, University of Athens Panepistimiopolis, Zografou 15 784, Greece*

[2] *Department of Physics, West Pomeranian University of Technology Al. Piastow 48, 70-311 Szczecin, Poland*

[3] *Department of Chemical and Environmental Engineering West Pomeranian University of Technology Pulawskiego 10, 70-322 Szczecin, Poland*

[4] *Catalysis Research Center, Hokkaido University Sapporo 001-0021 Japan*

Nanocomposites of nNi/N-TiO_2 ($n = 1\%$, 5% and 10%) were prepared by co-modification of a commercial amorphous titanium dioxide via impregnation with $Ni(NO_3)_3$ followed by calcination at 800°C in an ammonia atmosphere. An essential increase in the visible light photoactivity of the co-modified samples in comparison with single-modified ones was observed. Good photocatalytic properties, especially for samples with $n = 5\%$, were determined. The temperature dependence of ferromagnetic resonance/electron paramagnetic resonance (FMR/EPR) spectra was established. The FMR spectra of nickel agglomerates dominated the observed spectra in the whole region of temperatures. Additionally, the EPR spectra of free radicals and trivalent titanium ions were recorded at low temperatures. The greatest concentrations of trivalent titanium ions were observed for sample $n = 5\%$ and the lowest for sample $n = 10\%$. It is proposed that in the case of the sample with $n = 5\%$ the largest number of nickel ions is involved in processes causing the appearance of the largest numbers of trivalent titanium ions.

Magnetic properties study of $Ni_3[Fe(CN)_6]_2$ and γ-$Fe_2O_3/Ni_3[Fe(CN)_6]_2$ nanoparticles

N. Guskos[1,2], J. Typek[2], A. Guskos[2], P. Berczynski[2], D. Petridis[3]

[1] *Solid State Section, Department of Physics, University of Athens Panepistimiopolis, 15 784 Zografou, Athens, Greece*

[2] *Institute of Physics, West Pomeranian University of Technology Al. Piastow 48, 70-311 Szczecin, Poland*

[3] *Institute of Materials Science National Centre for Scientific Research "Demokritos" Aghia Paraskevi Attikis, 15 341 Athens, Greece*

Magnetic properties of two samples of $Ni_3[Fe(CN)_6]_2$ and γ-$Fe_2O_3/Ni_3[Fe(CN)_6]_2$ were investigated. 370 mg of g-Fe_2O_3/oleate was placed in 50ml of toluene and 3 drops of oleylamine were added for better dispersion of the capped magnetic oxide. 100 mg of $Ni_3[Fe(CN)_6]_2$ dispersed by sonication in 40ml of toluene containing 0.5 ml oleylamine was added to this mixture. The resulting mixture was heated up to 20 ml to remove most of the toluene and g-$Fe_2O_3/Ni_3[Fe(CN)_6]_2$ was precipitated by adding 20 ml of acetone after cooling. The solid was isolated by centrifucation, washed with water and acetone and dried at RT. A strange phenomenon for magnetization as a function of the magnetic field was obtained for the molecular sample. The hysteresis loop had an unusual shape, and negative and positive magnetic fields tended to saturate. Hysteresis was observed in the case of the samples with iron oxide at low temperature (Figure 1a). ZFC and FC modes showed the superparamagnetic state with blocking temperature $T_B = 38$ K at the applied magnetic field $H = 50$ Oe (Figure 1b).

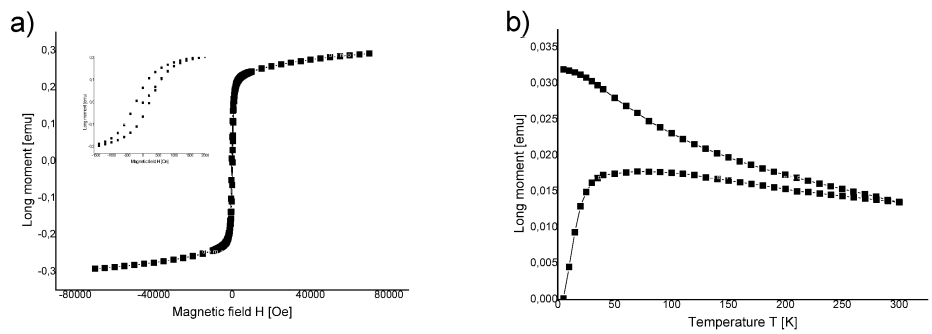

Figure 1: Temperature dependence of magnetization ZFC and FC modes at $H = 50$ Oe (a), and hysteresis loop (b) for sample γ-$Fe_2O_3/Ni_3[Fe(CN)_6]_2$

Magnetic properties of $TiO_2[(FeClN)_6]_2Fe_3$ and $TiO_2[(FeClN)_6]_2Co_3$

N. Guskos[1,2], G. Zolnierkiewicz[2], J. Typek[2], A. Guskos[2], P. Berczynski[2], D. Petridis[3]

[1] *Deparment of Solid State Physics, Faculty of Physics University of Athens Panepistimiopolis, 15 784 Zografou, Athens, Greece*

[2] *Institute of Physics, West Pomeranian University of Technology Al. Piastow 48, 70-311 Szczecin, Poland*

[3] *Institute of Materials Science, National Centre for Scientific Research "Demokritos" Aghia Paraskevi Attikis, 15 341 Athens, Greece*

The magnetic properties two nanocomposites of $TiO_2[(FeClN)_6]_2Fe_3$ (a) and $TiO_2[(FeClN)_6]_2Co_3$ (b) were investigated. The EPR spectra of trivalent iron ions in low symmetry crystalfields were recorded where for the sample with iron was one time greater (increasing concentration) (Figure 1). Hysteresis loops were observed in both samples where the loop was greater for the sample with cobalt (Figure 2). ZFC and FC modes of magnetic susceptibility showed that the sample with cobalt ions appeared to be in a superparamagnetic state with blocking temperature $T_B = 13(1)$ K. Opposite, there was no superparamagnetic state in the sample with iron. The following values of Curie temperature $T_C = 10$ K for the sample with cobalt and $T_C = 7$ K for the sample with iron were obtained at high temperature regions using reverse magnetic susceptibility for the applied magnetic field. Then, ferromagnetic interaction was observed.

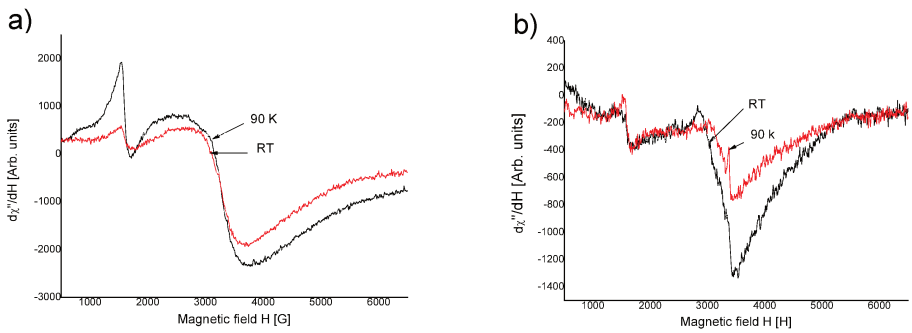

Figure 1: EPR/FMR spectra of $TiO_2[(FeClN)_6]_2Fe_3$ (a) and $TiO_2[(FeClN)_6]_2Co_3$ (b)

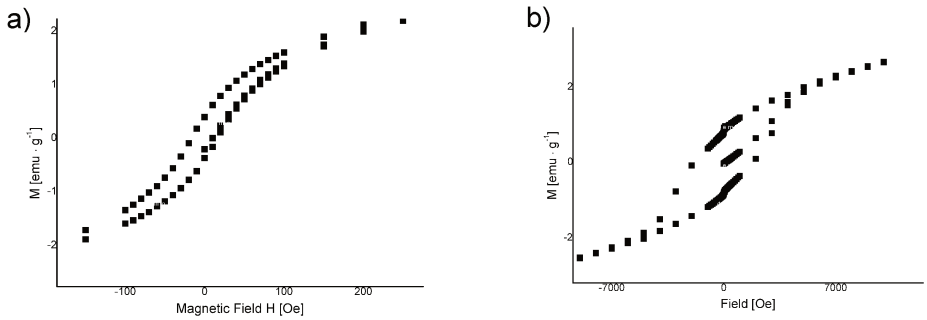

Figure 2: Magnetic field dependence of magnetization; a) $TiO_2[(FeClN)_6]_2Fe_3$ and b) $TiO_2[(FeClN)_6]_2Co_3$

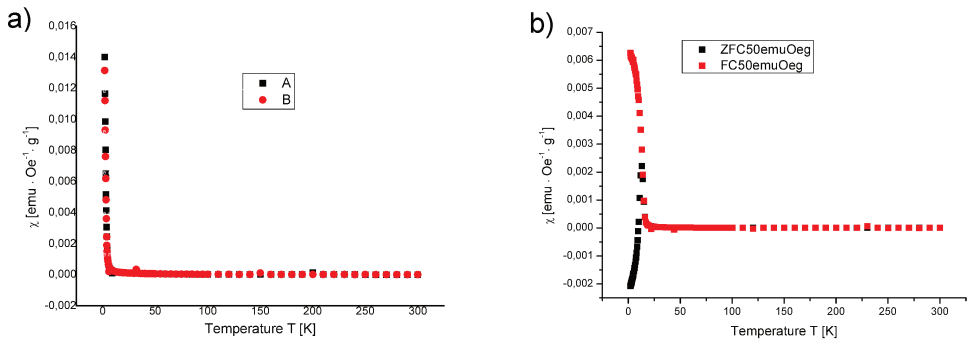

Figure 3: Temperature dependence of magnetic susceptibility at $H = 50$ Oe for ZFC and FC modes; a) $TiO_2[(FeClN)_6]_2Fe_3$ and b) $TiO_2[(FeClN)_6]_2Co_3$

FMR/EPR study of nanocrystalline $n\mathrm{MnO}/(1-n)\mathrm{ZnO}$ ($n = 0.6$, 0.7 and 0.8)

N. Guskos[1,2], G. Zolnierkiewicz[2], J. Typek[2], A. Guskos[2], K. Wardal[2], P. Berczynski[2], D. Sibera[3], U. Narkiewicz[3]

[1] *Department of Solid State Physics, Faculty of Physics, University of Athens Panepistimiopolis, 15784 Zografou, Athens, Greece*

[2] *Institute of Physics, West Pomeranian University of Technology Szczecin Al. Piastow 48, 70-311 Szczecin, Poland*

[3] *Institute of Chemical and Environmental Engineering West Pomeranian University of Technology Pulaskiego 10, 70-322 Szczecin, Poland*

Transition metal doped ZnO has received much attention in recent years due to its interesting and technologically useful properties. Its magnetic properties are widely studied, but reports claiming conflicting properties: intrinsic ferromagnetism, paramagnetism, extrinsic ferromagnetism, spin-glass behavior are found in the literature. Nanocrystalline $n\mathrm{MnO}/(1-n)\mathrm{ZnO}$ (for $n = 0.6$, 0.7 and 0.8) samples were prepared by the coprecipitation-calcination method. X-ray diffraction showed the presence of spinel, manganese oxide and zinc oxide phases in the system. Two phases: ZnO and $ZnMnO_3$ are observed in samples with a low nominal content of MnO. With increasing MnO concentration, the ZnO phase content decreases and the peak attributed to this phase disappears in the sample with $n = 0.6$. The peak of ZnO disappears because all the zinc is bonded in the spinel phase. In sample $n = 0.6$ and more, the phases $ZnMn_2O_4$ and Mn_3O_4 are found [1]. In particular, the mean crystallite size of Mn_3O_4 determined from Scherrer's formula was 24 nm, 37 nm, 45 nm for $n = 0.6$, 0.7, 0.8, respectively.

The magnetic properties of the $n\mathrm{MnO}/(1-n)\mathrm{ZnO}$ samples were investigated by the electron paramagnetic resonance (EPR) / ferromagnetic resonance (FMR)) methods. An EPR signal from the paramagnetic phase of Mn_3O_4 was observed at temperatures above 45 K and from defects/spurious phases in the low temperature range (Figure 1–3). As the index n increases the concentration of the Mn_3O_4 phase is also increasing (Figure 1–3). The FMR signal maximum was obtained at 24 K, 31 K, 27 K and for samples with $n = 0.6$, $n = 0.7$, $n = 0.8$, respectively. For sample $n = 0.95$ this maximum was at 34 K [2]. The EPR spectra in the high temperature range were centered at $g_{\mathrm{eff}} \sim 2$ and the linewidth and the integrated intensity strongly depended on the value of index n.

References

[1] Guskos N, Zolnierkiewicz G, Typek J, Sibera D, Narkiewicz U, Lojkowski W 2011 *Acta Phys. Pol. A* **120** 1074

[2] Guskos N, Dudek M, Zolnierkiewicz G, Typek J, Berczynski P, Lendzion-Bielun Z, Sibera D, and Narkiewicz U 2013 *J. Magn. Magn. Mater.* **326** 225–231

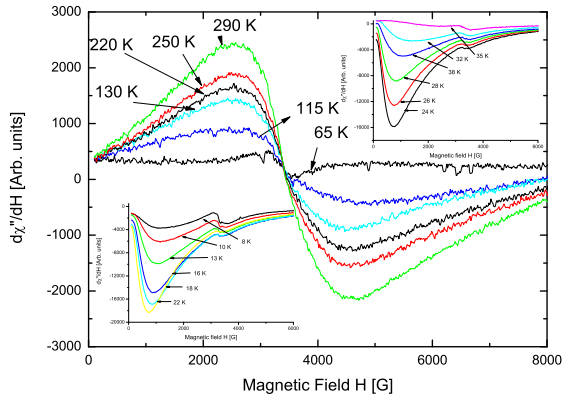

Figure 1: FMR/EPR spectra at different temperatures of $n\mathrm{MnO}/(1-n)\mathrm{ZnO}$ for $n = 0.6$

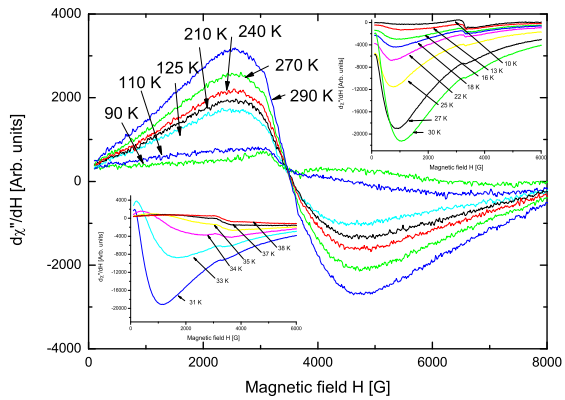

Figure 2: FMR/EPR spectra at different temperatures of $n\mathrm{MnO}/(1-n)\mathrm{ZnO}$ for $n = 0.7$

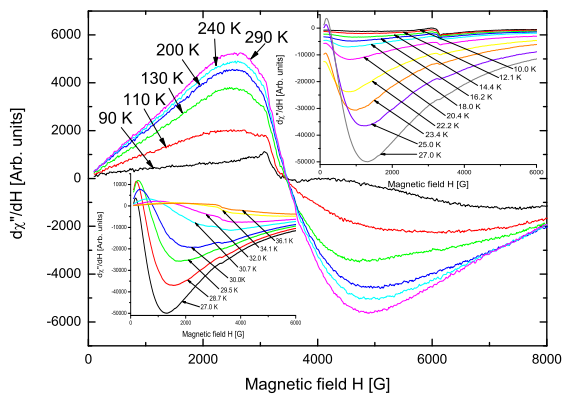

Figure 3: FMR/EPR spectra at different temperatures of $n\mathrm{MnO}/(1-n)\mathrm{ZnO}$ for $n = 0.8$

The ising spin glass model in the presence of a random field

I. A. Hadjiagapiou

Section of Solid State Physics, Department of Physics, University of Athens
Panepistimiopolis, 15 784 Zografou, Athens, Greece

The infinite-ranged Sherrington-Kirkpatrick Ising spin glass model in the presence of a Gaussian random magnetic field is studied by means of the so called replica trick. The randomness of both variables (exchange integral J_{ij} and random field h) is expressed by a joint Gaussian probability density function with a covariance ρ. Within the replica-symmetry hypothesis, the magnetization and Edwards-Anderson-order-parameter profiles, the phase diagram as well as the entropy are presented with respect to the temperature T and random field h. The de Almeida-Thouless instability region is reduced as the covariance ρ is increased. The entropy for small temperatures is negative in the absence of a random field, but as this field is switched on the respective range is reduced.

Acknowledgements
This research was supported by the Special Account for Research Grants of the University of Athens ($E\Lambda KE$) under Grant No. 70/4/4096.

Effect of surface-induced intralayer inhomogeneity on helical superstructures of liquid crystals

W. Jeżewski, I. Śliwa

Institute of Molecular Physics, Polish Academy of Sciences
M. Smoluchowskiego 17, 60-179 Poznan, Poland

A mechanism explaining the formation of distorted helical structures in thin ferroelectric chiral liquid crystal systems is presented. It is shown that the deformation of helical interlayer structures of thin smectic systems can be regarded as a consequence of the surface-induced spatial inhomogeneity in the distribution of the azimuthal molecular orientation within smectic layers. The nonuniformity of the intralayer azimuthal orientation of molecules is argued to generate a local depolarizing electric field of the strength varying not only in smectic layers but also between the layers. The resulting modulation of the depolarization level in the direction of helical axes is shown to distort helices. Using a simple model including the depolarization interaction, it is demonstrated that the degree of the helix deformation strongly changes under temperature variations [1]. Depending on temperature, the intralayer orientational inhomogeneity can cause a partial or even complete destruction of the helical ordering. The partially ordered smectic-liquid phase exhibits the occurrence of domains with non-helical and small-period helix structures, irregularly distributed along the smectic-layer normal. The appearance of such complex orientational superstructures of liquid crystals is argued to occur near molecular tilting transitions, as a result of the decay of long-range orientational correlations between molecules forming different smectic layers. Accordingly, the surface-induced destruction of helical long-range ordering of smectic liquid crystals can be treated as a mechanism of the transition between helical smectic phases and de Vries-type phases occurring in thin liquid crystal systems.

References

[1] W. Jeżewski, Phys. Rev. E **85**, 051702 (2012)

Rotational relaxation in isotropic phase and chiral nematic phase of liquid crystalline material in nonlinear dielectric spectra

P. Kędziora

Institute of Molecular Physics, Polish Academy of Sciences
M. Smoluchowskiego 17, 60-179 Poznan, Poland

The nonlinear dielectric spectroscopy (NDS) is a useful method to study the kinetics of intermolecular aggregation processes, conformational changes and strong intermolecular orientational correlations, such as those existing in liquid crystalline materials.

The NDS allows studying the orientational relaxation modes for a molecule in an isotropic fluid and in liquid crystalline phases. The studies of cholesteryl oleyl carbonate (COC) have shown that in the isotropic phase the molecule exhibits only one relaxation mode relevant to rotations of the longitudinal permanent dipole moment around the short axis. In the mesogenic phases the dipole moment reorientation can be described by two or three modes.

The nonlinear dielectric relaxation spectra allow observing some molecular fluctuations in the chiral nematic phase (N*), in the vicinity of the phase transition to the blue phase (BP). The fluctuations are limited to a very narrow interval of the temperature (2 K) and, between BP and N*, manifest themselves as domains with a supercooled blue phase structure [1].

The transition to the fluctuational region of the chiral nematic phase is also manifested by the appearance of a second, high-frequency orientational band associated with reorientations of the transversal dipole moment around the long molecular axis.

The fluctuations of the molecular dipole moment diminish as the temperature decreases, and the system evolves slowly to the homogeneous cholesteric phase. The "chemical" nonlinear dielectric effect (NDE) (positive) disappears and simultaneously the orientational bands (negative NDE) are shifted to lower frequencies and a third orientational band appears. This new relaxation of the negative effect is attributed to the processional motion around the director. It should be stressed that these bands which are due to the Langevin effect are connected with diffusional rotations of individual molecules.

Acknowledgements
This work was supported by Fonds voor Wetenschappelijk Onderzoek – Vlaanderen, Belgium, in the framework of the agreement for scientific cooperation with the Polish Academy of Sciences.

References
[1] P. Kędziora, K. W. Wojciechowski, *J. Phys. Chem. B*, **113**, 9123 (2009)

Spin localization in porous carbon-based systems with host-guest interactions

M. Kempiński[1], W. Kempiński[2], D. Markowski[2], M. Śliwińska-Bartkowiak[1]

[1] *Faculty of Physics AMU*
Umultowska 85 61-614 Poznan, Poland

[2] *Institute of Molecular Physics PAS*
M. Smoluchowskiego 17, 60-179 Poznan, Poland

In the presented work we want to compare the influence of various effects on the electronic properties of carbon nanoparticle textures. Spin localization observed with EPR in an exemplary carbon system of activated carbon fibers (ACF) depends strongly on the type of molecules adsorbed inside the ACF pores [1]. Several techniques were applied to find the parameter responsible for the observed differences.

We examined the host-guest interactions using contact angle measurements and numerical simulations and obtained the information on the wetting and quasi-high pressure effect in pores. The changes in the nanoparticle structure were resolved with X-ray diffraction. The results of the direct conductivity measurements allowed us to examine the influence of the adsorbed molecule dipole moment which seems to be the main factor determining the changes observed with EPR.

Acknowledgements
This research was partially supported by the Polish grant MNiSW DPN/N174/COST /2010 and COST MP0901 "NanoTP".

References

[1] M. Kempiński, M. Śliwińska-Bartkowiak, W. Kempiński, *Rev. Adv. Mater. Sci.* **14**, 163 (2007)

Kinetics of guest molecules insertion into nano-graphitic porous matrix

W. Kempiński[1], D. Markowski[1], M. Kempiński[2]

[1] *Institute of Molecular Physics PAS*
M. Smoluchowskiego 17, 60-179 Poznan, Poland

[2] *Faculty of Physics, A. Mickiewicz University*
Umultowska 85, Poznan, Poland

The electronic properties of modified activated carbon fibers (ACFs) by specific guest molecules located inside ACFs of different porosity are studied. Parameter T_0 which determines the potential barriers for charge carrier hopping transport in ACFs can be defined on the basis of the host-guest interaction [1,2]. The modification level of parameter T_0 is characterized by the kinetics of the dipolar molecule insertion into a porous matrix of ACFs.

Acknowledgements
This research was partially supported by the Polish grant MNiSW DPN/N174/COST /2010 and COST MP0901 "NanoTP".

References

[1] M. Kempiński, W. Kempiński, J. Kaszyński, M. Śliwińska-Bartkowiak, *Appl. Phys. Lett.* **88**, 2006, 143103
[2] W. Kempiński, D. Markowski, M. Kempiński, M. Śliwińska-Bartkowiak *Carbon* **57**, 2013, 533

Crystal structure and physical properties of layered misfit compound: $Ca_{25}Co_{22}O_{56}(OH)_{28}$

T. Klimczuk[1], H. W. Zandbergena[2], N. M. van der Pers[3], L. Viciu[4], V. L. Miller[4], R. J. Cava[4]

[1] *Faculty of Applied Physics and Mathematics, Gdansk University of Technology G. Narutowicza 11/12, 80-233 Gdansk, Poland*

[2] *National Center for HREM, Department of Nanoscience, Delft University of Technology Rotterdamseweg 137, 2682 AL Delft, The Netherlands*

[3] *Department of Materials Science, Delft University of Technology Rotterdamseweg 137, 2682 AL Delft, The Netherlands*

[4] *Department of Chemistry, Princeton University Princeton, NJ 08544, United States*

The high pressure synthesis, structure and magnetic properties of $Ca_{25}Co_{22}O_{56}(OH)_{28}$ are reported. The compound has a misfit structure, consisting of double, square calcium oxide hydroxide rock-salt-like layers between hexagonal CoO_2 layers. The misfit compound crystallizes in the monoclinic space group $C2/m$, and can be characterized by the coexistence of two subsystems with common a, c and $\beta = 95.745(8)$ parameters, and different b parameters for the rock-salt and hexagonal type planes. The compound shows Curie–Weiss paramagnetism with an antiferromagnetic Weiss temperature of 43 K and a reduced Co moment. Substantial deviations from Curie–Weiss behavior are seen below 50 K with no indication of magnetic ordering. No superconductivity was observed down to a temperature of 2 K.

Sol-gel method as a promising route of nanostructures preparation

B. Kościelska

Faculty of Applied Physics and Mathematics, Department of Solid State Physics
Gdansk University of Technology
G. Narutowicza 11/12, 80-233 Gdansk, Poland

In recent years much attention has been paid to V_2O_5, NbN, VN and $LiTi_2O_4$. These are materials with many commercial applications related to their remarkable physical and chemical properties. The interesting properties of vanadium oxides result from various metal oxidation states (from +II to +V) and different V-O coordination geometries what allows many applications in optical, electrical, electrochemical and thermochromic devices. The main application of V_2O_5, especially in a 1D structure, are industrial catalytic processes. NbN and VN are hard coating materials with a high melting point, hardness, chemical stability at high temperatures and high electrical conductivity. Interest in NbN layers is also focused on their superconducting properties. Their relatively high superconducting critical temperature (up to 16 K) allows them to be used in Josephson junctions and in several superconducting microelectronics applications. The last of the presented materials, $LiTi_2O_4$ is one of the most interesting materials in the family of oxide spinels. It stands out because of its superconducting properties and its possible application as a negative electrode material for lithium-ion batteries.

One common preparation method for the above mentioned materials (films, powders and 1D nanostructures) may be the sol-gel route [1–3]. The sol-gel way seems to be a very fast, easy and low cost process. What is more, owing to its high controllability, it gives a possibility of producing materials with a precisely defined stoichiometry. The structure, physical properties and manufacturing of V_2O_5, NbN, VN and $LiTi_2O_4$ via the sol-gel method will be presented in this lecture.

References

[1] B. Kościelska, *J. Non-Cryst. Solids* **354** (2008) 1549
[2] B. Kościelska, A. Winiarski, W. Jurga, *J. Non-Cryst. Solids* **356** (2010) 1998
[3] M. Łapiński, B. Kościelska, W. Sadowski, *J. of Alloys and Compounds* **536** (2012) 30

Study of icosahedral clusters in close-packed simple liquids

A. L. Kozub[1], J. Rybicki[1,2]

[1] *Faculty of Applied Physics and Mathematics, Gdansk University of Technology G. Narutowicza 11/12, 80-233 Gdansk, Poland*

[2] *TASK Computer Centre, Gdansk University of Technology G. Narutowicza 11/12, 80-233 Gdansk, Poland*

The local structure of liquid copper was determined using Steinhardt order parameters, with particular attention paid to icosahedral clusters. The positions of atoms were obtained from three sets of molecular dynamics simulations, with the forces obtained from: the Sutton-Chen (SC) potential, the Naval Research Laboratory total energy tight-binding (NRL-TB) method and the divide-and-conquer learn-on-the-fly (DCLOTF) method, respectively. A broad range of local geometries appeared, which is a typical result for close-packed liquids. Among them a number of icosahedral clusters were detected. The highest density of icosahedral clusters was obtained at the temperature of 1000 K for the NRL-TB and DCLOTF simulations and 1200 K for the SC simulations.

We propose various means of analysing the icosahedral clusters formed in liquid copper. The average number of the clusters, their lifetime and correlations between them at various temperatures were studied as a function of the approach used to generate the trajectories. Finally, We studied the formation and decay of icosahedral clusters.

Acknowledgements
The calculations were performed at the TASK Computer Centre (Gdansk, Poland).

Nanoporous Cu doped lithium titanate thin films – structure and optical properties

M. Łapinski, B. Kościelska, W. Sadowski

Department of Solid State Physics, Gdansk University of Technology
G. Narutowicza 11/12, 80-233 Gdansk, Poland

Recently, much attention has been given to materials in nanostructured forms. They often show novel and enhanced properties that are different from those of their corresponding bulk materials. Especially nanoporous films could exhibit anomalous optical, electronic, magnetic and other properties [1,2]. Among porous materials, nanostructured lithium titanate ($LiTi_2O_4$) thin films could be very interesting from the point of view of practical applications. Lithium titanate is a II type spinel oxide superconductor with relatively high (~ 13 K) superconducting transition temperature T_c. Above T_c lithium titanate shows metallic behaviour and can be used e.g. as electrodes for rechargeable lithium-ion batteries [3]. Since the discovery of superconductivity in lithium titanate, much scientific attention has been devoted to improve the transition temperature by doping by other atoms. Substitution of Ti atoms in lithium titanate by, for example, Al, B, Cr, Ge, Mn, Ni or V does not increase T_c [4]. It is only the Cu dopant that gives hope to increase the transition temperature [5].

One of the best methods of preparation of $LiTi_{2-x}Cu_xO_4$ is the sol-gel method, which is cheap, simple and reproducible. Lithium acetate, butoxytitanium and ethanol were used as reagents. Additionally copper nitrate was added as a Cu dopant source. The amounts of lithium, titanium and copper precursors were calculated for the $LiTi_{2-x}Cu_xO_4$ solution with x equal to 0, 0.05, 0.1, 0.15 and 0.2. Films were deposited on quartz glass substrates by a spin coating technique at a rate of 120 rps. The samples were subsequently dried at 100 °C for 10 hours in an argon atmosphere. Repeating the above procedure three times resulted in obtaining approximately 800 nm smooth thin films. After deposition, the samples were heated in an argon atmosphere at 550 °C for 20 hours.

The structure of the prepared samples was investigated by X-ray diffraction. All the patterns of the samples revealed a nanocrystalline structure. The scanning electron microscope investigations showed a homogeneous, porous morphology. Uniform pores were about 200 nm in size. The optical measurements showed high transmittance in the visible range of light for all the samples (the transmission coefficient of more than 70%). The absorption edge (λ_{cutoff}) of the examined films was in the range of 300 nm–310 nm and it was independent from the copper dopant amount. According to the quantum size effect, the optical results showed no relationship between the radii of crystallites and the copper dopant in the lithium titanate.

References

[1] Chen F, Kitai A H 2008 *Thin Solid Films* **517** 622

[2] Sadek A Z, Partridge J G, McCulloch D G, Li X Y, Yu X, Wlodarski W, Kalantar K 2009 *Thin Solid Films* **622** 1294
[3] Lapinski M, Koscielska B, Sadowski W 2012 *J. Alloy. Compd* **536** 30
[4] Sun C P, Huang Y F, Tai S T, Huang C L , Yang H D 2006 *Physica B* **378–380** 395
[5] Faran O, Volterra V 1995 *Physica C* **255** 329

Characterization of Fe-Co catalyst for CO_x-free hydrogen production via ammonia decomposition

Z. Lendzion-Bieluń, R. Pełka, W. Arabczyk

Institute of Chemical and Environment Engineering
West Pomeranian University of Technology
Pulaskiego 10, 70-322 Szczecin, Poland

The properties of a fused Fe-Co catalyst and an industrial iron catalyst for ammonia synthesis were compared in the work. The ammonia decomposition kinetics and the distribution of catalyst nanocrystallite sizes were determined. The fused Fe-Co catalyst was prepared by melting magnetite with promoter oxides (Al_2O_3, CaO, K_2O). Cobalt(II, III) oxide was also added during the melting process. The chemical composition of the prepared catalyst was found with the aid of the ICP-OES method: 1.05% Al_2O_3, 1.23% CaO, 0.21% K_2O, 4.8% Co_3O_4, and iron oxides – a complement to 100%. The phase composition before and after the ammonia decomposition tests was determined with the XRD method. The specific surface area of the catalyst reduced form was measured by the thermal desorption method. A comparision of the courses of nitriding processes of the Fe-Co and industrial iron catalyst during the ammonia decomposition reaction and the ammonia decomposition rate over the cobalt-doped catalyst is shown in Figure 1.

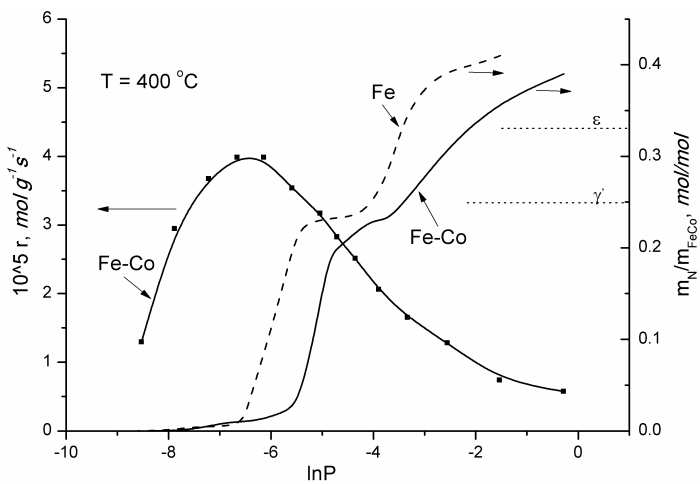

Figure 1: Rate of ammonia decomposition and mass change vs nitriding potential logarithm ($\ln P = \ln(p_{NH_3}/p_{H_2}^{1.5})$)

The values of the ammonia decomposition rate over the industrial iron catalyst at the process conditions are below the detection limit of the used appliances. the nitriding process for the Fe-Co catalyst starts at a higher nitriding potential.

Acknowledgements
Scientific work of one of the authors (R. Pełka) supported from the budget of the Iuventus Plus programme for science in 2012–2013, No. IP 2011040771

Influence of metallic sample construction elements on sputtering process in Line 440 magnetron setup

P. Lichograj[1], J. M. Olchowik[2]

[1] *Centre for Research on Innovation*
Pope John Paul II State School of Higher Education in Biala Podlaska
Sidorska 105, 21-500 Biala Podlaska, Poland

[2] *Institute of Renewable Energy Engineering, Lublin University of Technology*
Nadbystrzycka 40B, 20-618 Lublin, Poland

Magnetron sputtering is still one of many interesting techniques of material deposition and thin layer creation [1,2]. The possibility of deposition of different targets on the substrate allows creating various types of elements, such as electrodes, detectors, photovoltaic cells [3]. During the experiments the authors tested many combinations of materials but also analysed the possibility of atom migration from other targets (Line 440 – four target setups) or from the sample (substrate) construction elements. It is possible that the plasma created in a sputtering process has influence not only on the target but also on the setup environment. To explain this phenomenon, the authors decided to prepare samples with metallic elements, complete the process at various conditions (magnetron generator power, gas composition, temperature, etc.), and then, analyse its atomic composition for the search for atoms deposited from metal elements.

References

[1] A. A. Ogwu, T. H. Darma, E. Bouquerel, *Journal of Achievements in Materials and Manufacturing Engineering*, **24**, 2007
[2] K. Mech, R. Kowalik, P. Żabiński, *Archives of Metallurgy and materials*, **56**, 2011
[3] A. Chowdhuri, D. Haridas, K. Sreenivas, V. Gupta, *International Journal of Smart Sensing and Intelligent Systems*, **2**, 2009

Influence of electromagnetic field generated around copper conductor with current placed in vacuum chamber on process of RF and DC magnetron sputtering of thin films

R. Lichograj[1], J. M. Olchowik[2]

[1] *Centre for Research on Innovation*
Pope John Paul II State School of Higher Education in Biala Podlaska
Sidorska 105, 21-500 Biala Podlaska, Poland

[2] *Institute of Renewable Energy Engineering, Lublin University of Technology*
Nadbystrzycka 40B, 20-618 Lublin, Poland

Thin films deposited on magnetron sputtering are an important alternative to other methods [1]. There is a need to study and develop both RF magnetron sputtering and DC magnetron sputtering, due to their widespread use in technology [2,3].

The study focused on the influence of a conductor with current placed on glass samples in a vacuum chamber on the deposited magnetron single thin layers of Sn and Si.

The parameters of DC and RF Magnetron Sputtering were set at constant for all samples and types of applied layers to see the influence of the field. The sputtering process was also carried out with a copper conductor not connected to the power source and the parameters of the DC and RF Magnetron Sputtering remained unchanged.

The sputtering process operations were repeated several times for different values of the change in the electrical current or voltage source or when the current source was disconnected.

The electron microscope and the ellipsometer were used in order to examine the surface on which thin layers were applied.

References

[1] J. Musila, P. Barocha, J. Vlčeka, K. H. Namc, J. G. Hanc, *Thin Solid Films*, **475**, 2005
[2] K. Mech, R. Kowalik, P. Żabiński, *Archives of Metallurgy and materials*, **56**, 2011
[3] A. Chowdhuri, D. Haridas, K. Sreenivas, V. Gupta; *International Journal of Smart Sensing and Intelligent Systems*, **2**, 2009

Performance tests of polyether flame resistant auxetic foams

J. Lisiecki[1], S. Klysz[1,2], T. Blażejewicz[1], G. Gmurczyk[1], P. Reymer[1]

[1] *Air Force Institute of Technology*
Warszawa, Poland

[2] *University of Warmia and Mazury*
Olsztyn, Poland

The article presents the results of the tests carried out for flame resistant polyether foams processed according to the Mechanical-Chemical-Thermal process. The level of auxeticity, Poisson's ratio for the whole specimen under compression calculated from the measured engineering strains was verified using an ME46 video extensometer. The presented tests were chosen to estimate the performance of the final product, which is expected to be used as a seat cushion.

Firstly, the permanent strain after compression was defined using specially designed apparatus. The test was carried out according to the PN-EN ISO 1856 standard using two methods: A – after 22 hours under 50% compression in 70°C, and B – after 72 hours under 50% compression in room temperature. Humidity and temperature were recorded throughout the whole test using an LB-701 (no 470) thermohygrometer.

Secondly, fatigue under constant cyclic loading was tested according to the PN-EN ISO 3385 and PN-EN ISO 2439 standards using an MTS 370.10 LANDMARK test machine and a specially designed indenter. As a result, changes in the foam thickness as well as hardness, from before and after the test, were compared and discussed.

Thirdly, deflection under tension was defined according to Mil-S-27332B. Foam specimens, compressed twice to a 75% deflection with a speed of 250 mm/min using two perforated plates were then compressed to a 25, 50, 65, 75, 80 and 85% deflection with a speed of 50 mm/min and the applied force was measured. This allowed defining the characteristics of force versus strain and evaluate them using the values given in the standard.

Finally, the stress-strain characteristics under compression were defined according to the PN-EN ISO 3386-1-00 standard. Foam samples placed between two perforated plates were compressed three times to 30 and once up to 77% using an MTS testing machine, which allowed determining the stress-strain characteristics as well as to estimate the volume energy dissipated by the sample.

In the article the authors describe the manufacturing process, the setup and the results of the measurements including discussion of the results.

Acknowledgements
The financial support of Structural Funds in the Operational Programme – Innovative Economy (IE OP) financed from the European Regional Development Fund – Project Modern Material Technologies in Aerospace Industry, No. POIG.01.01.02-00-015/08-00 is gratefully acknowledged.

AFM/STM characterization of SnO_2 thin films obtained by magnetron sputtering

Z. Lubańska[1], J. M. Olchowik[2]

[1] *Centre for Research on Innovation*
Pope John Paul II State School of Higher Education in Biala Podlaska
Sidorska 105, 21-500 Biala Podlaska, Poland

[2] *Institute of Renewable Energy Engineering, Lublin University of Technology*
Nadbystrzycka 40B, 20-618 Lublin, Poland

Atomic force microscopy is one of the most popular methods used in surface imaging. This method allows measuring the surface topography and determining the dimensions of structures in a subatomic resolution [1]. Due to its properties, it can be applied to the measurement of conductor and semiconductor surfaces prepared in various processes. The experiment is focused on SnO_2 thin layers which can be used as transparent electrodes [2]. The authors are trying to illustrate the correlation between process parameters – creation of a semiconductor in magnetron sputtering by different process conditions (temperature and cooling, gas pressure and composition), the sample surface and its other electro-optical parameters.

References

[1] A. Bosseboeuf, M. Dupeux, M. Boutry, T. Bourouina, D. Bouchier, D. Débarre, *Microsc. Microanal. Microstuct.* **8** (1997) 261
[2] M. Batzill, U. Diebold, *Progress in Surface Science* **79** (2005) 47

Controlled release fertilizers as an example of functional materials

K. Lubkowski, B. Grzmil

West Pomeranian University of Technology, Szczecin
Institute of Chemical and Environment Engineering
Pulaskiego 10, 70-322 Szczecin, Poland

An increased production of fertilizers and soil fertilization are in contrast with relatively low nutrient assimilation by crops. Low effectiveness of nutrient assimilation causes serious problems in terms of environmental protection. The effectiveness of nutrient absorption may be improved through developing, producing and applying the so-called *slow or controlled release fertilizers* (SRF/CRF). These fertilizers gradually release mineral nutrients, providing proper nutrition to plants.

In a system in which a fertilizer granule is coated with an inert layer, water penetrates through a hydrophobic membrane into the granule's inside. Nutrients are dissolved and the arising osmotic pressure leads to either partial tearing off of the membrane or its expansion, which allows ion transport through the coating into the soil. Sulfur-coated urea (SCU) is an example of this kind of fertilizer. Other examples include: polyethylene-coated urea, polymer-coated superphosphate, natural gum, rosin, waxes, paraffins, various kinds of ester copolymers, urethane composites, epoxy and alkyd resins, polyolefines, polyacrylic acid, polyvinyl alcohol, epoxidized soybean oil or butadiene-methylstyrene block copolymers. The second kind of fertilizers is a system where the active component is dispersed in a polymer matrix. The first study into a matrix system was published in 1987, but the system has not been thoroughly studied, nor has it been used in industrial applications.

A drawback of SRFs is that there is still a considerable amount of useless polymer left in the soil after consumption of nutrients. A good and possible solution, although not used on a technological scale as yet, is to produce SRFs using biodegradable materials.

Investigations on anticorrosive properties of modified aluminium phosphate

K. Łuczka, K. Lubkowski, B. Grzmil

Institute of Chemical and Environment Engineering
West Pomeranian University of Technology
Pulaskiego 10, 70-322 Szczecin, Poland

Microwave synthesis of materials offers several advantages including shorter synthesis time, rapid heating, fast reaction, easy reproducibility, narrow particle distribution, high yield, high purity, efficient energy transformation and overall volume heating. Microwave heating is different from conventional heating in the way that heat is generated internally within the material instead of originating from an external heating source and a subsequent radiative transfer [1].

The objective of these studies was to elaborate a preparation method of nanoparticle aluminum phosphates modified with ammonium or/and ammonium and calcium with the use of inorganic compounds as precursors. Analytical-grade reagents were used. Phosphates were prepared by reaction of various substrates. Studies on the synthesis of aluminium ammonium calcium phosphates were performed with the use of a glass reactor and microwave radiation. The influence of process parameters (the molar ratio of substrates, concentration, temperature, pressure) on the phase composition and properties of products was determined. The phase composition of the obtained samples was studied using XRD analysis. The synthesized powder was characterized for morphology, particle-size, crystallinity, phases and elemental composition. The selected pigment with preferred physicochemical properties will be investigated in a corrosion test using two-component systems (epoxy and polyurethane coatings) or alkyd ones.

References

[1] Kalita S J, Verma S 2010 *Nanocrystalline hydroxyapatite bioceramic using microwave radiation: Synthesis and characterization* Materials Science and Engineering **C 30** 295–303

Magnetic properties of carbon nanotubes poly(ether-ester) nanocomposites

O. Manos[1], S. Glenis[1], A. Szymczyk[2], V. Likodimos[1,3], N. Guskos[1,2]

[1] *Department of Solid State Physics, University of Athens Panepistimiopolis, 15 784 Zografou, Athens, Greece*

[2] *Institute of Physics, West Pomeranian University of Technology Al. Piastow 17, 70-310 Szczecin, Poland*

[3] *Institute of Advanced Materials, Physicochemical Processes, Nanotechnology and Microsystems, NCSR "Demokritos" Aghia Paraskevi Attikis, 15 341 Athens, Greece*

The exceptional mechanical, electrical and thermal properties of carbon nanotubes (CNTs) attract particular research interest due to their potential application as filler material for polymer reinforcement and the development of advanced nanocomposite materials. Interface engineering and reduction of CNT agglomeration are key issues for the production of carbon nanotube reinforced polymers characterized by a sufficient interfacial stress transfer between nanotubes and the polymer matrix without compromising the inherent CNT properties. In this work, the magnetic and electronic properties of composites consisting of oxidized multi-wall carbon nanotubes (MWNTs) and single-wall carbon nanotubes (SWNTs) dispersed in elastomeric poly(ether-ester) matrices were studied by means of electron spin resonance (ESR) and dc magnetization measurements. Nanocomposites were prepared using the *in situ* polycondensation reaction process, where MWNTs and SWNTs are introduced as fillers at 0.5 wt% in poly(trimethylene terephthalate) (PTT) and poly(trimethylene terephthalate)-block-poly(tetramethylene oxide) (PTT-PTMO) block copolymers, during their synthesis. A significant reduction of the diamagnetic response of MWNTs was identified in the PTT/MWNTs 0.5 wt% composites, indicative of substantial hole doping related to the oxygen functional groups on the oxidized CNT's surface. Furthermore, ESR measurements on both PTT/MWNTs 0.5 wt% and PTT-PTMO/SWNTs 0.5 wt% revealed considerable enhancement of the spin susceptibility due to an excessive increase in the density of paramagnetic defects which are sensitive CNT-polymer interfacial coupling.

A preliminary study on the effect of missing ribs in hexagonal honeycombs

L. Mizzi[1], D. Attard[1], R. Gatt[1], A. Casha[2], J. N. Grima[1,3]

[1] *Metamaterials Unit, Faculty of Science, University of Malta Msida MSD 2080, Malta*

[2] *Department of Anatomy, Faculty of Medicine and Surgery, University of Malta Msida MSD 2080, Malta*

[3] *Department of Chemistry, Faculty of Science, University of Malta Msida MSD 2080, Malta*

When a material is uniaxially loaded, the lateral dimensions of the material normally change. Intuition suggests that they should become thinner. However, there exist materials which posses the inherent property of expanding when stretched. These materials, more commonly referred to as auxetic, exhibit a negative Poisson's ratio. This unexpected behaviour is very often associated to the internal geometric features of the material and mechanism/s that govern their deformation. A particular geometry which has attracted a lot of interest in view of its potential to exhibit such behaviour is the re-entrant honeycomb, which has been thoroughly studied in terms of its mechanical behaviour. However, most of the studies were based on perfect honeycombs and very few have focused on the effects of possible disorder and defects that may be present in such honeycombs. In view of this, in the work presented here, the effect that random defects may have on the in-plane mechanical properties of both re-entrant and conventional honeycombs are qualitatively studied. In particular, an analysis of the Young's moduli and Poisson's ratios for honeycombs with a varying number of randomly missing ribs is studied using the **E**mpirical **M**odelling **U**sing **D**ummy **A**toms (EMUDA) through custom-made force-fields implemented in *Cerius*^{2} molecular modelling software. The results obtained suggest that the magnitude of the Young's moduli and Poisson's ratios generally decreased as the number of defects increased. The extent of decrease was found to mainly depend on the number of defects present, which type of ribs are missing, i.e. whether vertical or inclined and also on the dominating deformation mechanism. Some interesting trends were observed for honeycombs with missing vertical ribs deforming through dilation when loaded in the horizontal direction, which were found to be very little affected by the introduction of such defects. This is in sharp contrast to honeycombs with missing inclined ribs deforming through the hinging mechanism or one which involved both hinging and stretching. In these cases, it was found that it is possible for a structure exhibiting conventional behaviour to become auxetic as the number of defects increases and vice versa. This trend, along with various other interesting behaviours is explained in terms of the changes in the geometry of the systems and their propensity to deform via other mechanisms.

Preparation of visible light-active TiO_2 by thermal modification with arenes

A. W. Morawski, E. Kusiak-Nejman, A. M. Wanag

West Pomerania University of Technology
Institute of Chemical and Environment Engineering
Pulaskiego 10, 70-322 Szczecin, Poland

Titanium dioxide is a semiconductor which has been tested as a photoactive nanostructural material for water treatment for almost four decades. Different kinds of TiO_2 modification have been proposed considering the postulates of sustainable development. One of such modifications is the thermal modification of starting titania by carbon from different carbonic precursors (sucrose, glucose, aliphatic alcohols, arenes).

In this study TiO_2 (anatase phase) was conducted in arene atmosphere in a tubular furnace at 400°C for 4 hours to prepare TiO_2/C nanomaterials. Arenes (benzene, naphthalene and anthracene) were used as carbon dopants.

On the basis of UV-Vis/DR analysis it was possible to find insignificant changes in band gap energy but it was also noted that calcination of starting TiO_2 with arenes led to improve absorption in the visible range. It could be explained by changes in the colour of photocatalysts from white for starting titania, TiO_2 calcined at 450°C and TiO_2/C photocatalyst modified with benzene to grayish brown for the TiO_2 photocatalyst modified with arenes. It was also noted that the TiO_2 nanophotocatalysts modified with benzene and naphthalene were characterized as visible-active materials during phenol decomposition. The enhanced activity of the tested TiO_2/C materials in the case of benzene modification could be explained by the presence of some optimal carbon content in the photocatalyst sample. It is possible to observe a decrease

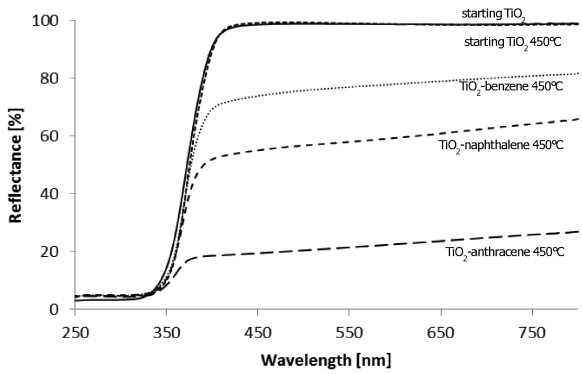

Figure 1: UV-Vis/DR absorption spectra of starting TiO_2, TiO_2

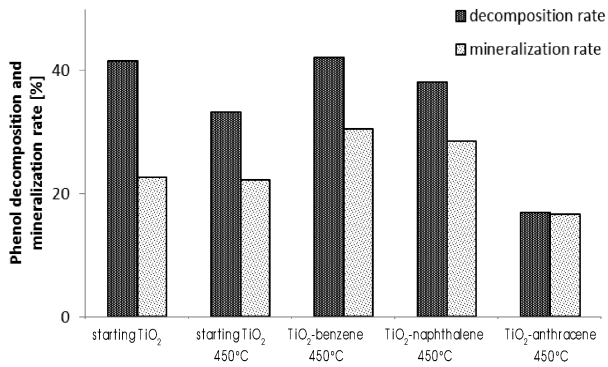

Figure 2: Decomposition and mineralization rates of phenol calcined at 450°C and TiO_2 calcined at 450°C modified with arenes solution for TiO_2, TiO_2 calcined at 450°C and TiO_2 calcined at 450°C and TiO_2 calcined at 450°C modified with arenes

in the decomposition and mineralization rate for samples modified with naphthalene and anthracene due to a too high amount of carbon in these materials. It was proved that the photocatalytic activity of carbon modified titania nanomaterials strongly depended on the carbon content in TiO_2/C photocatalysts.

Acknowledgements
This work was supported by grant No. 506-10-011-4524/6 (National Science Centre, Poland).

Magnetic properties of system Co_xMo_3N + Cr

D. Moszyński[1], N. Guskos[2,3], A. Guskos[3], U. Narkiewicz[1]

[1] *Institute of Chemical and Environmental Engineering*
West Pomeranian University of Technology
Pulaskiego 10, 70-322 Szczecin, Poland

[2] *Department of Solid State Physics, Faculty of Physics, University of Athens*
Panepistimiopolis, 15 784 Zografou, Athens, Greece

[3] *Institute of Physics, West Pomeranian University of Technology*
Al. Piastow 48, 70-311 Szczecin, Poland

Cobalt molybdenum oxide hydrate, $CoMoO_4 \cdot xH_2O$, was impregnated with chromium nitrate, $Cr(NO_3)_3$, and samples containing from 0.5 wt% to 2 wt% of chromium were prepared. An oxidic precursor was then reduced in the stream of ammonia at 700°C for 5 h. Two different phases of cobalt molybdenum nitrides: Co_2Mo_3N and Co_3Mo_3N were identified in the obtained materials by X-ray diffraction analysis. Moreover, the Co_2Mo_3N phase content decreased with the increasing concentration of chromium. The material doped with 0.5 wt% of chromium contained 23 wt% of Co_2Mo_3N, while the material doped with 2 wt% of chromium – only 6 wt% of Co_2Mo_3N.The surface area of the materials analyzed by the BET method changed with the chromium concentration, as well. The BET area increased from 13 m^2/g to 17 m^2/g as the chromium concentration changed from 0.5 to 2 wt% of chromium, respectively. The temperature dependence of magnetization for the ZFC and FC modes was observed in the temperature range from 2 K up to room temperature (RT). A hysteresis loop was observed for the all samples at low temperatures, and up to RT for one of them. Only one sample showed blocking temperature of about 50 K.

Formation and structure of Al-Zn based magnetic fluids

S. Mudry, I. Shtablavyi, Yu. Kulyk, B. Sokolyuk

Physics of Metals Department, Ivan Franko National University of Lviv
Kyrylo and Mephodiy 8, 79005 L'viv, Ukraine

Aluminum-based alloys and their composites have proven to be the most promising in terms of practical application as multi functional materials. Mostly, the Al-based composites are used as structural materials in automotive, shipbuilding and aircraft industries in which small particles are a reinforcement phase.

Composites with a liquid metal matrix and ferromagnetic filler can be used as magnetic fluids. The possibility of controlling the magnetic fluid behavior with the help of a magnetic field offers great opportunities for the practical use of such composites with a metal matrix.

The main problem at the formation of magnetic fluids with a liquid metal matrix is to avoid the chemical interaction between the liquid matrix and the ferromagnetic particles. For that reason the phase formation process in Al-Zn alloys filled with magnetite particles at room temperature and in the process of heat treatment were studied in this work.

The X-ray diffraction and scanning electron microscopy methods were used for phase identification in order to investigate the thermal and composition stability of a composite.

Acknowledgements
This work was supported by a grant from the Fundamental Researches State Fund of Ukraine (No 0113U002789).

Nanoscale structure in liquid PbTe doped with Bi_2Te_3

S. Mudry, A. Korolyshyn, I. Shtablavyi, V. Vus

Physics of Metals Department, Ivan Franko National University of Lviv
Kyrylo and Mephodiy 8, 79005 L'viv, Ukraine

A pseudo-binary PbTe-Bi_2Te_3 system is of interest due to a possibility of obtaining materials with enhanced thermoelectric properties by means of concentration and change of the cooling condition. For that reason it is important to study the structure in the liquid state and its variation for melts of different composition at different temperatures, especially at temperatures which are close to solidification. The structure was studied for molten PbTe and alloys with additions of 2; 5 and 10 mol.% of the Bi_2Te_3 compound and at temperatures of 5 K above the liquidus point in phase diagram.

The X-ray diffraction method was employed to obtain angular dependence of scattered intensity from the surface of the melts under investigation. Experimental data were recorded by means of a high temperature X-ray diffractometer which permitted to reach a high accuracy of the diffraction patterns which were used to calculate the structure factors and pair correlation functions. From these functions the main structure parameters – the most probable distance to the nearest neighbor atoms, the number of neighbors, the size of clusters were determined. Analyzing these parameters by comparing with those for crystalline phases we determined the kind of structural units and their parameters. We estimated also the degree of chemical ordering and the dependence of such ordering versus the content of Bi_2Te_3. For more detailed information on the short range order structure variation the model interpretation of structure parameters was also performed. The available literature data on the physical-chemical properties of the PbTe-Bi_2Te_3 pseudo-binary system were also compared with the results on structure studies of this work. It was shown that the structure of PbTe-enriched melts had an atomic distribution that was significantly different from the random atomic distribution and was highly sensitive to the content of Bi_2Te_3.

Acknowledgements
This work was supported by a grant from the Fundamental Researches State Fund of Ukraine (0113U002789).

Gradient filled segmented block copolymer urethane elastomers with improved abrasion resistance

M. Nachman, S. Paszkiewicz, E. Senderek, Z. Rosłaniec

Institute of Materials Science and Engineering West Pomeranian University of Technology Al. Piastow 19, 70-310 Szczecin, Poland

Urethane elastomers (PUR) possess a unique combination of properties: excellent rubber elasticity, good mechanical properties and enhanced abrasion resistance. They are the most abrasion-resistant of all elastomeric materials. Many physical and chemical properties of urethane elastomers can be modified by the addition of nanofillers [1]. The aim of this study was to utilize the magnetic properties of nanocrystalline iron carbides (Fe_3C) and nitrides (ε-Fe_3N) to manufacture gradient filled polyurethane with unilaterally increased abrasion resistance.

Gradient-filled thermoplastic multiblock polyurethane elastomers with a nanocrystaline filler, containing different concentrations of polyether soft segments were synthesized to prepare a nanocomposite with high abrasive wear resistance. The materials were obtained by the prepolymeryzation method with oligomeric polyether (PTMO), butylene glycol and methylenediphnyl 4,4-diisocyanate, then cast into molds. A magnet was placed under the molds to obtain a gradient distribution of the filler in polyurethane. Two types of nanocrystalline fillers with magnetic properties: nanocrystalline iron carbide (Fe_3C) in a matrix of carbon and nanocrystalline iron nitride (ε-Fe_3N) in a matrix of carbon-enriched nitrogen were used. The details of the method of obtaining nanofillers and their characteristics have been described elsewhere [2]. The resulting composite materials were characterized by unilaterally enhanced abrasion resistance. Moreover, the addition of the filler used in a small amount of 0.8 wt.% did not significantly affect the density of the material, which was extremely important to the weight of the finished product.

Acknowledgements
This work is sponsored by financial support of the West Pomeranian University of Technology.

References

[1] Boczkowska A, Czechowski L, Jaroniek M, Niezgoda T 2010 *Mechanik* **7** 470–474
[2] Narkiewicz U, Pełech I, Rosłaniec Z, Kwiatkowska M, Arabczyk W 2007 *Nanotechnology* **18** 405–601

Soft polydisperse dimers exhibit negative Poisson's ratio at zero temperature

J. W. Narojczyk, K. W. Wojciechowski, M. Kowalik

Institute of Molecular Physics, Polish Academy of Sciences
M. Smoluchowskiego 17, 60-179 Poznan, Poland

Influence of atomic size polydispersity on Poisson's ratio [1] of cubic systems consisted of di–atomic molecules (dimers) is studied by computer simulation. The simulations, performed in the NVT ensemble, are restricted to static systems, i.e. the zero temperature case ($T = 0$ K). The dimers are arranged in such a way that the positions of their centres of mass and their orientations are aperiodic but the constituting atoms form a perfect (or slightly distorted in the polydisperse case) f.c.c. lattice. Such a phase is called the *degenerate crystal* (DC) [2]. Figure 1 shows one of many examples of the DC structure.

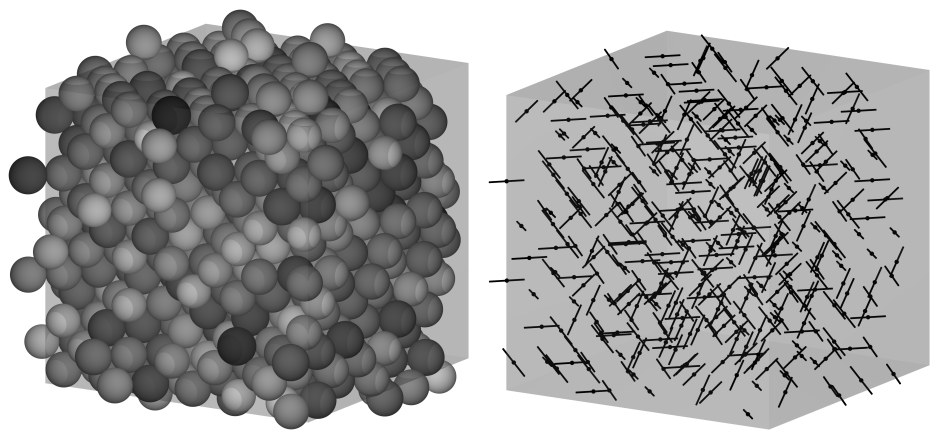

Figure 1: Example of microscopic structure of DC polydisperse dimer system. The structure shown consists of 432 dimers and has the polydispersity parameter δ equal to 3%. On left the atoms are drawn in the shades of gray, indicating their size relative to other atoms. The darker the color, the larger the atomic diameter. The gray cube indicates the periodic box. On right dimer center positions and orientations for the structure in left are represented by points and line segments connecting the atomic centers.

Size polydispersity concerns all atoms in the model. Interactions are short-ranged – restricted to nearest-neighbouring atoms, i.e. those sharing a common wall of their Voronoi polyhedra. The atoms interact with soft, repulsive n-inverse-power potential.

Poisson's ratio is the negative ratio of the relative change in the transverse dimension to the relative change in the longitudinal dimension when infinitesimal change

of the longitudinal stress is applied [1]. In the case of anisotropic materials, Poisson's ratio ($\nu_{\alpha\beta}$) may depend on both the longitudinal (α) and transversal (β) direction. It is known that, in general, the disorder of crystalline lattice leads to the increase of average Poisson's ratio, both in the case of isotropic [3–6] and anisotropic [7–9] systems. However, in the case of cubic systems a direction exists ($\beta = [1\bar{1}0]$) for which, polydispersity has the opposite effect, when the sample is deformed in $\alpha = [110]$. In this case it has been found, that increasing polydispersity leads to a *decrease* of the Poisson's ratio [8,9], down to *negative* values. For unconstrained, polydisperse cubic system (f.c.c. spheres), the decrease was insignificant [8], and negligible in the limit of hard interactions. Negative Poisson's ratio was observed for a range of soft interactions. For f.c.c. dimers, the increasing polydispersity decreases $\nu_{[110][1\bar{1}0]}$ *significantly*, down to ≈ -0.8, in the range of hard interactions [9]. Various models of dimers were studied [10] and the observed effect was found to be robust with respect to model details. Hence, this effect can be of interest from practical applications perspective.

Acknowledgements
Part of the simulations was performed at Poznan Supercomputing and Networking Center (PCSS).

References

[1] L. D. Landau and E. M. Lifshitz, *Theory of Elasticity*, Pergamon Press, London, 1986
[2] K. W. Wojciechowski, Degenerate crystalline phase in a two-dimensional system of hard dimers, *Modern Physics Letters B*, 5:1843–1851, 1991
[3] K. W. Wojciechowski and J. Narojczyk, Influence of disorder on the Poisson's ratio of static solids in two dimensions, *Reviews on Advanced Materials Science*, 12:120–126, 2006
[4] J. W. Narojczyk and K. W. Wojciechowski, Computer simulation of the Poisson's ratio of soft polydisperse discs at zero temperature, *Materials Science (Poland)*, 24:921–927, 2006
[5] J. W. Narojczyk and K. W. Wojciechowski, Elastic properties of two-dimensional soft discs of various diameters at zero temperature, *Journal of Non-Crystalline Solids*, 352: 4292–4298, 2006
[6] J. W. Narojczyk and K. W. Wojciechowski, Elasticity of periodic and aperiodic structures of polydisperse dimers in two dimensions at zero temperature, *Physica Status Solidi (b)*, 245:2463–2468, 2008
[7] J. W. Narojczyk, A. Alderson, A. R. Imre, F. Scarpa, and K. W. Wojciechowski, Negative Poisson's ratio behavior in the planar model of asymmetric trimers at zero temperature, *Journal of Non-Crystalline Solids*, 354:4242–4248, 2008
[8] J. W. Narojczyk and K. W. Wojciechowski, Elastic properties of the fcc crystals of soft spheres with size dispersion at zero temperature, *Physica Status Solidi (b)*, 245:606–613, 2008
[9] J. W. Narojczyk and K. W. Wojciechowski, Elastic properties of degenerate f.c.c. crystal of polydisperse soft dimers at zero temperature, *Journal of Non-Crystalline Solids*, 356:2026–2032, 2010,
[10] J. W. Narojczyk, K. W. Wojciechowski and M. Kowalik, Partially auxetic properties of polydisperse soft dimer systems at zero temperature, *Journal of Chemical Physics*, submitted

Low-temperature static magnetic properties and FMR spectroscopy of Mg-Zn nanoferrites

B. V. Padlyak[1,2], N. Guskos[3,4], G. Zolnierkiewicz[4], A. V. Kopayev[5], I. P. Yaremiy[5]

[1] *Sector of Spectroscopy, Institute of Physical Optics Dragomanov 23, 79005, Lviv, Ukraine*

[2] *Division of Spectroscopy of Functional Materials Institute of Physics, University of Zielona Gora Szafrana 4a, 65-516 Zielona Gora, Poland*

[3] *Solid State Section, Department of Physics, University of Athens Panepistimiopolis, 15 784 Zografou, Athens, Greece*

[4] *Institute of Physics, West Pomeranian University of Technology Al. Piastow 48, 70-311 Szczecin, Poland*

[5] *Physical & Technical Faculty, Vasyl Stefanyk PreCarpathian National University Shevchenko 57, 7-000, Ivano-Frankivsk, Ukraine*

Mg-Zn crystalline ferrites represent very important magnetic materials for radiofrequency and microwave engineering applications. Mg-Zn ferrites also are very interesting materials from the scientific point of view, particularly for studying the nature of magnetism in complex oxide crystals as, in contrast to other ferrites with a spinel structure, the magnetic structure of Mg-Zn ferrites is relatively simple. The magnetic structure and a wide range of magnetic properties of bulk Mg-Zn ferrites result from a different distribution of Fe^{3+} ($3d^5$, $^6S_{5/2}$) ions between two crystallographically non-equivalent sites in the Mg-Zn lattice with a tetrahedral (A-sites) and octahedral (B-sites) coordination to oxygen. Magnetic moments of tetrahedral (A) and octahedral (B) magnetic sub-lattices are different and antiparallel. Therefore, Mg-Zn ferrites belong to non-compensated antiferromagnetics (or ferrimagnetics according to Neel). At the atomic level the ferrimagnetism phenomenon is explained by a stronger exchange interaction between Fe^{3+} ions of (A) and (B) sub-lattices (A–B interaction) in comparison with the exchange interaction between Fe^{3+} ions, localized only in sub-lattice (A) (A–A interaction) or in sub-lattice (B) (B–B interaction). However, a variation of inter-atomic distances caused, for example, by differences in the ionic radii of non-magnetic ions, which substitute Fe^{3+} ions in sub-lattices (A) and (B), the A–A or B–B exchange interactions can be comparable with the A–V exchange interaction.

The transition from bulk Mg-Zn ferrites to man-sized Mg-Zn ferrite materials with dimensions comparable and close to inter-atomic distances can essentially change their magnetic structure and properties which need more detailed investigation. The magnetic structure and properties (magnetic susceptibility, magnetization, hysteresis loop) and X-band ($\nu \cong 9.4$ GHz) ferromagnetic resonance (FMR) spectra of the series

of Mg-Zn nanoferrites with different compositions were investigated and analysed in the wide temperature (2–300 K) and magnetic field (0–±80 kOe) ranges.

Ferrite nanoparticles with $Mg_xZn_{1-x}Fe_{2\pm y}O_4$ ($x = 0$, 0.5, 0,532, 0.56, 0.588; $y = 0$, 0.033) chemical compositions were obtained by the sol-gel auto-combustion method using the nanotechnology process. According to the X-ray analysis the obtained nanopowders of Mg-Zn ferrites consisted of one crystalline phase with a spinel structure. The technological conditions of the Mg-Zn nanoferrites synthesis led to changes in the nanoparticle size. The size of particles in the obtained Mg-Zn ferrites evaluated using the Scherre's formula was in the 20–40 nm range. Difference thermal analysis (DTA) did not show any structural phase transitions in the obtained series of Mg-Zn nanoferrites at heating up to 1000°C. The lattice parameters of the nanocrystalline Mg-Zn ferrites were less than that in the corresponding nanoferrites, obtained by the ceramic method.

It was shown by the XANES (X-ray Absorption Near Edge Structure) spectroscopy that the iron was incorporated into the crystal lattice of the Mg-Zn nanoferrites in the trivalent state (Fe^{3+}). The static (DC) magnetic properties of the Mg-Zn nanoferrite series were investigated in the 2–300 K temperature range using a Quantum Design Magnetic Property Measurements System MPMS XL-7 with a Superconducting Quantum Interference Device (SQUID) magnetometer. All the investigated Mg-Zn nanoferrites are characterised by magnetic hysteresis. The shape of hysteresis loops and their parameters essentially depends on the chemical composition of the Mg-Zn nanoferrites and temperature. The parameters of observed hysteresis loops in the series of Mg-Zn nanoferrites were determined and analysed.

The observed temperature dependencies of static magnetic properties of Mg-Zn nanoferrites are directly connected with their magnetic structure. In particular, the temperature dependencies of magnetic susceptibility, measured at zero-field cooling (ZFC) and field cooling (FC) regimes, show that the $ZnFe_2O_4$ nanoferrite is characterised by two blocking temperatures (T_B), located in the low temperature range and above the room temperature that is good evidence at the applied 1000 Oe field. The $ZnFe_2O_4$ nanoferrite reveals strong ferromagnetic interaction in the high-temperature and antiferromagnetic interaction in the low temperature ranges.

The X-band FMR spectra of the obtained series of Mg-Zn nanoferrites also essentially show dependence on temperature in the 4–290 range. The lineshape and parameters (g-factor, giromagnetic ratio, peak-to-peak derivative linewidth, and peak-to-peak derivative amplitude) of the FMR signals, observed in the obtained Mg-Zn nanoferrites were determined at different temperatures and analysed in comparison with other nanocrystalline and bulk ferrites.

Real time quantum tunneling

G. J. Papadopoulos

Department of Physics, Solid State Physics Section, University of Athens
Panepistimiopolis, 15 784 Zografou, Athens, Greece

A real time scheme for the tunnelling effect past a barrier, within the semi-classical approximation, as a first step, is presented. The semi-classical propagator across a truncated hyperbolic barrier is obtained analytically in terms of the energy required for a particle to flee from a given position on one side of the barrier to a given position on the other side in a specified time. Given the particle's initial state in the form of a wave packet the propagator is used to obtain the wave function on the barrier's other side. The wave function, then, supplies both the probability and current densities as they evolve in time.

Mechanical and thermal stability of PTT-b-PTMO/graphene nanocomposites

S. Paszkiewicz[1], A. Szymczyk[2], E. Piesowicz[1], M. Nachman[1], K. Kwiatkowski[1], Z. Rosłaniec[1]

[1] *Institute of Material Science and Engineering, West Pomeranian University of Technology Al. Piastow 19, 70-310 Szczecin, Poland*

[2] *Institute of Physics, West Pomeranian University of Technology Al. Piastow 19, 70-310 Szczecin, Poland*

Nanocomposites based on PTT-b-PTMO (polyether-ester (PEE)) and graphene (3-layer thick, Angstron Materials) with the 0.1–1.0 wt.% nanofiller content were prepared by *in situ* condensation polymerization [1,2]. The graphene was found to be dispersed homogenously in the polymer matrix (TEM, SEM) (Figure 1). The thermal property and the mechanical property of the nanocomposites were studied. When the graphene content was 1%, the composite had a desired comprehensive property. At this composition, the thermal degradation onset temperature and the thermal deformation temperature of PTT-b-PTMO were increased and the tensile strength of the PEE was increased by 12% with a slight decrease in elasticity. The mechanism of PEE stabilization by graphene is associated with the transfer of free radicals on the carbon planes [3]. Due to its radical accepting capacity, graphene is expected to interrupt the chain propagation, leading to antioxidant action in polymers.

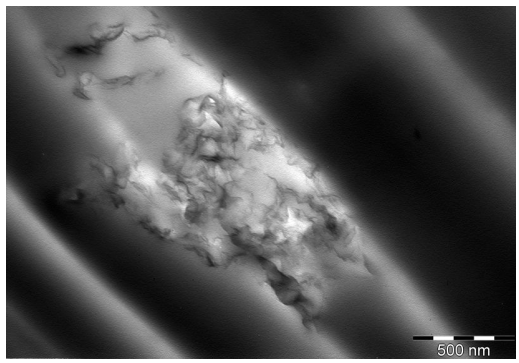

Figure 1: TEM micrograph of PTT-b-PTMO/1.0 wt.% graphene, $\times 75,000$

Acknowledgements
This work is sponsored under the European Project MNT ERA NET 2012 (APGRAPHEL Project).

References

[1] Szymczyk A, Paszkiewicz S, Rosłaniec Z 2013 *Polym Bull* **70** 1575–90
[2] Szymczyk A 2012 *J. Appl Polym Sci* **126** 796–807
[3] Zeynalov E B, Friedrich J F 2008 *Open Mater Sci Journal* **2** 28–34

Different ways to remove iron, cobalt and iron-cobalt catalysts from CNTs

I. Pełech, A. Jędrzejewska, A. Kaczmarek, U. Narkiewicz

Institute of Chemical and Environment Engineering
West Pomeranian University of Technology
Pulaskiego 10, 70-322 Szczecin, Poland

Carbon nanotubes (CNTs) are successfully used for many different applications due to their excellent electrical, thermal and mechanical properties. Most often theses materials are produced using the chemical vapour deposition technique because in this way it is possible to obtain a high yield. Unfortunately, CNTs are usually formed by bundles which are strictly entangled with a large amount of impurities like other carbonaceous materials (amorphous carbon and graphite) along with small catalytic metal particles. Therefore, in order to evaluate their unique properties for practical use, they have to be at first separated and purified.

In the available papers several purification processes, both chemical and physical, have been reported, depending on the nanotube morphology (single-walled or multi-walled), growth process and the metal catalyst. In most cases physical methods are included: filtration or high temperature annealing. The second area is focused on the use of chemical methods such as gas-phase oxidation, reduction in the gas phase, liquid phase oxidation and electrochemical oxidation. It has been found in many studies that oxidation, acid and filtration methods cannot be successfully applied to a CNT produced by CVD, because in this case it is not possible to remove catalyst particles and other contaminants. An important drawback is a too long purification process. An alternative method to purification of carbon nanotubes can be acid digestion with microwave heating. This method appears to be the most promising technology for large-scale purification, avoiding long processing times or multiple stages, utilizing minimal acid volumes under optimised conditions.

In this work an effective purification method for the removal of different kinds of catalyst from as-grown nanotubes is reported. CNTs obtained on iron, cobalt or iron-cobalt catalysts without a support were applied as the raw material. Two methods of purification of carbon nanotubes were employed: acid digestion under reflux and microwave assisted acid purification. The samples before and after treatment were characterized using different techniques. The phase composition of the samples was determined using X-ray diffraction (XRD) analysis (X'Pert PRO Philips diffractometer) with CuKα radiation. The removal degree of metal particles was determined using a thermobalance. The thermogravimetric analysis was performed on DTA-Q600 SDT TA Instruments apparatus with the heating rate of 10°C/min from room temperature to 900°C in air. Raman measurements were obtained using 785 nm (1.58 eV) excitation laser lines with a Renishaw InVia Raman Microscope spectrometer. It was found that the microwave assisted acid purification method demonstrated a significant

efficiency improvement over the traditional acid reflux and could be used to remove different kinds of metal particles. Similar amounts of catalyst particles were removed from the samples treated using nitric acid under reflux for 24 h and from the samples after digestion with microwave heating for 30 min only.

Acknowledgements
This work was supported under the project: LIDER/25/58/l-3/11/NCBR/2012 financed by the National Centre for Research and Development.

Double effect of CNT chlorination – surface functionalization and catalyst removal

I. Pełech[1], A. Jędrzejewska[1], D. Moszyński[1], R. Pełech[2]

[1] *Institute of Chemical and Environment Engineering*
West Pomeranian University of Technology
Pulaskiego 10, 70-322 Szczecin, Poland

[2] *Institute of Organic Chemical Technology, West Pomeranian University of Technology*
Pulaskiego 10, 70-322 Szczecin, Poland

CNTs possess excellent physical and chemical properties and have wide-range potential applications. However, only some of these properties and applications have been verified or implemented in a practical use. To a great extent, this situation can be ascribed to the difficulties in getting high-purity CNTs. As the as-prepared CNTs are usually accompanied by carbonaceous or metallic impurities, purification is an essential issue to be addressed. Pristine carbon nanotubes are also unsuitable for manufacturing of composite materials with large molecule species, such as polymer chains, because CNTs as a bulk material have a pronounced tendency to agglomerate in a polymer matrix. It is likely that chemical functionalization will facilitate the dispersion and stabilize carbon nanotubes to prevent agglomeration.

In this paper a chlorination method is proposed for simultaneous purification and functionalization of carbon nanotubes, thus increasing the range of their application. Carbon nanotubes were obtained by the CVD method through ethylene decomposition on nanocrystalline iron or cobalt or bimetalic iron-cobalt catalysts. Additionally, commercially available multi-walled carbon nanotubes (Nanocyl NC7000) were used. The effects of the temperature (50, 150, 250 and 400°C), the time of reaction (2–10 h), the type of catalyst (Fe, Co, Fe/Co) on the effectiveness of treatment and functionalization were tested. Using the XPS method and the Mohr method the presence of chlorine species on the surface of chlorinated samples was confirmed. The quantitative analysis of the metal impurity content was validated by means of thermogravimetric analysis. The phase composition of the samples was determined using the X-ray diffraction method and the morphology of carbon nanomaterials was studied using Transmission Electron Microscopy

Acknowledgements
This work was supported under the project: LIDER/25/58/l-3/11/NCBR/2012 financed by the National Centre for Research and Development.

Influence of experimental conditions on purification and surface modification of CNTs during microwave assisted acid digestion method

I. Pełech[1], U. Narkiewicz[1], A. Jędrzejewska[1], D. Moszyński[1], R. Pełech[2]

[1] *Institute of Chemical and Environment Engineering West Pomeranian University of Technology Pulaskiego 10, 70-322 Szczecin, Poland*

[2] *Institute of Organic Chemical Technology, West Pomeranian University of Technology Pulaskiego 10, 70-322 Szczecin, Poland*

Carbon nanotubes are separated from catalyst traces most often by an acid reflux in the presence of e.g. nitric or sulfuric acid. It is known that oxygen functional groups can be introduced on the carbon nanotubes surface during acid treatment. Nevertheless, this method is time-consuming. An alternative route to the modification of carbon nanotubes is a microwave assisted method.

In this work multi-walled carbon nanotubes were synthesized in a high temperature furnace (Carbolite, STF 16/180) using the ethylene – argon mixture (1:1) on an iron catalyst at 700°C under atmospheric pressure. After synthesis the samples were submitted to oxidation at 400°C or hydrogenation at 500°C. Additionally, commercially available multi-walled carbon nanotubes (Nanocyl NC7000) were used.

The carbon nanotubes were modified using nitric and hydrochloric acid treatment with microwave heating. The samples after synthesis or pretreatment under air atmosphere or pretreatment under hydrogen atmosphere were next immersed in a Teflon vessel filled with 100 ml of nitric or hydrochloric acid. Then, the whole content was placed in a reactor heated with microwaves. The influence of pretreatment, the kind of acid, nitric acid concentration, pressure and reaction time were investigated. After digestion the samples were washed and filtered with a 0.1 μm PTFE (polytetrafluoroethylene) membrane in deionized water to pH ~ 7. Finally the samples were dried in an oven at 100°C for 24h.

The obtained results were compared with the results achieved using the traditional acid digestion method. In this case the same materials were immersed in 100 ml of hydrochloric or nitric acid and boiled under reflux. Next, the suspension was washed and filtered with a 0.1μm PTFE (poly-tetrafluoroethylene) membrane in deionized water to pH ~ 7. Finally the samples were dried in an oven under 100°C for 24h.

The removal degree of metal particles was confirmed by X-ray diffraction (XRD) analysis (X'Pert PRO Philips diffractometer) using Cu Kα radiation and the amount of ash was determined using a thermogravimetric method. The thermogravimetric analysis was performed on DTA-Q600 SDT TA Instruments apparatus with the heating rate of 10°C/min from room temperature to 900°C in air. The Raman measure-

ments were obtained using excitation laser lines 785 nm (1.58 eV) with a Renishaw In-Via Raman Microscope spectrometer. The X-ray photoelectron spectra were obtained using Mg Ka (hm 5 1253.6 eV) radiation with a SES 2002 spectrometer operating at constant transmission energy AU6 (EP 5 50 eV).

Acknowledgements
This work was supported under the project: LIDER/25/58/l-3/11/NCBR/2012 financed by the National Centre for Research and Development

Chemical and physical properties of nanocrystalline iron of different nanocrystallite sizes

R. Pełka, Z. Lendzion-Bieluń, R. Wróbel, W. Arabczyk

Institute of Chemical and Environment Engineering
West Pomeranian University of Technology
Pulaskiego 10, 70-322 Szczecin, Poland

The pre-reduced iron ammonia synthesis catalyst, produced by fusing magnetite with small amounts of metal oxide promoters (Al_2O_3, CaO and K_2O), was used as a raw material for obtaining iron nanocrystallites of specified sizes. The average size of iron nanocrystallites as determined by XRD is 20 nm and $\sigma = 18$ nm (the parameter characterizing the size distribution width). The specific surface area is 10 m^2/g (BET).

The passive layer in the catalyst was reduced with hydrogen (30 dm^3 H_2/(h g)) in a tubular differential reactor at a temperature of 500°C. Then, the sample was oxidized at 500°C in a stream of nitrogen (20 dm^3 N_2/(h g)), saturated with water vapour (0.02 bar of H_2O) to oxidation degree $\alpha = 0.2$. Two phases (metallic iron and magnethite) were present in the sample after oxidizing. Metallic iron was selectively dissolved with a dilute solution of nitric acid (V). The magnetite remaining after etching was reduced with hydrogen at 375°C. Then, the sample was nitrided with ammonia in the above mentioned reactor at a temperature of 375°C. The processes of oxidation and nitriding were performed under conditions assuring that the rate of the chemical process was limited by the surface chemical reaction rate. If so, nanocrystallites undergo a phase transition in the order of their size, from the smallest to the largest.

The phase composition, average sizes and size distributions of crystallites were determined by the XRD method. Nanocrystallite size distributions of iron and magnetite were determined by the Pielaszek method. Chemical composition analyses of catalyst samples were performed by the ICP method. The specific surface areas were determined by the BET method.

Samples of nanocrystalline iron with narrower diameter ranges (parameter $\sigma = 3$–8 nm) and different average crystallite sizes, 10–20 nm (P1), 20–25 nm (P2), 25–30 nm (P3), respectively, as compared to the P0 sample, were obtained. These values did not

wt%	P0	P1	P2	P3
Al_2O_3	3.16	3.78	3.32	3.32
CaO	3.50	0.64	0.25	0.34
K_2O	0.79	0.13	0.16	0.17
SiO_2	0.36	0.17	0.02	0.07

Table 1: Chemical composition of samples P0, P1, P2, P3

change after the nitriding process. The nature of size distributions and the average size of nanocrystallites in the obtained samples affected the nitriding process, as indicated by changes in the shape of the TG curves.

The specific surface areas were within the following ranges: 40–50 m^2/g (P1), 20–25 m^2/g (P2), 10–15 m^2/g (P3).

The ICP results after nitriding and reduction of nitrides are presented in Table 1.

Acknowledgements
The scientific work financed by the Ministry of Science and Higher Education from the State budget resources for science in 2010–2013 – Scientific Project No. N N209 413039.

Poisson's ratio of two-dimensional auxetic foams

A. A. Pozniak[1], J. Smardzewski[2], K. W. Wojciechowski[3]

[1] *Department of Technical Physics, Poznan University of Technology*
Nieszawska 13A, 60-965 Poznan, Poland

[2] *Department of Furniture Design, Faculty of Wood Technology*
Poznań University of Life Sciences
Wojska Polskiego 38/42, 60-627 Poznan, Poland

[3] *Institute of Molecular Physics, Polish Academy of Sciences*
M. Smoluchowskiego 17, 60-179 Poznan, Poland

A material or structure whose Poisson's ratio is negative is often referred to as an auxetic. In contrast to common materials, it expands its lateral dimensions when stretched and gets thinner under compressive strain. This behavior renders the mechanical properties of auxetics strongly counterintuitive. Among many various classes of materials revealing Negative Poisson's Ratio (*NPR*), there is an interesting group of auxetics originating from conventional foams. As has been shown by Lakes [1] and later by Grima [2], a conventional foam can be subjected to multi-axial compression and spontaneously induced NPR can be observed after stress removal (by heating and/or chemical treatment). Although the effect of the compression induced drop in Poisson's ratio has been known for years, its microscopic mechanisms are not fully understood. Trying to shed light on the phenomenon we propose a foam model undergoing certain modifications and observe the influence of these modifications on the effective Poisson's ratio.

An analysis of two-dimensional foams is presented in this work. There are two structural models considered, see Figure 1, where (a) is a classic honeycomb structure (called Y-model) while (b) presents a kagomé-like structure (called Δ-model). The second structure (Figure 1b) clearly emerges from the first one (Figure 1a) by proper modification of the joints.

To propose a reliable two-dimensional foam structure model, the compressed specimen has to fulfill a crucial condition of isotropy. The latter can be reached by introduction of some disorder to the structures presented in Figure 1. It should be noted that a structural disorder is introduced in such a way that the lattice topology should remain unchanged. The second modification bases on the material properties, namely three different ratios of joints (brighter parts of the structure) to the ribs (black) hardness are taken.

The influence of the structure and the hardness of joints on the effective Poisson's ratio was studied using Finite Element Methods [3]. It has been shown [4] that all the considered structures spontaneously transform into NPR ones at 10 percent linear compression. The harder the joint forming material, the lower the effective Poisson's ratio. Furthermore, for the Δ-model based structure, the drop in Poisson's ratio accompanying biaxial compression was more significant than in the Y-model.

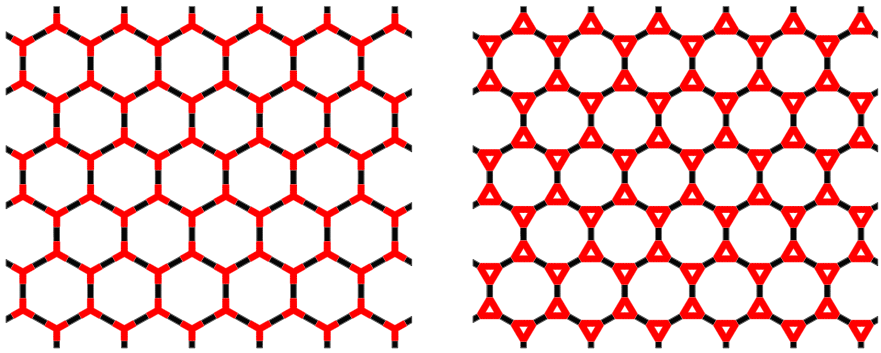

Figure 1: Ordered examples of 6×6 structures (a) before and (b) after joint modification

Finally, the models were studied by two different approaches. The first one utilized the plane stress elements, while the second made use of the Timoshenko beam formalism. It has been shown that the beam–based approach, which completely ignores overlaps of the beams but is much faster and requires less memory, gives qualitatively correct estimates of Poisson's ratio.

Acknowledgements
This work was supported by the grant NCN 2012/05/N/ST5/01476. Some of the simulations were performed at the Poznan Supercomputing and Networking Center (PCSS). This research was also supported by the PL-Grid Infrastructure.

References

[1] R. S. Lakes, *Science*, **235** (4792), 1038, 1987
[2] J. N. Grima, D. Attard, R. Gatt, and R. N. Cassar, *Advanced Engineering Materials*, **11** (7), 533, 2009
[3] D. Hibbit, B. Karlsson, and P. Sorensen, *ABAQUS/Standard Analysis User's Manual, ver. 6.10*, 2010
[4] A. A. Pozniak, J. Smardzewski, and K. W. Wojciechowski, *Smart Materials and Structures*, 2013, in print

Structural transformations and magnetic properties of amorphous films of Gd-Fe system

V. I. Prysyazhnyuk, O. G. Mykolaychuk

Ivan Franko National University of Lviv
Kyrylo and Mephodiy 8, 79005 L'viv, Ukraine

Magnetic properties of films and bulk samples of binary compounds of a Gd-Fe system ($GdFe_2$, $GdFe_5$ and Gd_2Fe_{17}) and also the agency of structure formation on magnetic properties were explored. Amorphous films were deposited on teflon substrates by the thermal evaporation method. The temperature of the substrates had two values, 300 and 500 K.The percentage ratio of the polycrystalline phase was incremented with an increase in the substrate temperature or at annealing of films. The thickness of films was measured by an MIO-1 optical interferometer (it was equal to 200 nanometers). A UEMV-100K electronic microscope and a PRON-2 high-temperature attachment were used for structural studies of films. A modernised vibrating magnetometer was used for magnetic studies.

The hysteresis curves for volume and thin-film samples show that these materials belong to the class of magneto-soft compounds. It is necessary to note also significant differences in the nature of hysteresis loops for the volume and thin-film samples of all the compounds of this system. The absolute values of the coercive force for amorphous and polycrystalline films and volume compounds were determined. The coercive force decreases at formation of amorphous films by 2 times in comparison with the volume samples. The formation of a polycrystalline phase in films gives rise to the coercive force increasing by 1.5 times in comparison with the volume samples (polycrystalline films become more magneto-hard). The manner of crystallisation whether in the process of film formation on the warmed-up substrate, or in the process of annealing of amorphous films after their deposition is of no importance for the absolute value of the coercive force. Nevertheless, different structures are formed in such cases as has been shown by previous structural research [1].

References

[1] V. Prysyazhnyuk, O. Mykolaychuk, *J. of Non-Cristalline Solids*, 2006, **352**, 4299

Zinc oxide nanostructure prepared by sol-gel method

M. Prześniak, E. Herczyńska, B. Kościelska, W. Sadowski

Department of Solid State Physics, Gdansk University of Technology
G. Narutowicza 11/12, 80-233 Gdansk, Poland

ZnO is an important n-type semiconductor material with excellent mechanical, chemical and thermal stability at room temperature. Zinc oxide has also remarkable optic features. Especially, due to the wide band-gap, ZnO is suitable for short wavelength optoelectronic devices. Moreover, ZnO also exhibits sensitivity of electrical resistivity to gases such as ethanol, acetylene, CO, NO and NO_2. These properties are evidence that ZnO is one of the most preferred materials for optoelectronic and gas sensor applications. However, the most important issue, especially for potential sensor applications seems to be a ZnO nanostructure. Therefore, it seems to be vital to develop a nanostructure manufacturing method. The nanostructure metal oxide semiconductors play an important role for sensing gas and humidity. Nanostructures have a large specific surface. Sensors constructed of nanostructures are characterized by greater sensitivity. It has been possible to synthesize ZnO in a large number of different nanostructures.

In the present work, we focused on synthesis and characterization of ZnO powders prepared by the sol-gel method. This synthesis method has a great potential to fabricate nanostructured metal oxides for commercial applications due to the fact that this method is very simple and relatively cheap. The starting solution was prepared by mixing zinc acetate dihydrate, absolute ethanol, deionized water and acetic acid. Bulk xerogel powders were annealed at various temperatures ranging from 250°C to 450°C. The structure of the samples was characterized by X-ray diffraction method (XRD), scanning electron microscope (SEM). ZnO nanostructures were manufactured with the proposed method.

Dynamics in crowded environment – application of dynamic lattice liquid model

A. Sikorski[1], P. Polanowski[2]

[1] *Department of Chemistry, University of Warsaw*
Pasteura 1, 02-093 Warsaw, Poland

[2] *Department of Molecular Physics, Technical University of Łódź*
Żeromskiego 116, 90-924 Łódź, Poland

Extensive and systematic simulation studies of two-dimensional fluid motion in a complex crowded environment were performed. In contrast to other works [1] we focused on cooperative phenomena that occurred where the motion of particles was taking place in a dense crowded system. Our main goal was to answer the question how fluid molecules moved in an environment which had a complex structure, taking into consideration the fact that the motion of fluid molecules was highly correlated. The Dynamic Lattice Liquid (DLL) model, which can work at the highest fluid density, was employed [2]. It became the basis for a parallel algorithm, which took into account coincidences of attempts of elementary molecular motion resulting in local cooperative structural transformations. Within the frame of the DLL model we considered cooperative motions of fluid particles in an environment that contained static obstacles. We studied the dynamic properties of the system, such as the mean square displacement and the relaxation time of the position as a function of concentration of obstacles. The changes of hydrodynamic interactions were also investigated by studies of the distribution of the cooperative loop length. The subdiffusive motion of particles was found in the crowded system [3]. It was also shown that the percolation threshold determined from the dynamic behavior of the mobile particles was considerably lower than that determined from the cluster analysis.

References

[1] Zhou H-X, Rivas G, Minton A P 2008 *Annu Rev. Biophys.* **37** 375–397
[2] Polanowski P, Pakula T 2003 *J. Chem. Phys.* **118** 11139
[3] Ben-Avraham D, Havlin S 2000 *Diffusion and reactions in fractals and disordered systems*, Cambridge University Press, Cambridge, chapt. 6

Evolution of charge along DNA

C. Simserides

Physics Department, University of Athens
Panepistimiopolis, 15 784 Zografou, Athens, Greece

Initially, an introduction to the DNA double helix is made. The necessary tight-binding parameters which describe the charge transfer along DNA, either at a base-pair level or at a single-base level and either for electrons or for holes is discussed. The pi molecular structure of the DNA bases (adenine (A), thymine (T), cytosine (C), and guanine (G)) obtained by the linear combination of atomic orbitals method is needed. The calculated HOMO and LUMO wave functions and energies of the DNA bases are then used to calculate the corresponding energies and wave functions of the two B-DNA base-pairs (A-T and G-C). Then, these results are used to obtain a complete set of the hopping matrix elements between successive base-pairs (as well as between neighboring bases considering all possible combinations i.e. complementary bases of the same base-pair, successive bases of the same strand and diagonally located bases of opposite strands) both for electrons and holes. The HOMO and LUMO energies and the hopping matrix elements are then used to obtain the temporal and spatial evolution of charge along DNA for various types of DNA.

Field-induced dependence of rotational diffusion processes in smectic films deposited on solid surface

I. Śliwa[1], M. Iwamoto[2], A. A. Vakulenko[3], A. V. Zakharov[3]

[1] *Institute of Molecular Physics, Polish Academy of Sciences*
M. Smoluchowskiego 17, 60-179 Poznan, Poland

[2] *Department of Physical Electronics, Tokyo Institute of Technology*
O-okayama 2-12-1, Meguro-ku, Tokyo 152-8552, Japan

[3] *Saint Petersburg Institute for Machine Sciences, Russian Academy of Sciences*
Saint Petersburg 199178, Russia

We have carried out a numerical study of the structural, thermodynamic, and motional properties of ultra-thin smectic films deposited in vacuo on a solid surface and subjected to external electric field **E** [1]. A molecular model based upon the random walk theory is applied for calculating the rotational self-diffusion (RSD) coefficient D both in the bulk of the smectic film and in the vicinity of the bounding surfaces. The RSD coefficient is presented as explicit function of temperature, of the molecular moment of inertia, and of the orientational distribution function (ODF) of the smectic film. The mean-field theory, which takes into account the effects of surface enhanced pair interactions in the bounding layers, as well as of the film thickness, on the ordering processes in the ultra-thin liquid crystal (LC) film deposited on the solid surface and subjected to external electric field, has been proposed. In the framework of that approach, the set of OPs and the Helmholtz free energy per 8CB molecule in the wide temperature range have been calculated. It has been shown that both the enhanced LC/solid, LC/vacuum pair interactions and the externally applied electric field have an important influence on the RSD coefficient and may extend the range of stability of these smectic films to temperatures higher than T_{AN} (bulk). It has been shown that the number of perturbed layers from each bounding surfaces, LC/solid and LC/vacuum, for a chosen set of the model parameters W_0 and W_1, is equal to eight. It means that the OPs, as well as the RSD coefficient vary rapidly with growth of i, to the values of the bulk OPs and RSD coefficient, and further increasing in the film thickness does not influence the magnitude of the OPs and the RSD coefficient. A reasonable agreement between the theoretically predicted and the experimentally obtained data of the RSD coefficient in the bulk of 4-*n*-octyl-40-cyanobiphenyl phase has been obtained.

References

[1] M. Iwamoto, I. Śliwa, A. A. Vakulenko and A. V. Zakharov, *Chem. Phys. Lett* **566**, 32 (2013)

Elasticity of two-dimensional Yukawa model

K. V. Tretiakov, K. W. Wojciechowski

Institute of Molecular Physics, Polish Academy of Sciences
M. Smoluchowskiego 17/19, 60-179 Poznan, Poland

The Yukawa potential is one of widely used approximations in modeling of colloidal suspensions [1–3]. Recently, the equilibrium properties and phase diagram of two-dimensional Yukawa systems have been obtained [4,5]. In the present study, the elastic properties of a crystalline two-dimensional Yukawa system are determined. Monte Carlo simulations in the NpT ensemble with variable shape of the periodic box are used as the simulation method [6].

The particles, interacting through hard-core repulsive Yukawa potential, form a triangular structure and, hence, the system elastic properties can be described by only two elastic constants: the bulk modulus B and the shear modulus μ. The effects of the Debye screening length (κ^{-1}) on the elastic properties of the system are studied. It is found that the elastic moduli increase with the density and their growth rate depends largely on the screening length: the smaller the screening length the more accelerated the increase in the elastic moduli with density (see Figure 1).

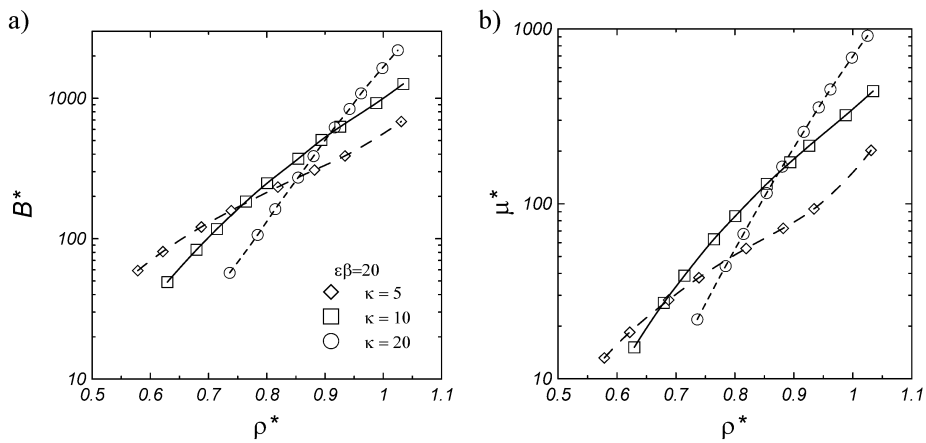

Figure 1: Density dependence of: (a) bulk modulus, (b) shear modulus, for different screening length values

Acknowledgements
This work was supported by the grant NN202 261 438 of the Polish Ministry of Science and Higher Education. Some of the calculations were performed at the Poznan Supercomputing and Networking Center (PCSS).

References

[1] J. P. Hansen and I. R. McDonald, *Theory of Simple Liquids* (Academic press, Amsterdam, 2006)
[2] F. E. Azhar, M.Baus, and J. P. Ryckaert, *J. Chem. Phys.* **112**, 5121 (2000)
[3] A. P. Hynninen and M. Dijkstra, *Phys. Rev. E* **68**, 021407 (2003)
[4] R. Asgari, B. Davoudi, and B. Tanatar, *Phys. Rev. E* **64**, 041406 (2001)
[5] P. Hartmann, G. J. Kalman, Z. Donko, and K. Kutasi, *Phys. Rev. E* **72**, 026409 (2005)
[6] K. W. Wojciechowski, K. V. Tretiakov, and M. Kowalik, *Phys. Rev. E* **67**, 036121 (2003)

Poisson's ratio of spheres interacting through hard-core repulsive Yukawa model

K. V. Tretiakov, K. W. Wojciechowski

Institute of Molecular Physics, Polish Academy of Sciences
M. Smoluchowskiego 17/19, 60-179 Poznan, Poland

A hard-core repulsive Yukawa potential [1] is one of well-known potentials in the field of condensed matter, where it has been used to model colloidal suspensions [2,3]. Studies of the phase diagram of this model have shown that particles can crystallize in bcc or fcc phases depending on the parameters of potential and external parameters [2,3]. As the bcc phase is stable only in a narrow strip of the potential parameters and external conditions, this work concentrates on the study of Poisson's ratio of the fcc phase. Monte Carlo simulations [4] are used to investigate the effects of the Debye screening length on the Poisson's ratio of the system.

It has been found that Poisson's ratio is negative in the direction $[110][1\bar{1}0]$ and its value decreases with an increase in the screening length (see Figure 1) [5].

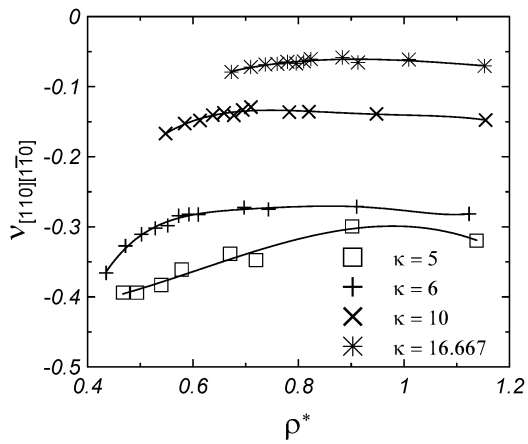

Figure 1: Density dependence of Poisson's ratio in direction $[110][1\bar{1}0]$ for different screening length values

Acknowledgements
This work was supported by the grant NN202 261 438 of the Polish Ministry of Science and Higher Education. Some part of the calculations were performed at the Poznan Supercomputing and Networking Center (PCSS).

References

[1] J. P. Hansen and I. R. McDonald, *Theory of Simple Liquids* (Academic Press, Amsterdam, 2006)
[2] F. E. Azhar, M. Baus, and J. P. Ryckaert, *J. Chem. Phys.* **112**, 5121 (2000)
[3] A. P. Hynninen and M. Dijkstra, *Phys. Rev. E* **68**, 021407 (2003)
[4] K. W. Wojciechowski, K. V. Tretiakov, and M. Kowalik, *Phys. Rev. E* **67**, 036121 (2003)
[5] K. V. Tretiakov and K. W. Wojciechowski, *Phys. Status Solidi B* (2013), in print

Study of magnetic properties of new vanadate $Cu_{13}Fe_4V_{10}O_{44}$

J. Typek[1], G. Zolnierkiewicz[1], M. Bobrowska[1], N. Guskos[1,2], A. Blonska-Tabero[3]

[1] *Institute of Physics, West Pomeranian University of Technology, Szczecin Al. Piastow 48, 70-311 Szczecin, Poland*

[2] *Department of Solid State Physics, Faculty of Physics, University of Athens Panepistimiopolis, 15 784 Zografou, Athens, Greece*

[3] *Department of Inorganic and Analytical Chemistry West Pomeranian University of Technology Al. Piastow 42, 71-065 Szczecin, Poland*

The $Cu_{13}Fe_4V_{10}O_{44}$ compound is a new vanadate which has been obtained recently in the ternary oxide system CuO-V_2O_5-Fe_2O_3. It is known from literature that the components of this system as well as the phases forming in its side systems, are active in such catalytic processes as, for example, oxidation reactions of: benzene to phenol, methanol to formaldehyde, isobutane to isobutene or toluene to benzaldehyde. Therefore, the $Cu_{13}Fe_4V_{10}O_{44}$ compound, forming with the involvement of all the components of the CuO-V_2O_5-Fe_2O_3 system, can be considered as a phase with potential catalytic properties. The basic physicochemical characterization of $Cu_{13}Fe_4V_{10}O_{44}$ has been already established. This compound has a sort of brown colour, its density is up to 3.97(5) g/cm^3. It crystallizes in a monoclinic system and melts incongruently at 790(5)^{o}C. The IR spectrum and the SEM image of this new compound are also given. The $Cu_{13}Fe_4V_{10}O_{44}$ compound was obtained by the standard solid-state reaction method, according to the following equation:

$$2Cu_5V_2O_{10(s)} + Cu_3Fe_4V_6O_{24(s)} = Cu_{13}Fe_4V_{10}O_{44(s)} \quad (1)$$

The DC susceptibility measurements were carried out in the 2–300 K temperature range using an MPMS-7 SQUID magnetometer and in magnetic fields up to 70 kOe in ZFC and FC modes. The EPR study was performed on a conventional X-band ($\nu = 9.4$ GHz) Bruker E 500 spectrometer with the 100 kHz magnetic field modulation. The measurements were carried in the 4–290 K temperature range using an Oxford Instrument helium-flow cryostat.

Figure 1 shows the temperature dependence of the DC magnetic susceptibility χ in the ZFC mode registered at four different magnetic fields. The inset shows the low temperature $\chi(T)$ curves in an expanded scale. Table 1 shows the magnetic parameters of the $Cu_{13}Fe_4V_{10}O_{44}$ compound calculated from the DC magnetization measurements. In the paramagnetic phase, the Curie-Weiss law, $\chi(T) = C/(T - T_{CW})$, allows calculating the effective magnetic moment (see Table 1) which is significantly smaller than expected for the sum of four iron ion magnetic moments in the formula unit.

Magnetic field [kOe]	Cooling mode	Curie constant C [10^{-1} emu K/g Oe]	Effective moment [μ_B/f.u.]	Curie-Weiss constant T_{CW} [K]	Neel temperature [K]
0.1	ZFC	7.73	11.82	−109.3	2.49
	FC	7.64	11.74	−105.8	2.49
1	ZFC	8.17	12.14	−101.8	2.70
	FC	8.01	12.02	−98.6	2.45
10	ZFC	7.86	11.91	−96,9	2.75
	FC	7.96	11.98	−99,5	2.50
70	ZFC	7.85	11.90	−97.9	2.40
	FC	7.79	11.86	−96.3	2.70

Table 1: Values of magnetic parameters of the $Cu_{13}Fe_4V_{10}O_{44}$ compound calculated from the DC magnetization measurements

Below 3 K a phase transition to the AFM phase was detected. The Neel temperature depends on the external magnetic field indicating the important role of spin clusters in the paramagnetic state.

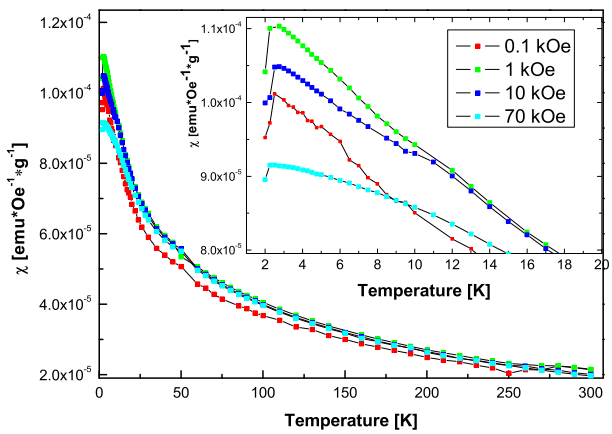

Figure 1: Temperature dependence of DC magnetic susceptibility χ in ZFC mode registered at four different magnetic fields. The inset shows the low temperature $\chi(T)$ curves in an expanded scale

The EPR measurements point out to an important role of the short-range AFM correlations of Fe^{3+} magnetic moments in the paramagnetic phase. The evidence for it is that, for $T > 2T_{\mathrm{N}}$, the EPR resonance shows an incognizant g-shift and T-dependence (see Figure 2) of the line broadening expected for a short range magnetic interaction in AFM materials above the Neel temperature T_{N}: $\Delta H(T) = \Delta H_0 + C_1(T - T_{\mathrm{N}}^{\mathrm{EPR}})^{-n}$, with $\Delta H_0 = 617(18)$ G, $C_1 = 11(1) \cdot 10^3$ G/K$^{-0.879}$, $T_{\mathrm{N}}^{\mathrm{EPR}} = 2.7(5)$ K, $n = 0.88(5)$. The EPR integrated intensity (Figure 3) was fitted by the Curie-Weiss type equation, $I_{\mathrm{int}}(T) = I_0 + \frac{C_2}{(T - T_{\mathrm{CW}})}$, with $I_0 = 5.373 \cdot 10^{10}$, $C_2 = 1.13 \cdot 10^{12}$, $T_{\mathrm{CW}} = -60.2$ K.

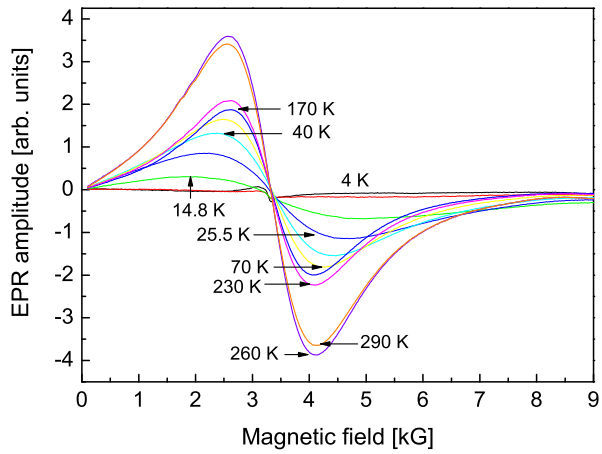

Figure 2: Some of EPR spectra of $Cu_{13}Fe_4V_{10}O_{44}$ registered at different temperatures

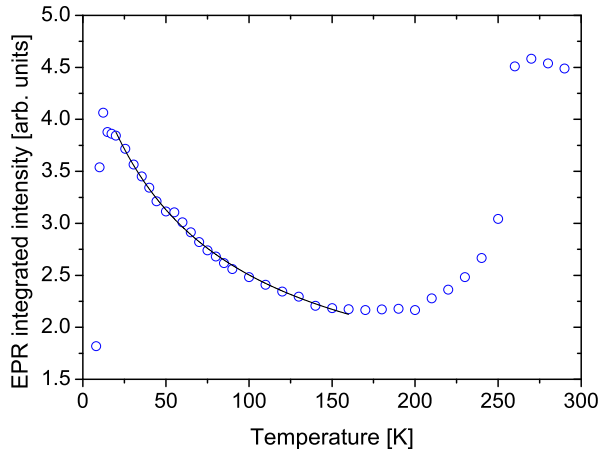

Figure 3: Temperature dependence of the EPR integrated intensity of the $Cu_{13}Fe_4V_{10}O_{44}$

Magnetic properties of $Cu_{3.9}Fe_{3.4}V_6O_{24}$ with lyonsite structure

J. Typek[1], G. Zolnierkiewicz[1], M. Bobrowska[1], N. Guskos[1,2], A. Blonska-Tabero[3]

[1] *Institute of Physics, West Pomeranian University of Technology, Szczecin Al. Piastow 48, 70-311 Szczecin, Poland*

[2] *Department of Solid State Physics, Faculty of Physics, University of Athens Panepistimiopolis, 15 784 Zografou, Athens, Greece*

[3] *Department of Inorganic and Analytical Chemistry West Pomeranian University of Technology, Szczecin Al. Piastow 42, 71-065 Szczecin, Poland*

Mineral lyonsite, with the formula α-$Cu_3Fe_4V_6O_{24}$, has been discovered in the summit crater fumaroles of the Izalco volcano (El Salvador). Attempts to synthesize α-$Cu_3Fe_4V_6O_{24}$, conducted in laboratory by the conventional solid-state reaction method led to its different form, i.e. β-$Cu_3Fe_4V_6O_{24}$ with a structure closely related to another mineral called howardevansite. The lyonsite-type phase can be synthesized in laboratory by this method, however, the composition of a phase obtained in such a way differs from that describing the mineral, and furthermore, it has a certain range of homogeneity, which can be expressed by $Cu_{3+1.5x}Fe_{4-x}V_6O_{24}$ ($0.551 < x < 0.778$). The crystal framework of lyonsite can accommodate different elements with different oxidation states and cation stoichiometries as well as cationic vacancies. Therefore, this structure type can be adopted by a wide range of phases.

Members of the lyonsite family can be described by the formula $A_4(BO_4)_3$, where B is a tetrahedrally coordinated high oxidation state cation and A is usually an octahedrally coordinated lower oxidation state cation. The isolated B-site tetrahedra form an octahedral channel occupied by one of the A-site cations and are connected by chains of AO_6 units.

Phases with lyonsite-type structure are undoubtedly worth conducting a comprehensive study. It is known from the literature that some of these phases have very interesting catalytic or conductive properties. On the other hand, phases with a lyonsite-type structure are known for their conductive properties, they belong to the family of NASICON ion conductors. A comprehensive study of the physicochemical properties of lyonsite-type phases can provide better understanding of the mechanism of the mentioned catalytic processes and conductivity.

The synthesis of $Cu_{3.9}Fe_{3.4}V_6O_{24}$ was performed by the standard solid-state reaction method. A mixture of the initial composition: 45.35 mol% CuO, 19.77 mol% Fe_2O_3 and 34.88 mol% V_2O_5, corresponding to the formula $Cu_{3.9}Fe_{3.4}V_6O_{24}$, was homogenized by grinding and heated in air in four stages: 560°C (20 h) + 580°C (20 h) + 700°C (20 h) + 740°C (20 h) until the monophase sample was obtained according

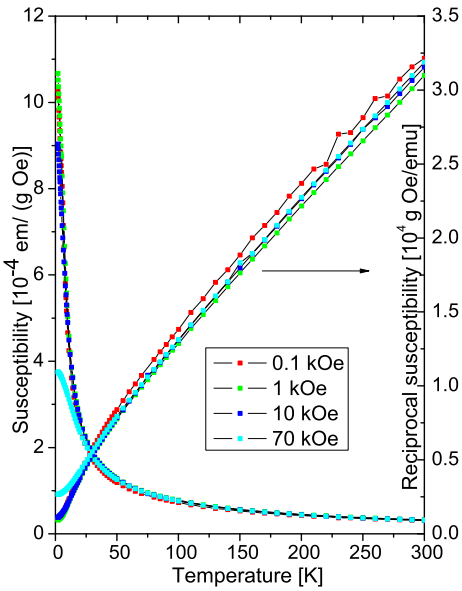

Figure 1: Temperature dependence of DC magnetic susceptibility $\chi(T)$ (left axis) and reciprocal susceptibility $\chi^{-1}(T)$ (right axis) in ZFC mode measured at four different magnetic fields ($H = 0.1$, 1, 10, 70 kOe) for $Cu_{3.9}Fe_{3.4}V_6O_{24}$ compound

to the reaction:

$$3.9CuO_{(s)} + 1.7Fe_2O_{3(s)} + 3V_2O_{5(s)} = Cu_{3.9}Fe_{3.4}V_6O_{24(s)} \quad (1)$$

The electron paramagnetic resonance study (EPR) was carried out on a conventional X-band ($\nu = 9.4$ GHz) Bruker E 500 spectrometer with the 100 kHz magnetic

Magnetic field [kOe]	Cooling mode	Curie constant C [10^{-1} emu K/g Oe]	Effective moment [μ_B/f.u.]	Curie-Weiss constant T_{CW} [K]	Neel temperature [K]
0.01	ZFC FC	24	4.65	−134	5.97 –
0.1	ZFC FC	102	9.58	−42	2.75 –
1	ZFC FC	109	9.90	−42	2.50 –
10	ZFC FC	106	9.76	−39	– –
70	ZFC FC	106	9.76	−40	– –

Table 1: Values of magnetic parameters of $Cu_{3.9}Fe_{3.4}V_6O_{24}$ compound calculated from DC magnetization measurements. The Curie-Weiss law was applied in the 70–250 K range

field modulation. The measurements were carried in the 4–300 K temperature range using an Oxford Instrument helium-flow cryostat. The DC susceptibility measurements were carried out in the 2–300 K temperature range using an MPMS-7 SQUID magnetometer and in magnetic fields up to 70 kOe in the ZFC and FC modes.

Both the DC magnetization and EPR studies indicate a dominating AFM interaction in the $Cu_{3.9}Fe_{3.4}V_6O_{24}$ compound spin system leading to the AFM state at low temperatures (and low magnetic fields).

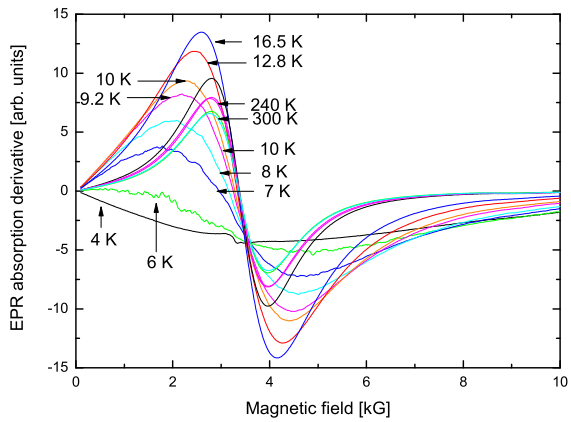

Figure 2: Selection of the registered EPR spectra of $Cu_{3.9}Fe_{3.4}V_6O_{24}$ at different temperatures

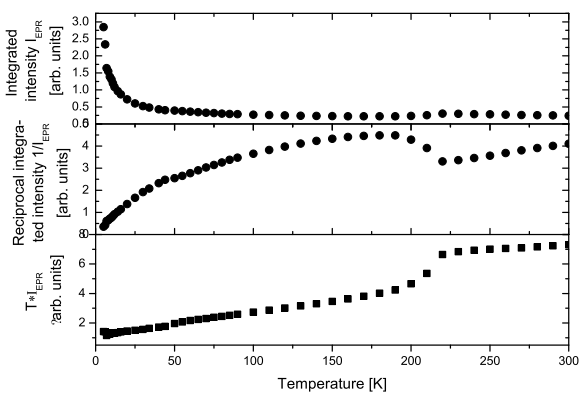

Figure 3: Temperature dependence of EPR integrated intensity (upper panel), reciprocal of integrated intensity (middle panel) and product of integrated intensity and temperature (lower panel)

Cluster structure of molten $Cu_3Ge(Sn)$ alloys

V. Vus[1], A. Yakymovych[2], S. Mudry[1]

[1] *Department of Metal Physics, Ivan Franko National University Lviv Kyrylo and Mephodiy 8, 79005 L'viv, Ukraine*

[2] *Department of Inorganic Chemistry / Materials Chemistry, University of Vienna Waehringer 42, A-1090 Vienna, Austria*

Copper-based alloys have a wide application first of all due to such properties of copper as high electrical and thermal conductivity, easy joining, excellent formability, high corrosion resistance and others. Current application of copper alloys is becoming wider including micro- and nanoelectronics, dental casting and other areas. For that reason it is important to study the properties of Cu-based alloys and first of all those that are related to the nanoscale structure and nanotechnologies.

Nanoporous metals and metal alloys have attracted considerable interest of scientists due to the unique properties and industrial application as novel functional materials. Most of the investigations have been carried out in the solid state and a possibility of a similar structure for liquids has been practically hardly studied at all. On the other hand, the existence of a micro-heterogeneous structure in liquid metal alloys with various kinds of structural units (associates, clusters, etc.) should lead to the formation of vacancies between them. In other words, the packing density of atoms in volumes between short-range order microregions is small and could be interpreted as "nanoporous areas". Such a micro-heterogeneous structure is pronounced in liquid alloys with chemical compounds in the solid state. For this reason Cu_3Ge and Cu_3Sn compounds in the liquid state are investigated in this work. The microstructure was investigated using X-ray diffraction and viscosity measurements.

The viscosity coefficient measurements were carried out by means of an oscillating crucible. The analysis of the temperature dependence of the viscosity coefficient allowed marking the deviation from the Arrhenius law and was attributed to the changes in both the interaction between unlike kind atoms and the size of clusters.

In order to confirm the assumption about structure changes we also studied the structure by means of the X-ray diffraction method. The structure factors obtained for these alloys were compared with those for liquid components. The existence of a shoulder on the right-hand side of the principal peak allowed us to suppose that chemically ordered microgroups were the main structural units responsible for such deviation. Such volume distribution of atoms leads to formation of microregions with a dense and rarefied arrangement of the atoms. Therefore, this structure could be considered as a "nanoporous-like structure".

Also, structural transitions of a local short-range order forming various type microregions were interpreted by combining the studies of viscosity as a structure-sensitive property and the structure data in a wide temperature range above the liquidus.

Structure and microstructure of arsenic and vanadium doped lanthanum ortho-niobate

S. Wachowski, A. Mielewczyk-Gryń, M. Gazda

Department of Solid State Physics, Faculty of Applied Physics and Mathematics
Gdansk University of Technology
G. Narutowicza 11/12, 80-233 Gdansk, Poland

High temperature proton conductors (HTPCs) are promising materials due to their applications in solid oxide fuel cells, hydrogen separators, hydrogen pumps and gas sensors [1]. Current state-of-art HTPCs are perovskite oxides such as barium cerates and zirconates [2,3]. Those materials have the highest reported proton conductivity among HTPCs. On the other hand, they exhibit poor chemical and mechanical stability, especially in carbon dioxide- and sulfur-rich atmospheres [2,3]. More recently new materials from the ABO_4 group have been reported to have high proton conductivity and good mechanical and chemical stability at elevated temperatures. Among those 2% Ca-oped on A-site lanthanum orthoniobate have the highest reported proton conductivity of 10^{-3}S/cm at 900°C [4].

Various doping strategies can be applied to obtain different structural and electrical properties of the designed material. The lanthanum niobate has two crystal structures (monoclinic below and tetragonal above 500°C), which is deleterious for future application due to a change of crucial material properties during phase transition. Proper isovalent doping on B-site can change the phase transition temperature even below room temperature [5]. Such properties are crucial for future applications of the material, and thus, it is very important to determine the dependence between doping and the properties of the material.

In this work synthesis of lanthanum orthoniobate was made. Doping by arsenic or vanadium in 5% to 20% was introduced. The relationship between the doping type and the percentage and structure and microstructure of the material was investigated.

Samples were prepared by solid state synthesis. The obtained materials were examined with the X-ray diffraction method at room temperature using Phillips X'Pert Pro MPD with CuKα radiation. The patterns were analysed by the Rietveld refinement method using the LHPM1 program [7]. The pseudo-Voigt profile function was applied.

The microstructure of the samples was studied by Scanning Electron Microscope Quanta 250FEG with the Bruker Energy-dispersive X-ray spectroscopy system.

During the experiment the phase content was examined in terms of the doping type and percentage.

X-ray diffraction measurements provided basic information about the influence of doping on the structure, the unit cell parameters and the average crystallite size. Scanning electron micrographs were obtained for sample microstructure studies and

energy-dispersive X-ray spectroscopy measurements were performed for a more accurate phase content analysis.

Figure 1. presents X-ray diffraction spectra of As-doped samples. The change in the spectra with the doping concentration indicates that the structure changes and that a tetragonal structure is eventually achieved at room temperature.

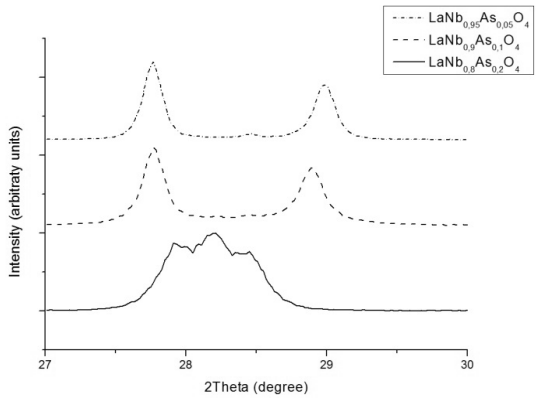

Figure 1: X-ray diffraction spectra of As-doped lanthanum niobate

References

[1] H. Iwahara, Y. Asakura, K. Kotahira, M. Tanaka, *Solid State Ionics*, **168** (2004)
[2] K. Kotahira, Y. Kochci, T. Shimura, H. Iwahara, *Solid State Ionics*, **138** (2000)
[3] K. Gdula-Kasica, A. Mielewczyk-Gryń, T. Lendze, S. Molin, B. Kusz, M. Gazda, *Crystal Research and Technology*, **45** (2010)
[4] R. Haugsrud, T. Norby, *Nature materials*, **5** (2006)
[5] A. B. Santibanez-Mendieta, E. Fabbri, S. Licoccia, E. Traversa, *Solid State Ionics*, **216** (2012)
[6] The X'PERT PLUS Rietveld algorithm is based on the source of the program LHPM1 (April 11, 1988) of R. J. Hill and C. J. Howard, X'Pert Plus, ©1999 Philips Electronics N. V.

Blocking temperature of $n\mathrm{Fe_2O_3}/(1-n)\mathrm{ZnO}$ nanocomposites as determined by DC magnetization and ferromagnetic resonance

K. Wardal[1], J. Typek[1], G. Zolnierkiewicz[1], N. Guskos[1,2], U. Narkiewicz[3]

[1] *Institute of Physics, West Pomeranian University of Technology Al. Piastow 48, 70-311 Szczecin, Poland*

[2] *Department of Solid State Physics, Faculty of Physics, University of Athens Panepistimiopolis, 15 784 Zografou, Athens, Greece*

[3] *Department of Inorganic and Analytical Chemistry West Pomeranian University of Technology Al. Piastow 42, 71-065 Szczecin, Poland*

As the wide-gap ZnO nanoparticles have numerous potential applications in electro-optical devices, transparent ultraviolet protection films, and spintronic devices, the study of magnetic properties of $n\mathrm{Fe_2O_3}/(1-n)\mathrm{ZnO}$ ($n = 0$–1) nanocrystals gains importance. We studied four samples: three samples consisting of concentrated nanopowders (with $n = 0.2$, 0.4, 0.7) obtained by the traditional wet chemistry method followed by calcination, and one sample containing the same $n = 0.7$ nanopowder embedded at a concentration of 0.1 wt.% in a PEN-b-PTMO polymer by DC magnetization and ferromagnetic resonance (FMR) methods. The only magnetic phase present in all the investigated samples was $\mathrm{ZnFe_2O_4}$.

Blocking temperature T_B is one of the most important magnetic characteristics of a nanomaterial which could severely limit its applications. Above T_B, nanoparticles are in the so called superparamagnetic phase (narrow lines in the FMR spectrum). The value of T_B could be determined from the maximum of the temperature dependence of ZFC magnetization. As can be seen in Figure 1 the largest values of T_B are obtained for both types of the $n = 0.7$ samples. This could be explained as a result of the strongest magnetic system (highest concentration of iron) in all the investigated samples. The fact that T_B is in general higher in the $n = 0.2$ sample than in the $n = 0.4$ sample could by explained by assuming the existence of larger size agglomerates in the $n = 0.2$ sample than in the $n = 0.4$ sample.

From FMR measurements T_B could be determined from the temperature dependence of the integrated intensity I_{int}. The peak in the $I_{\mathrm{int}}(T)$ curve is often interpreted as occurring at T_B, although this subject is still under debate. The blocking temperature calculated from FMR is usually much higher than the temperature obtained from static magnetization. In Figure 2 a comparison of T_B determined by both the methods is shown. The polymer sample ($n = 0.7$, polymer) displays consistently smaller values of T_B compared to sample ($n = 0.7$) what indicates weaker magnetic interaction between nanoparticles in the polymer. In Figure 3 the temperature dependence of the

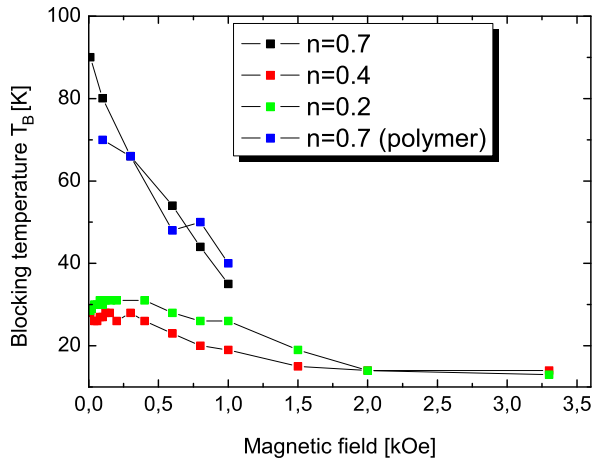

Figure 1: Values of blocking temperature as function of static magnetic field in four investigated samples determined from ZFC magnetization

temperature gradient of FC and ZFC magnetization difference for the three investigated samples is presented. It is argued that the T_B distribution (due to the different sizes of nanoparticles) can be extracted from the ZFC and FC curves. Comparing the obtained curves for our three samples it is evident that sample $n = 0.7$ contains nanoparticles with a broader distribution of sizes in comparison to the nanoparticles in the $n = 0.2$ and $n = 0.4$ samples.

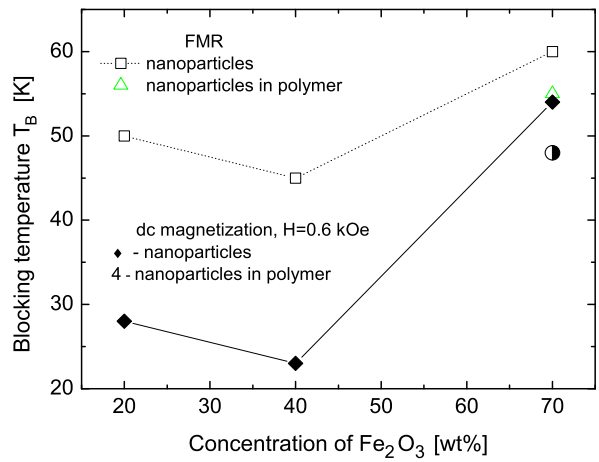

Figure 2: Comparison of blocking temperatures determined from FMR (upper curve) and DC magnetization (lower curve) measurements

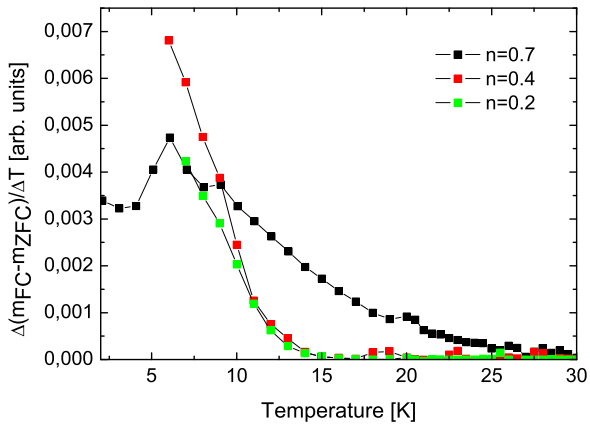

Figure 3: Temperature dependence of temperature gradient of FC and ZFC magnetization difference for three investigated samples

Simulation of branched polymers – a Monte Carlo study

E. Wawrzyńska[1,2,3], S. Eisenhaber[3], P. Parzuchowski[1], G. Zifferer[3], A. Sikorski[2]

[1] *Faculty of Chemistry, Warsaw University of Technology Noakowskiego 3, 00-664 Warsaw, Poland*

[2] *Department of Chemistry, University of Warsaw Pasteura 1, 02-093 Warsaw, Poland*

[3] *Institut of Physical Chemistry, University of Vienna Währinger Str. 42, A-1090 Wien, Austria*

Dendrimers are radially symmetric molecules with a well-defined, homogeneous and perfectly monodisperse structure made of branched repeating units emerging from a central core. In general, they have a globular shape with diameters in the nanometer scale which makes them ideal candidates for nanotechnology applications. Concomitant with the progress in the research of dendrimers, other branched polymers: star-branched and hyperbranched polymers have started to attract increasing attention. The above mentioned types of polymers are structured differently. While dendrimers consist of dendritic and terminal units, hyperbranched polymers are randomly branched molecules and possess also linear units in their structures. Star-branched polymers in turn, are composed of several linear polymer chains connected to a common core. Dendrimers, hyperbranched polymers and star-branched polymers are an interesting area for findings of new and unusual properties. In spite of the fact that enormous progress has been made in the potential applications of dendrimers and hyperbranched polymers during the last decade, we still have only a vague answer concerning how the polymer structure type affects the target applications. The synthetic methodology has been significantly improved, however, from the point of view of material science and medicine, further development of theoretical investigations of dendrimers and hyperbranched polymers is needed to fully understand all the properties of these materials. Clearly the simulation of branched polymers is still in infancy and many discoveries still lie ahead [1,2]. The present study concerns investigations of physical properties of dendrimers and hyperbranched polymers in the infinite dilution limit based on coarse-grained model systems using a dynamic Monte Carlo method: The polymer chains are represented by sequences of lattice points restricted to a simple cubic lattice. Configurations are dynamically produced by use of pivot moves and micro relaxations starting from a non reversal random walk configuration after conversion into a self avoiding one, accepting only moves resulting in a configuration with fewer overlaps. For data generation a new configuration is accepted according to the Metropolis Rosenbluth algorithm allowing variation of the solvent quality from bad to good solvent conditions introducing the solvent implicitly

via contacts between segments [3]. The size, shape and local structure of the whole molecule and branches, as well as the mutual orientation of branches were calculated as functions of the chain architecture, the degree of branching, the number of generations (in case of dendrimers) and the total chain length emphasizing scaling laws of mean square dimensions and characteristic shape data in the limit of the infinite chain length.

Acknowledgements
This research has been supported by the International PhD Programme MPD/2010/4 (The European Union, The European Regional Development Found), the European Union in the framework of European Social Fund through the Warsaw University of Technology Development Programme and Scholarship Foundation of the Republic of Austria.

References
[1] Inoue K 2000 *Progr. Polym. Sci.* **25** 453
[2] Lallana E, Fernandez-Trillo F, Sousa-Herves A et al. 2012 *Pharm. Res.* **29** 902–921
[3] Zifferer G 1999 *Macromol. Theory Simul.* **8** 433

Synthesis of multifunctional hyperbranched polymers soluble in supercritical carbon dioxide

E. Wawrzyńska[1], A. Sikorski[2], J. Gregorowicz[3], Z. Fraś[3], P. Parzuchowski[1]

[1] *Faculty of Chemistry, Warsaw University of Technology Noakowskiego 3, 00-664 Warsaw, Poland*

[2] *Department of Chemistry, University of Warsaw Pasteura 1, 02-093 Warsaw, Poland*

[3] *Polish Academy of Science, Institute of Physical Chemistry Kasprzaka 44/52, 01-224 Warsaw, Poland*

Benefiting from the unique type of architecture, nanometer dimensions, versatility of functionality, dendrimers have shown promise in the field of nanomedicine, inter alia, as drug-delivery carriers. Hyperbranched polymers possess some of the features of dendrimers, including a high degree of branching, multifunctionality, a more spherical shape than linear polymers and the presence of nanocavities. Hyperbranched polymers are conveniently prepared and therefore, they are less expensive in comparison to dendrimers, which are prepared under tedious multistep reaction schemes. The commercially viable technology needs a continuing effort to lessen the cost of synthesizing macromolecules capable of carrying drug molecules and improving the preparation of macromolecular drug-delivery systems. Therefore, our present research investigates the design and synthesis strategy of multifunctional hyperbranched polymers with the objective to develop effective drug delivery systems (DDS) [1,2].

The influence of the degree of branching, the presence and amount of spacer units between branching points, the chemical character of terminal groups and the type of the hyperbranched polymer on solubility in a supercritical carbon dioxide (temperature, pressure and concentration) was studied. The research was carried out for hyperbranched polyesters (dimethylolpropionic acid derivatives) and polyethers (polyoxetanes).

Acknowledgements

This research has been supported by the Polish Foundation of Science International PhD Programme MPD/2010/4 (The European Union, The European Regional Development Found) and the Polish National Science Centre Research Grant N N209 028440.

References

[1] Paleos C M, Tsiourvas D and Sideratou Z 2007 *Molecular Pharm.* **4** 169
[2] Frechet J, 2003 *J. Polym. Sci. Part A, Polym. Chem.* **41** 3713
[3] Tryznowski M et al. 2012 *Macromolecules* **45** 6819

Highly efficient calculation method of bond order parameters

S. Winczewski[1,2], J. Rybicki[1,2]

[1] *Department of Solid State Physics, Gdansk University of Technology G. Narutowicza 11/12, 80-233 Gdansk, Poland*

[2] *TASK Computer Center, Gdansk University of Technology G. Narutowicza 11/12, 80-233 Gdansk, Poland*

The bond order parameters method [1] is widely used to characterize the local particle structure of computer simulated materials [2–4]. The computing process of bond order parameters involves very frequent evaluation of spherical harmonics which makes the method computationally extremely expensive.

A new computational scheme for the evaluation of bond order parameters was proposed and implemented. The performed numerical experiments showed that the developed new algorithm increased the efficiency of bond order parameters evaluation by 20–40 times, thus making the method applicable to the characterization of the structure of large-scale atomic systems.

Acknowledgements
This work was co-financed by the European Union within European Regional Development Fund, through grant Innovative Economy (POIG.02.03.00-00-096/10).

References

[1] Steinhardt P J, Nelson D R and Ronchetti M 1983 *Phys. Rev. B* **28** 784
[2] Wang Y, Teitel S and Dellago Ch 2005 *J. Chem. Phys.* **122** 214722
[3] Moroni D, ten Wolde P R and Bolhuis P G 2005 *Phys. Rev. Lett.* **94** 235703
[4] Desgranges C and Delhommelle J 2008 *Phys. Rev. B* **77** 054201

X-ray absorption fine structure analysis as a very sensitive local structural probe

A. Witkowska

Department of Solid State Physics, Faculty of Applied Physics and Mathematics
Gdansk University of Technology
G. Narutowicza 11/12, 80-233 Gdansk, Poland

The X-ray Absorption Spectroscopy (XAS) is a powerful technique providing information on the structure of the environment around selected atomic species and also on the electronic and magnetic properties of matter. This insight can be obtained from analysis of the quantum interference pattern, usually detectable above any inner shell absorption edge, generated by scattering of the photoelectron on the potential of the surrounding atoms. The observed oscillations are usually referred to as the X-ray Absorption Fine Structure (XAFS). The particular assets of an XAFS are its element specificity and its sensitivity on the local structure giving a possibility to obtain detailed information without the presence of any long range ordering. For these reasons, this is really a unique technique for structural analysis of multicomponent and disordered systems. The applications of this spectroscopy cover a wide range of scientific disciplines ranging from physics, chemistry, materials science, biology and earth sciences.

The lecture will be devoted to the presentation of this technique. The first part will focus on the history and general theory of the method and on some aspects of the XAFS experiment. Especially, a description of a synchrotron laboratory and the XAS experimental set-up will be presented, and the sample and measurement optimization will also be discussed. The second part of the lecture will be dedicated to XAFS application to structural analysis of disordered systems. Additionally, detailed results of a multiple-scattering extended X-ray absorption fine structure (MS EXAFS) data analysis of liquid metals (e.g. Pb, Cu), heavy-metal oxide glasses (e.g. lead-silicate glass) and nanoparticles (e.g. Pb, Pt, PtCo) will be shown. In the summary, the advantages and disadvantages of the technique will be underlined.

References

[1] G. Bunker 2010 *Introduction to XAFS*, Cambridge University Press
[2] P. Willmott 2011 *An Introduction to Synchrotron Radiation*, John Wiley and Sons, Ltd.
[3] A. Filipponi et al. 2009 *GNXAS extended suite of programs for advanced x-ray absorption data-analysis: methodology and practice*, TASK Publishing, Gdansk, Poland, ISBN 978-83-908112-8-4

Simple models of auxetic foams

K. W. Wojciechowski[1], A. A. Poźniak[2]

[1] *Institute of Molecular Physics, Polish Academy of Sciences*
M. Smoluchowskiego 17/19, 60-179 Poznan, Poland

[2] *Department of Technical Physics, Poznan University of Technology*
Nieszawska 13A, 60-965 Poznan, Poland

Poisson's ratio is the negative ratio of the relative change in the transverse dimension to the relative change in the longitudinal dimension when infinitesimal change of the longitudinal stress is applied [1]. Foams of negative Poisson's ratio have been manufactured by Lakes in 1987 [2]. Materials exhibiting negative Poisson's ratio are known as auxetics [3]. In this lecture, recent progress in theoretical and simulation modeling of auxetic foams will be presented.

Acknowledgements
This work was supported by the grant NCN 2012/05/N/ST5/01476. Part of the simulations was performed at Poznan Supercomputing and Networking Center (PCSS).

References
[1] L. D. Landau and E. M. Lifshitz, *Theory of Elasticity*, Pergamon Press, London (1986)
[2] R. S. Lakes, *Science* **235**, 1038 (1987)
[3] K. E. Evans, *Endeavour* **15**, 170 (1991)

Investigating the auxetic potential of nematic side-chain liquid crystalline polymers: a computational study

C. Zerafa[1], A. C. Griffin[2], K. W. Wojciechowski[3], M. R. Dudek[4], J. N. Grima[1,5]

[1] *Department of Chemistry, Faculty of Science, University of Malta Msida MSD 2080, Malta*

[2] *School of Materials Science and Engineering, Georgia Institute of Technology 801 Ferst Drive, Atlanta, GA 30332-0295 USA*

[3] *Institute of Molecular Physics, Polish Academy of Sciences M. Smoluchowskiego 17, 60-179 Poznan, Poland*

[4] *Institute of Physics, Zielona Gora University 65-069 Zielona Gora, Poland*

[5] *Metamaterials Unit, Faculty of Science, University of Malta Msida MSD 2080, Malta*

Considerable advances have been recently made by Griffin et al. in the synthesis of nematic liquid crystalline polymers (LCPs) designed to exhibit negative Poisson's ratio [1–3]. These polymers contain laterally attached rod-like units, which are aligned along the direction of the main polymer chain in the unstressed state but rotate to the orthogonal direction when stretched. This re-orientation of laterally attached rods is thought to push neighbouring chains apart as shown in Figure 1a, thus giving rise to lateral expansion and potentially also a negative Poisson's ratio.

Force-field based molecular modelling simulations were performed using Accelrys® Materials Studio V.6.0 on polymeric systems based on Griffin's LCPs in an attempt to understand better the behaviour of these systems when they are stretched. Systems of various sizes were studied, where each unit cell contained from 4 up to 256 repeating units, whose chemical structure is shown in Figure 1b, in different systems (with a $2 \times 2 \times 1$ and $8 \times 8 \times 4$ configuration, respectively). The starting structure was optimised in such a way as to give a highly packed dense system, hence this system can represent (within the simulation error) the density close to the highest density possible at atmospheric pressure.

A strain was applied for several steps along the direction of the main chain (the Z-direction) by increasing the length of cell (parameter c) by 1.75% in each single step, which was kept constant while the energy of the structure was minimised using the PCFF force-field [4]. The calculations suggest that Poisson's ratio is clearly negative in the b_y direction and positive in the a_x direction, whilst the transverse area seems to decrease with increasing strain (see Figure 2). The simulations show that the system is anisotropic in a direction transverse to the director of the nematic phase and it is

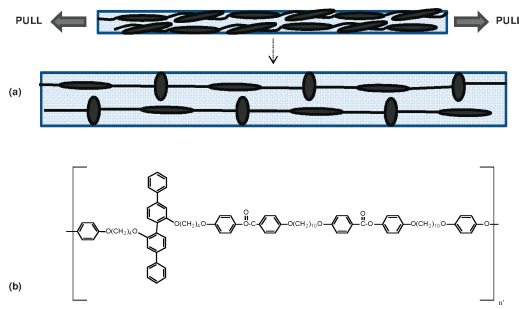

Figure 1: (a) Schematic figure showing the re-orientation of the laterally attached rods in the nematic LCPs after stretching along the main chain direction; (b) The repeating unit of the studied polymer

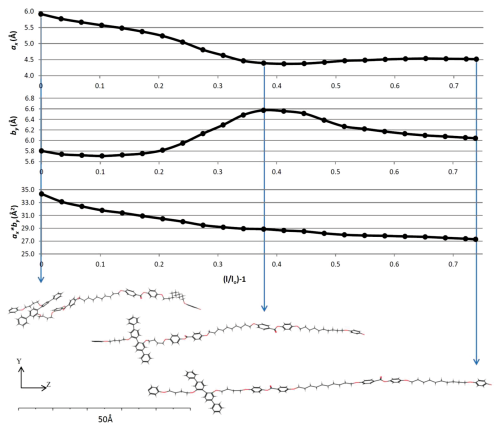

Figure 2: Dependence of the parameters a_x, b_y, and the cross section area $a_x b_y$ on the 'strain' (excess relative length) of the sample, $l/l_0 - 1$, for one of the studied systems (containing 256 monomers in an $8 \times 8 \times 4$ configuration); the figure also includes snapshots of a representative repeating unit in the system at three different strains

necessary to investigate even larger systems in order to confirm whether this effect survives in the bulk nematic phase. Theoretical modelling by analytic studies and computer simulation of a simplified (geometric) model are also being performed to complement this study.

Acknowledgements
This research is funded by a grant awarded to Christine Zerafa through the Strategic Educational Pathways Scholarship (Malta). These scholarships are part-financed by the European Union – European Social Fund (ESF) under Operational Programme II – Cohesion Policy 2007–2013, "Empowering People for More Jobs and a Better Quality of Life". She is grateful to authorities of the Institute of Molecular Physics, Polish Academy of Sciences (IFM PAN), and for hospitality at the Institute of Physics, Uni-

versity of Zielona Gora. She is also grateful for the hospitality and the financial support of the Georgia Institute of Technology, which made her visit to Atlanta possible. This research has been carried out using computational facilities procured through the European Regional Development Fund, Project ERDF-080 'A Supercomputing Laboratory for the University of Malta' (http://www.um.edu.mt/research/scienceeng/erdf_080). Part of the simulations was performed at the Poznan Supercomputing and Networking Center.

References

[1] C. B. He, P. W. Liu, and A. C. Griffin, *Macromolecules*, **31** (1998) 3145
[2] C. B. He, P. W. Liu, P. J. McMullan, and A. C. Griffin, *Phys. Stat. Sol. B*, **242** (2005) 576
[3] C. B. He, P. W. Liu, C. W. Smith, and K. E. Evans, *Macromol. Chem. Phys.*, **206** (2005) 233
[4] H. Sun, S. Mumby, J. Maple, and A. Hagler, *J. Am. Chem. Soc.*, **116** (1994) 2978

INDEX OF AUTHORS

Domain-Oriented Services and Resources of Polish Infrastructure for Supporting Computational Science in the European Research Space –

PLGrid Plus

ACC CYFRONET AGH, Kraków coordinator | ICM UW, Warsaw | PSNC, Poznań | TASK, Gdańsk | WCNS, Wrocław

PLGrid Plus project serves Polish scientific communities enabling extensive cooperation among them, as well as international cooperation in the scope of research activities in the area of e-Science.

The e-infrastructure requirements of the scientific communities are highly diversified and depend on the scientific field. The differences may relate to computing power and type of computing infrastructure, software resources and databases, as well as a unique measuring/research equipment, which is a part of the infrastructure.

To harmoniously support, in terms of IT, both, the development of scientific research in the various problem areas and researchers, it is necessary to fit the characteristics of the IT infrastructure to problems being the subject of research, which is the most important task implemented within the PLGrid Plus project.

Currently, domain-specific solutions are being created for the following groups of users, representing the strategic areas and important topics for the Polish and international science:

www.plgrid.pl
www.plgrid.pl/plus

The new services will provide a significant extension of the Polish computing infrastructure, which has been built since 2008 within the PL-Grid project. Currently, scientists use 7 million CPU-hours on average and execute about 1 million jobs per month. They have access to computing resources including more than 230 TFlops of computing power and more than 3.6 PBytes of storage space. Within the PLGrid Plus project it is planned to extend these resources three times.

All interested in cooperation, please contact us through the Helpdesk system: **helpdesk AT plgrid.pl**

INVITATION

We invite scientists from these and other areas to take advantage of the PLGrid Plus project offer: we will jointly prepare the specific computing environments for each research group, i.e., services, tools and computing infrastructure (including software), tailoring them to your needs.

INNOVATIVE ECONOMY
NATIONAL COHESION STRATEGY

The PLGrid Plus project is co-funded by the European Regional Development Fund as part of the Innovative Economy program

EUROPEAN UNION
EUROPEAN REGIONAL DEVELOPMENT FUND